

Title	Study on dinosaur locomotion mechanism based on mechanical functional morphology of musculoskeletal system
Author(s)	伊東, 和輝
Citation	大阪大学, 2024, 博士論文
Version Type	VoR
URL	<a href="https://doi.org/10.18910/96053">https://doi.org/10.18910/96053</a>
rights	
Note	

*Osaka University Knowledge Archive : OUKA*

<https://ir.library.osaka-u.ac.jp/>

Osaka University

DOCTORAL DISSERTATION

---

**Study on dinosaur locomotion mechanism  
based on mechanical functional morphology  
of musculoskeletal system**

---

Kazuki ITO

December, 2023

Graduate School of Engineering,

OSAKA UNIVERSITY





OSAKA UNIVERSITY

*Abstract*

Graduate School of Engineering

Doctor of Engineering

**Study on dinosaur locomotion mechanism based on mechanical functional morphology of musculoskeletal system**

by Kazuki ITO

Dinosaurs are terrestrial vertebrates with unparalleled diversification over 160 million years of lineage. They range from bipedal to quadrupedal and from small to the largest species in history, covering almost the entire diversity of legged terrestrial vertebrates in size. From these points, the ultimate goal of this study is to construct a general design principle of terrestrial locomotion that can be applied to diverse body sizes or locomotor types by understanding the locomotor mechanism of dinosaurs. Locomotion in terrestrial vertebrates is emerged from the musculoskeletal system and interaction with the environment. The skeleton supports the body, and the mechanical function of the muscular system maintains the posture of the skeleton. The muscular system is composed of many elements, such as muscles and tendons, and the active and passive functions interact to coordinate the movement of the skeleton and realize locomotion. Therefore, it is important to clarify the essential mechanism of dinosaur locomotion based on the correlation between the morphology and mechanical function of the musculoskeletal system (this is called mechanical functional morphology here). In many previous approaches to reconstruct the musculoskeletal system, the muscular system has been estimated based on the morphological homology of extant sisters of dinosaurs (e.g., crocodiles and avians). However, the mechanical significance of muscles and tendons is unclear in estimates based on morphology alone. Therefore, in this study, I proposed an approach to construct dinosaur locomotion based on the mechanical functional morphology of the musculoskeletal system of extant sisters. First, in preparation, I dissected extant sisters to hypothesize the fundamental locomotion mechanism. Next, I developed physical models of the musculoskeletal system of the dissected species and verified the feasibility of the hypotheses. From this approach, I revealed the stance mechanism of the crocodylian hindlimbs based on the passive coordination of the muscular system and interaction with the environment. Furthermore, I revealed the mechanical backgrounds of the Engage-Disengage Mechanism observed in the intertarsal joint of ratites. Finally, I attempt to construct locomotion mechanisms by applying the mechanical functional morphology of extant sisters to the dinosaur skeleton. As a result, I succeeded in realizing the stance of the hindlimbs of the dinosaur skeleton based on the stance mechanism of a crocodylian hindlimb. Through these approaches, I was able to construct dinosaur locomotion based on the mechanical functional morphology of the musculoskeletal system. However, this dissertation only clarified the stance mechanism of dinosaur hindlimbs, which is only the beginning of the way to realize the terrestrial locomotion of dinosaurs.



# Contents

<b>Abstract</b>	<b>iii</b>
<b>1 General introduction</b>	<b>1</b>
1.1 Introduction . . . . .	1
1.2 Previous method . . . . .	1
1.3 Problems with previous method . . . . .	3
1.4 Scope of this study . . . . .	4
1.5 Approach . . . . .	5
1.6 Contents of this dissertation . . . . .	6
<b>2 Elucidation of the fundamental locomotion mechanism in Crocodilians I</b>	<b>9</b>
2.1 Introduction . . . . .	9
2.2 Dissection of <i>Crocodylus porosus</i> and minimum configuration for semi-erect limb posture . . . . .	10
2.3 Crocodilian hindlimb robot . . . . .	11
2.4 Results . . . . .	13
2.4.1 Semi-erect limb posture provided by the passive interlocking mechanism . . . . .	13
2.4.2 Function of coudifemoralis longus muscle tendon and gastrocnemius . . . . .	15
2.4.3 An additional passive element . . . . .	16
2.5 Discussion and Conclusions . . . . .	17
<b>3 Elucidation of the fundamental locomotion mechanism in Crocodilians II</b>	<b>21</b>
3.1 Introduction . . . . .	21
3.2 Crocodilian hindlimb robot . . . . .	22
3.3 Results . . . . .	22
3.3.1 Functions of the iliotibials as a passive element . . . . .	22
3.3.2 Effect of the iliotibialis on erect-limb posture . . . . .	23
3.4 Conclusions . . . . .	27
<b>4 Elucidation of the fundamental locomotion mechanism in avians</b>	<b>29</b>
4.1 Introduction . . . . .	29
4.2 Materials and methods . . . . .	31
4.3 Result . . . . .	31
4.3.1 EDM and muscle and ligaments arrangement of the emu hindlimb . . . . .	31
4.3.2 EDM in the intertarsal joint of the physical model . . . . .	32
4.3.3 Design of articular surface, critical for achieving the EDM . . . . .	33
4.4 Discussion . . . . .	36
4.5 Conclusions . . . . .	38

---

<b>5</b>	<b>Construction of locomotion mechanisms in dinosaurs</b>	<b>41</b>
5.1	Introduction . . . . .	41
5.2	Material and Method . . . . .	42
5.2.1	Skeletal model of <i>Protoceratops andrewsi</i> . . . . .	42
5.2.2	Stance mechanism based on the passive interlocking of the musculo-tendinous system in crocodilian hindlimb . . . . .	43
5.3	Result . . . . .	44
5.3.1	Reconstruction of the <i>Protoceratops</i> hindlimb musculoskeletal tendinous system . . . . .	44
5.3.2	Design of the <i>Protoceratops</i> hindlimb robot . . . . .	45
5.3.3	Experiment of upright standing and maintaining the posture . . . . .	46
5.4	Conclusions . . . . .	47
<b>6</b>	<b>General discussion</b>	<b>49</b>
6.1	Evaluation of the efficacy of the proposed approach . . . . .	49
6.2	Summary of this dissertation . . . . .	50
6.3	Future work . . . . .	52
	<b>Acknowledgements</b>	<b>55</b>
	<b>Bibliography</b>	<b>57</b>

# List of Figures

1.1	The methods for understanding locomotion mechanisms based on the morphology and mechanical function of the musculoskeletal system of archosaurs. . . . .	5
1.2	A method for estimating the locomotion of dinosaurs based on the locomotion mechanism of closely related species of dinosaurs. . . . .	7
2.1	A: The hindlimb and the trunk of the dissected crocodile (excluding the head, tail, and skin) in lateral view, with the schematics of the positions of the major bones (femur, tibia, fibula, and metatarsals) and the muscles (CFL and GE) and the tendon (CFLT) of interest. The photo is inverted for ease of comparison with the right hindlimb robot described later in this paper. B: A schematic representation of the crocodilian musculoskeletal system. The arrows indicate the positive directions of the joint rotations. . . . .	10
2.2	The Y-shaped junction of the hindlimb where the CFLT connects to the GE tendon. The purple and red arrows indicate the GRF and the traction force of the CFL, respectively. . . . .	11
2.3	The crocodilian hindlimb robot. A: Schematic illustration of the crocodilian robot skeletomuscular system and the sensor placement in the lateral and anterior views. B: The vertical and horizontal sliders constrain the motion of the robot. The red and blue arrows indicate the direction of the sliding in the guide mechanism. A ballast connecting to some pulleys provides resistance for forward movement. The green arrow indicates the connection. . . . .	12
2.4	A sequence of movement of the hindlimb robot in response to changes in the MPA pressure. As the pressure increases, the hip and knee joints gradually extend, causing the hip joint to move forward. A video of this experiment (sv_1.mp4) is available in Supplemental material. . . . .	14
2.5	A: The relative angles of the hip, knee, and ankle joints according to time. B: The tension of the CFL, CFLT, and GE in response to changes in the internal pressure of the MPA. The experiment was conducted 10 times. The darker lines indicate the average of all tests, while lighter lines represent individual test results. The MPA pressure is indicated by the black line. . . . .	14
2.6	Movement of each joint in case of CFLT absence. A: Each joint angle. B: Tension acting CFLT and GE, and GRF. . . . .	15
2.7	A sequence of hindlimb motion during the continuous increase of pressure of MPA without CFLT. A video of this experiment (sv_2.mp4) is available in Supplemental material. . . . .	16

2.8	Moment arms of the hip joint for three cases, $r_{YJ}$ (yellow), $r_{LE}$ (purple), and $r_{FT}$ (green); and the direction of CFL traction force (arrows). A: The CFLT and GE are properly connected. B: The CFLT is disconnected. C: The GE is disconnected. . . . .	16
2.9	Movement of each joint when GE disconnected. A: Each joint angle. B: Tension acting CFL and CFLT, and GRF. . . . .	17
2.10	A sequence of hindlimb motion during the continuous increase of pressure of MPA without GE. A video of this experiment (sv_3.mp4) is available in Supplemental material. . . . .	17
2.11	Comparison of ankle joint angles (A) and tension profiles of CFL (B), CFLT (C), and GE (D) under two conditions: one with the additional passive element GI and one without. . . . .	18
2.12	A sequence of motion using the additional passive element GI to prevent passive plantarflexion of the ankle joint. A video of this experiment (sv_4.mp4) is available in Supplemental material. . . . .	19
3.1	The hindlimb robot reconstructing the passive musculotendinous system and an MPA as the CFL. . . . .	23
3.2	The effect of IT as the biarticular muscle for the hip and knee joints. . . . .	24
3.3	The effect of IT as the biarticular muscle for the hip and knee joints. The path of IT extends according to the hip extension, and the knee joint extends if the IT length keeps constant. . . . .	24
3.4	Hip joint angle and maximum knee joint flexion angle. . . . .	25
3.5	The minimum musculotendinous structure (red lines) of the hindlimb robot for maintaining the erect-limb posture. . . . .	25
3.6	Representative sequence of standing up and propulsive motion. The above row indicates the motion in the absence of the IT. Below is the case using IT. . . . .	26
3.7	Ground reaction force around the calcaneum. . . . .	26
4.1	Ostrich ( <i>Struthio camelus</i> ) at Fukuyama City Zoo (A) and right posterior postcranial skeleton in lateral view (B). . . . .	30
4.2	Physical model using 3D-printed right hindlimb of ostrich [65]. . . . .	32
4.3	Experimental setup (A) and sequential photographs of experiment for flexion (B) . . . . .	33
4.4	Dissected intertarsal joint of emu. In the medial view (A-D), the orange and blue lines represent the LCML and LCM, respectively. In the lateral view (E-H), the orange and blue lines represent the MFB and LCL, respectively. The black line indicates the outline of the distal end of the tibiotarsus. . . . .	34
4.5	Joint elastic force (A), displacements of LCML and LCM (B), and displacements of the MFB and LCL (C). . . . .	36
4.6	Extended (A and B) and flexed (C and D) postures of replicated intertarsal joint. . . . .	37
4.7	Designed Cam surface. The cam surface is represented by the dash-dot line (DrM) and the solid line (CrM). DrM' and CrM' represent the virtual extensions of the DrM and CrM. . . . .	38

---

4.8	Cam surface and intertarsal joint motion. The cam surface is represented by the dash-dot line (DrM) and the solid line (CrM). The transparent images of the medial side of the tibiotarsal distal end are superimposed as the origin of the LCML matches the center of the base circle of the DrM, showing the distal end functions as a cam, and the tarsometatarsus functions as the follower. . .	39
5.1	A reconstructed skeleton of <i>Protoceratops andrewsi</i> (cast) at the Museum of Dinosaur Research, Okayama University of Science. . . . .	42
5.2	A. The schematic diagram of the stance posture maintenance mechanism in crocodylian hindlimbs. B. summarized representations of generated forces. . .	44
5.3	Reconstructed musculoskeletal tendinous system to achieve a stance posture in <i>Protoceratops</i> . . . . .	45
5.4	A. Left lateral view of <i>Protoceratops</i> hindlimb region showing the positions of joint axes. B. Anterior view of the hindlimb region. C. Experimental system using the physical model of the <i>Protoceratops</i> hindlimb. . . . .	46
5.5	A sequence of movement of <i>Protoceratops</i> hindlimb robot in response to the change of the MPA pressure. . . . .	47
5.6	The relative angle of each joint according to the MPA pressure. The lighter solid lines represent the variations in the relative angles over ten trials, while the darker solid line represents their averages. . . . .	48
6.1	The process of constructing the universal terrestrial locomotion framework. . .	53





# List of Tables

4.1	Lengths of ligaments LCML and LCM . . . . .	35
4.2	Displacements of ligaments MFB and LCL . . . . .	35



# List of Abbreviations

## Method

**EPB** Extant Phylogenetic Bracket

## Mechanism

**EDM** Engage-Disengage Mechanism

## Anatomy

**CFL** CaudoFemoralis Longus

**CFLT** CaudoFemoralis Longus Tendon

**GE** Gastrocnemius Externus

**GI** Gastrocnemius Internus

**IT** IlioTibialis

**MFB** Muscle of Fibularis Brevis tendinous

**LCM** Ligament of Collaterale Mediale

**LCML** Ligament of Collaterale Mediale Longum

**LCL** Ligament of Collaterale Laterale



## Chapter 1

# General introduction

### 1.1 Introduction

Dinosaurs are one of the most successful groups of terrestrial vertebrates to have ever existed on Earth. They first appeared approximately 230 million years ago during the Triassic period and flourished for approximately 150 million years, with over 1,000 known species[1], [2]. Their morphological diversity ranged from bipedal to quadrupedal, and they varied in size from small species weighing only a few kilograms to giants weighing over 20 tons, such as *Apatosaurus louisae*, which had a length of 21 meters[3], [4]. In terms of the maximum size, some dinosaurs surpassed even the largest extant terrestrial vertebrates, such as the African elephant[5].

Dinosaurs also had diverse body shapes, including those with unique head structures and those with exceptionally long necks and tails. For quadrupedal species, it is known that the center of mass (the load supported by the front and rear limbs) also varied[6]. From a locomotion perspective, dinosaurs appeared to possess versatile adaptations to their body shapes, sizes, and walking modes. Furthermore, they likely evolved sophisticated locomotor designs that adapted to the terrestrial physical environment over their long evolutionary history. Suppose we could identify the design principle. In that case, it might be possible to engineer locomotion systems capable of agile movement on land, applicable to a wide range of body shapes and potentially advancing fields such as walking robotics. In addition, understanding the principles of dinosaur locomotion could lead to more accurate estimates of their motion capabilities, which cannot be directly observed. Furthermore, a better understanding of dinosaur locomotion mechanisms provides valuable insight into the common principle of terrestrial vertebrate locomotion, including extant and extinct animals.

In light of the above, the objective of this research is to elucidate the mechanisms by which dinosaurs achieved locomotion.

### 1.2 Previous method

The locomotion of terrestrial vertebrates is realized through a musculoskeletal system comprising multiple bones and soft tissues such as muscles and tendons. Therefore, in understanding the mechanism of locomotion, the morphology of the musculoskeletal system is crucial information, and in particular, the arrangement and bonding of soft tissues such as muscles and tendons are factors that determine the movement of the skeleton. However, the morphology of these soft tissues poses a significant challenge to the elucidation of dinosaur locomotion. This is because most of the elements that make up the musculoskeletal system are primarily preserved only in bones. Nevertheless, reconstructing the arrangement of the

musculoskeletal system is essential to understanding locomotion. To address this issue, researchers on dinosaur musculoskeletal reconstruction often use a method known as “extant phylogenetic bracketing (EPB),” which is used to estimate lost characters or behaviors of extinct species [7], [8]. EPB is based on the following idea. First, as a premise, animals within a given clade tend to share anatomical characteristics. Based on this, two or more extant taxa, the closest living relatives or descendants of the target extinct group, are selected to bracket the extinct group. Then, the lost information on the extinct species is estimated based on the shared information between the extinct and extant species. In the case of dinosaurs, it is common to construct a phylogenetic framework that includes crocodylians, the closest living relatives, and avians, the descendants of dinosaurs.

Suppose we use EPB to reconstruct the lost soft tissues of dinosaurs. For example, we focus on a muscle that exists in either of the species that bracket the extinct species and infer whether it existed in dinosaurs. First, the presence of the muscle in question and the associated osteological information are confirmed in the bracketing extant species. Osteological information includes the bone of origin or insertion of the muscle and traces of muscle attachment. Next, the correlation between this information in all bracketing extant species is confirmed. Finally, it is inferred whether dinosaurs had the muscle in question by checking whether the osteological information confirmed in extant species is present in the dinosaur skeleton.

This method has been used to estimate the detailed arrangement of forelimb muscles [9]–[12] and hindlimb muscles [13]–[16] in dinosaurs based on the musculoskeletal systems of crocodylians and avians, and a generally uniform muscle arrangement has been revealed in the skeletons of several dinosaur species. Furthermore, a kinetic model has been constructed using muscle systems estimated based on EPB and estimates of the range of motion of joints and the muscle force that each muscle can exert, and this has been successfully used to assess the locomotor abilities of dinosaurs [16], [17]. On the other hand, studies that have assessed these dinosaurs’ locomotor abilities have produced unnatural results. For example, Bishop et al. conducted a study to assess the extent to which the hindlimb musculoskeletal dynamic model of the small bipedal theropod *Coelophysis* could support its own weight in stance [16]. The results showed that in the standing posture generally expected of dinosaurs (a slightly crouched posture with hip and knee joints flexed, similar to that of avians), the body weight could not be supported under static conditions for several predicted muscle force patterns, or could only be supported by less than twice the body weight. It was therefore suggested that *Coelophysis* adopted an upright, human-like posture, in which case it could support a load of about three times its own weight. Sellers et al. also constructed a simplified musculoskeletal kinetic model of the limb musculature of the large theropod (*Arginosaurus huinculensis*) and estimated gait by exploring the muscle activation pattern that maximizes the distance traveled within a given metabolic cost and time based on genetic algorithms [18]. In this report, it was reported that the estimated muscle forces did not allow for a gait pattern that fully utilized the joint range of motion estimated from the skeleton. Bishop et al. and Sellers et al. attributed these problems to a failure to consider the passive function of the musculoskeletal system.

### 1.3 Problems with previous method

Many studies have reconstructed the morphology of the dinosaur musculoskeletal system based on the Extant phylogenetic bracketing proposed by Witmer. However, the results of Bishop et al. and Seller et al. mentioned that there are problems with the reconstructing locomotion. The main reason for this is that Bishop et al. and Seller et al. suggested that there may be a lack of understanding of the passive function of the musculoskeletal system. So why was the passive function not considered in the reconstruction of locomotion using the musculoskeletal system based on EPB?

There are two main reasons for this problem. The first is the problem of the evidence used to infer EPB. The inference of the presence of muscles based on EPB is based solely on morphological information, such as the presence of the muscle in question in the bracketing species and the osteological information indicating the origin and insertion of the muscle in question in the bracketing species and dinosaurs. Therefore, it does not include any mechanical evidence in the inference. Therefore, even if the muscle in question was present in dinosaurs and played an important role in locomotion, it may not have been considered if it was not present in either of the bracketing species or did not leave traces on the bone. In particular, soft tissues such as tendons and membranes that do not function as actuators are not considered in the reconstruction of locomotion. In addition, in EPB, it is difficult to reconstruct the characteristics that do not leave traces on the bone, such as bonding between muscles or tendons. However, such connections between muscles and tendons bring about mechanical interactions, and if these are not sufficiently considered, the magnitude and direction of the force vectors transmitted to the skeleton may be significantly different from those assumed when the muscles and tendons have a single origin and insertion. These problems are likely due to the lack of accuracy in the morphology of the muscle system and the lack of a foothold in considering passive functions.

The second reason is that the passive functions of the muscle system in dinosaur locomotion have not been well understood. Previous studies [16]–[18] have focused only on the active function of the muscle system and have not explicitly considered the passive behavior of the muscles. On the other hand, Bishop et al. suggested that in order to maintain the posture of the metatarsophalangeal joint, a certain amount of torque was applied by a virtual actuator in addition to the torque exerted by the muscles. This torque is thought to be provided by the passive stretching of tendons and ligaments to maintain joint posture and by collisions between bones. Sellers et al. also showed that plausible locomotion could be easily achieved by imposing restrictions on the range of motion of the joints that do not originate from the active action of the muscles. This restriction of the range of motion is thought to be due to a passive elastic structure of the muscle system, which is still unknown in dinosaurs. From these considerations, it is possible that muscles not only actively contract but also exert an elastic force by passively extending to their natural length and that they act as a limiter to limit the range of motion of the joint by preventing further extension.

In addition, the function of passive elements that do not have active functions, such as tendons, is known to play an essential role in the mechanism of locomotion in extant terrestrial vertebrates. For example, ungulates such as horses have multiple tendons that span multiple joints from the distal leg to the proximal leg, and this passive muscle system produces the back-and-forth movement of the hindlimb by coordinating the movement of the hip joint and the movement of multiple joints of the distal leg, and by supporting the weight



by mechanically constraining the joints by the ground reaction force when the limb contacts the ground [19]–[21]. This function of coordinating joint movements by passive elements of the muscular system is found not only in mammals but also in the limbs of avians. The musculoskeletal system of the limbs of birds also has a mechanism that passively flexes the knee, ankle, and metatarsophalangeal joints in conjunction with the flexion movement of the hip joint, as does the horse [22], [23]. In this way, passive elements such as tendons create a mechanism for restricting joint movement and coordinating multiple joints by connecting to bones and muscles. In addition, it is known that the musculoskeletal system of running birds such as emus has a mechanism that passively extends and flexes the intertarsal joint by the shape of the articular surface of the bone and the elastic force of the muscle system [24].

These findings suggest that passive functions of the musculoskeletal system, such as restriction of joint range of motion and coordination, are deeply rooted in terrestrial vertebrate locomotion. Furthermore, the existence of these functions suggests that not all joint control for locomotion is performed by the active action of muscles but that the morphology of the musculoskeletal system autonomously controls some joint movements. In other words, locomotion in terrestrial vertebrates is achieved by a combination of the active function of the musculoskeletal system and the passive function of the musculoskeletal system. From the above, the locomotion mechanism of dinosaurs should be considered with the passive function of the musculoskeletal system.

## 1.4 Scope of this study

So, how can we think about the locomotion mechanism of dinosaurs, in which the active and passive functions of the musculoskeletal system are harmonized? If we infer the musculoskeletal system of dinosaurs based on EPB, as in previous studies [16], [17], the existence of all soft tissues is determined by the attention of the EPB user and the correlation within the bracketing relationship. As a result, the morphology of the musculoskeletal system reconstructed based on EPB has no meaning other than phylogenetic correlation. Furthermore, it is not clear what role each component of the musculoskeletal system plays in achieving terrestrial locomotion. In this case, when attempting to reconstruct locomotion based on this musculoskeletal system, it is necessary to rely on some index-based optimization of muscle firing timing or information that does not originate from the dinosaur musculoskeletal system, such as the gait trajectories of other organisms or electromyography. However, locomotion is originally achieved by the mechanical function that emerges from the interaction of each element in the morphology of the musculoskeletal system. In other words, understanding the relationship between the morphology and mechanical function of the musculoskeletal system that realizes locomotion (mechanical functional morphology) leads to the understanding of the natural locomotion mechanism of dinosaurs.

Therefore, in this study, we aim to construct the locomotion of dinosaurs based on the mechanical functional morphology of the musculoskeletal system. In this study, as in EPB, we also use information on crocodylians and avians; they are extant sisters of dinosaurs. However, instead of applying the morphological correlative of extant sisters to the dinosaur skeleton, we take the approach of applying the mechanical functional morphology of the musculoskeletal system for locomotion to the dinosaur skeleton. This approach allows us to construct a dinosaur musculoskeletal system in which the morphology of the system and the

mechanical functions necessary for locomotion are linked. Of course, the mechanism itself is that of crocodylians and avians, but since their skeletons are similar to those of dinosaurs, they are likely to share the locomotion mechanism.

## 1.5 Approach

We propose a method to elucidate the locomotion mechanism of dinosaurs in which the active and passive functions of the musculoskeletal system are harmonized. As a first step, it is necessary to understand the walking mechanism of crocodylians and avians based on the mechanical functional morphology of the musculoskeletal system, which forms the basis of the dinosaur musculoskeletal system. There are several studies on the locomotion of crocodylians and avians based on detailed musculoskeletal dynamic models [25], [26]. However, these studies do not consider the effect of the passive elongation of the muscles on joint motion. In addition, the attachment of muscles and tendons to multiple bones or other muscles is not considered. However, anatomical descriptions of the musculoskeletal system of crocodylians and avians show that many muscles have multiple attachments to other tissues, not just one origin and insertion [22], [27]–[30]. Moreover, the passive behavior of the muscular system may achieve coordinated joint motion, such as the reciprocal apparatus of horses [19]–[21]. From these facts, it is necessary to examine how the forces generated by muscle traction and interaction with the environment are transmitted through the arrangement and connection of the muscle system to move the joints. Therefore, in this study, in order to understand the locomotion mechanism of crocodylians and avians in more detail, we propose a method to hypothesize the locomotion mechanism realized by the morphology of the musculoskeletal system based on anatomy and physically reproduce it with a robot to evaluate its feasibility (Fig.1).

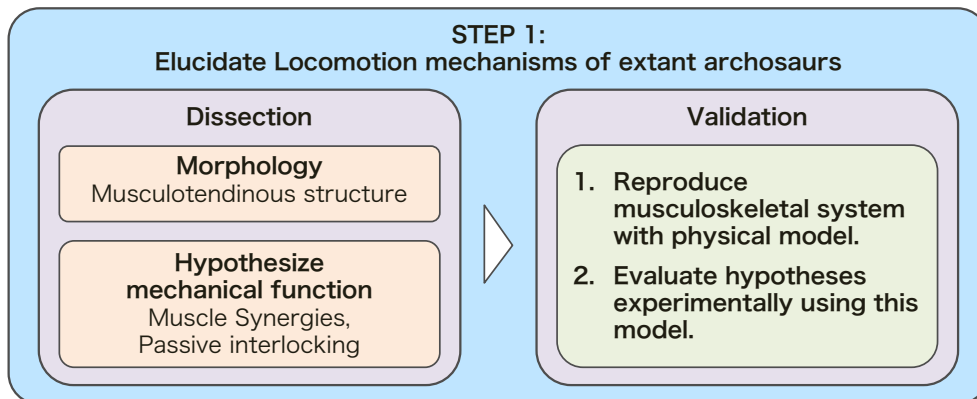


FIGURE 1.1: The methods for understanding locomotion mechanisms based on the morphology and mechanical function of the musculoskeletal system of archosaurs.

In biological dissection, the function of the muscles around the limbs of crocodylians and avians is predicted in advance based on the functional anatomical descriptions of the muscles [22], [27]–[30] and the electromyography of the muscles during gait [31], [32], and the arrangement and bonding of the muscles are observed in detail based on this prediction. In addition, each muscle or tendon is manually pulled, or a force equivalent to the ground reaction force is applied to the foot to examine the joint motion and the mechanical effects on

other muscles and tendons. Based on these experimental verifications, hypotheses are made about each muscle and tendon's active and passive actions and the locomotion mechanism realized by their coordinated action.

Next, the bones involved in the locomotion of crocodylians and avians are modeled in 3D by CT scanning or photogrammetry, and the bones are reconstructed with joints to create a movable skeletal physical model. This skeletal physical model plays the role of a platform for verifying the function of the muscle system. On this platform, the muscle system involved in the mechanism hypothesized in the biological dissection task is constructed. The active action of the muscles is reproduced by a linear actuator (a McKibben-type artificial muscle or a motorized pulley), and wires reproduce the muscles and tendons that do not use active action. The musculoskeletal system of the limb is constructed in a physical model following the above procedure. Finally, this physical model is used to verify the feasibility of the hypotheses about the mechanical function of each muscle or muscular system and to elucidate the locomotion mechanism based on the mechanical functional morphology of the musculoskeletal system. This series of processes is referred to as STEP1. However, since the musculoskeletal system of terrestrial vertebrates is very complex, this STEP1 should not attempt to reveal the complete locomotion mechanism at once. Locomotion is subdivided into the stance phase of standing and the extension movement of the joints, the swing phase of the flexion movement of the joints, and, in some cases, the function of a muscle, and the basic mechanisms of locomotion are revealed one by one.

After revealing the fundamental mechanism of locomotion that can be realized by crocodylians and avians based on STEP1, the next step is to apply it to the skeleton of dinosaurs and verify whether the mechanism of closely related species can also be realized in dinosaurs, as STEP2 (Fig.2).

First, a physical model of the dinosaur skeleton is constructed as a platform for verifying the function of the muscle system in the same way as STEP1. In this model, the muscle system necessary for the mechanism of closely related species is constructed. At this time, the origin and insertion of each muscle and tendon in the bone are determined based on the reconstruction of the dinosaur muscular system based on EPB [9]–[16]. Those not attached to the bone follow the arrangement of the extant sister. The physical model of the dinosaur musculoskeletal system is constructed following the above procedure. In this model, the active behavior of the muscles of the extant sister, which is the basis revealed in STEP1, is applied to the dinosaur physical model to verify whether locomotion can be realized.

Based on the above two steps, the fundamental mechanism of locomotion based on the morphology and function of dinosaurs is gradually revealed.

## 1.6 Contents of this dissertation

Again, this study aims to elucidate the locomotion mechanism of dinosaurs, in which the active and passive functions of the musculoskeletal system are well combined. To this end, based on the method proposed in the previous section, we first reveal the fundamental mechanism of locomotion of crocodiles and avians, which are closely related to dinosaurs. Then, we apply the fundamental mechanism revealed by the extant sisters of dinosaurs to the dinosaur skeleton to construct the musculoskeletal system and verify whether it can achieve the same movement as the extant sisters. Ultimately, this study aims to construct the locomotion mechanisms of dinosaurs by integrating the fundamental mechanisms based on

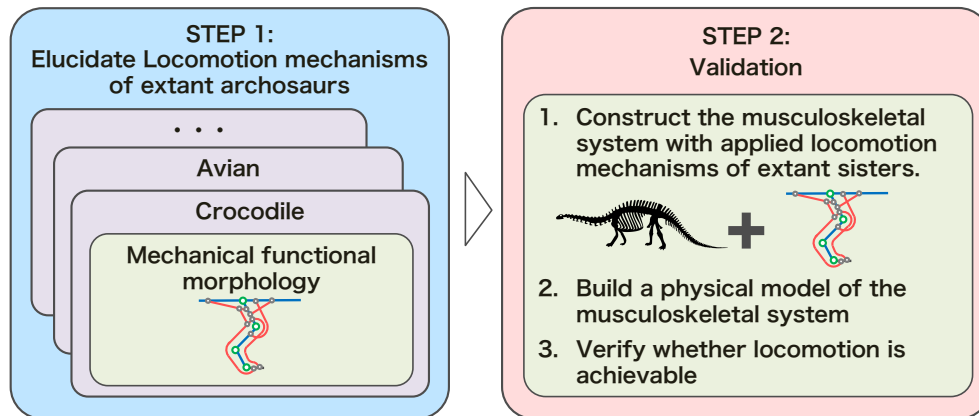


FIGURE 1.2: A method for estimating the locomotion of dinosaurs based on the locomotion mechanism of closely related species of dinosaurs.

crocodiles and avians. In this dissertation, we describe three attempts to understand the fundamental mechanism of locomotion of crocodiles and avians, which corresponds to STEP1 of the proposed method, and an attempt to apply the fundamental mechanism revealed from crocodiles to dinosaurs, which corresponds to STEP2. This dissertation consists of six chapters, including this chapter. The following is an outline of the contents:

Chapter 2, which follows this chapter, describes an attempt to understand the fundamental mechanism of locomotion of crocodiles, which corresponds to STEP1 of the proposed method. Here, focus on the mechanism that enables the crocodile's hind limbs to achieve a stance posture in locomotion on land, as dinosaurs do. First, we dissect the crocodile's hind limbs and hypothesize the mechanism of the hind limbs' stance and propulsion based on the passive coordination of the muscular system and the interaction with the environment. Next, we reproduce the musculoskeletal system of the crocodile's hind limbs with a physical model to verify the feasibility of the hypothesis.

Chapter 3 describes the function of a passive muscle that assists the stance and propulsion mechanism of the crocodile's hind limbs described in Chapter 2. First, attaching the muscle to the physical model of the crocodile's hind limb skeleton, which is a platform for verifying the muscular system function described in Chapter 2, experimentally reveals that the muscles passively coordinate the movement of the two joints. Furthermore, by integrating this function with the stance and propulsion mechanism, describe the function of increasing the frictional force around the calcaneus during the stance phase.

Chapter 4, as an attempt corresponding to STEP1 of the proposed method in avians, describes in detail the mechanism of the passive extension or flexion of the joint known as the Engage-Disengage Mechanism (EDM) observed in the intertarsal joint of running avians by biological dissection and reproduction with a physical model. Furthermore, describes that the shape of the distal tibiotarsal joint surface can be quantitatively designed using the arrangement and displacement of the ligaments that create the EDM.

Chapter 5 describes an attempt corresponding to STEP2 of the proposed method, which applies the fundamental locomotion mechanism of closely related species of dinosaurs to the dinosaur skeleton. Here, try that the stance mechanism of the crocodile's hind limbs, described in Chapters 2 and 3, is applied to the dinosaur skeleton. First, construct a physical model of the dinosaur's hind limb skeleton, which is a platform for verifying the function of the muscular system, and apply the muscular system that creates the stance mechanism

of the crocodile's hind limbs to it. Next, using this model, we verify whether the dinosaur's hind limb skeleton can achieve a stance posture based on the passive coordination of the muscular system and the interaction with the environment, as in the crocodile's hind limbs.

In the last chapter, Chapter 6 summarizes the attempts to elucidate the locomotion mechanism of dinosaurs, in which the active and passive functions of the musculoskeletal system are well combined, based on the proposed method. Finally, the future prospects of this study will be discussed, and this dissertation will be concluded.

## Chapter 2

# Elucidation of the fundamental locomotion mechanism in Crocodylians I

### Note

This chapter is the author's version of the following article:

**Kazuki Ito**, Tetusya Kinugasa, Kentaro Chiba, Yu Okuda, Ryuji Takasaki, Sayaka Hida, Tsukasa Okoshi, Ryota Hayashi, Koji Yoshida, and Koichi Osuka, “The robotic approach to the passive interlocking mechanism in the hindlimb musculoskeletal system of *Crocodylus porosus*” , *Advanced Robotics*, Vol. 37, No. 18, pp. 1187-1197, DOI: 10.1080/01691864.2023.2256375, 2023.

### 2.1 Introduction

The musculoskeletal systems of animals have tremendous degrees of freedom, and therefore the mere imitations of the systems in robots were considered not feasible. At the same time, recent integrations between animal anatomy and robotics reveal that animals have mechanisms that significantly reduce the degrees of freedom and achieve specific functions. The horse appendicular skeletons, for example, have a reciprocal apparatus that autonomously generates gaits through passively functioning muscular systems [19], [21] and a stay apparatus that supports their own weight during the stance phase through the interaction with the ground [19], [21]. Incorporating the passive interlocking system into robotics successfully achieved natural and efficient robot locomotion [33], [34]. Passive interlocking mechanisms have also been reported in birds for the autonomous generation of hindlimb movements and self-weight support [22], [24], and it is incorporated in robots to produce smooth and efficient locomotion [34], [35].

Non-avian reptiles, hereafter referred to as reptiles for the sake of simplicity, are another major terrestrial vertebrates that have been suggested to have passive interlocking mechanisms, although it has not been addressed in robotic studies. In lizards and crocodylians, the caudifemoralis longus muscle (CFL) and its branched tendon (CFLT) interlock to achieve femoral retraction and knee fixation [36], [37]. Additionally, crocodylians differ from the other known reptile in that their CFLT is further connected to the gastrocnemius externus muscle (GE) [29], [38], [39]. It can thus be hypothesized that the unique crocodylian passive interlocking mechanisms composed of CFL, CFLT, and GE may be related to their more

erected limb posture than in other reptiles, which is suggested to improve locomotion speed and effectiveness in reptiles and mammals [40], [41]. In this study, we first describe the musculoskeletal structures of crocodilian hindlimbs with special regard to the putative passive interlocking mechanism. We then incorporate the mechanism into a robot to test the hypothesis that the contribution of the passive interlocking mechanism achieves the crocodilian semi-erect postures.

## 2.2 Dissection of *Crocodylus porosus* and minimum configuration for semi-erect limb posture

A pelvic region with hindlimbs of a captive *Crocodylus porosus* was dissected (Figs. 2.1 and 2.2). The specimen was the freshly frozen specimen of a naturally died corpus of an adult female of unknown age, provided by the Oniyama Jigoku in Beppu City, Oita, Japan. The crocodile had a mass of 106 kg and a length of 2.8 m at its death. The specimen was placed in a prone position (Fig. 2.1A), allowing ground reaction forces (GRFs) to be applied or removed to the sole of the foot to identify the muscles that function during the semi-erect limb posture. The CFL originates from the third to fifteenth caudal vertebrae ( $P_0$ ) and inserts the fourth trochanter of the femur ( $P_1$ ), as shown in Fig. 2.1B. The CFLT branches off from the CFL at  $P_2$  slightly distal to the insertion at  $P_1$ , and joins the GE at  $P_3$ , located near the lateral femoral epicondyle ( $P_4$ ), which is the origin of the GE. The CFLT and GE together form a Y-shaped junction at  $P_3$ . The GE descends along the tibia and inserts onto the calcaneum and the ventrodistal aspect of the metatarsus ( $P_5$ ).

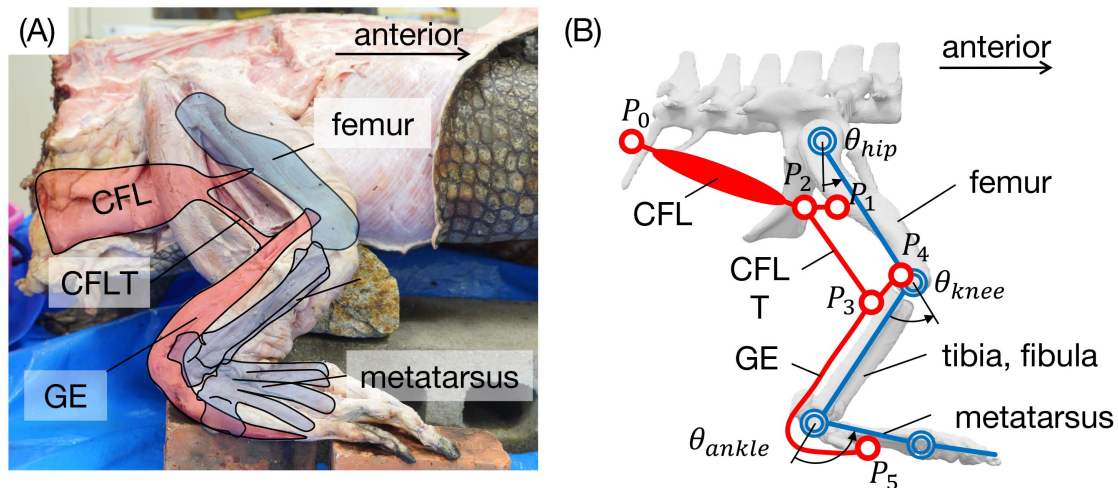


FIGURE 2.1: A: The hindlimb and the trunk of the dissected crocodile (excluding the head, tail, and skin) in lateral view, with the schematics of the positions of the major bones (femur, tibia, fibula, and metatarsals) and the muscles (CFL and GE) and the tendon (CFLT) of interest. The photo is inverted for ease of comparison with the right hindlimb robot described later in this paper. B: A schematic representation of the crocodilian musculoskeletal system. The arrows indicate the positive directions of the joint rotations.

The CFL is the largest muscle near the hindlimb and is primarily responsible for generating the propulsive force of the hindlimb [29], [38], [39]. The CFL contraction pulls both  $P_1$  and  $P_4$  simultaneously. The biarticular muscle GE flexes the knee joint and plantarflexes



the ankle joint upon contraction [38], or even passively by pulling  $P_4$  distally in response to the GRF acting on the sole (Fig. 2.2), under the assumption that GE is a passive element of constant length. The connection between the CFL and GE through the CFLT highlights the importance of considering the potential novel functions that may arise from the coordination of these two muscles. When both GRF and CFL contraction forces are applied, the tensions exerted on the CFLT and GE at the Y-shaped junction  $P_3$  balance each other, thereby maintaining the knee joint in an extended position, corresponding to the semi-erect limb posture shown in Fig. 2.2. Furthermore, the additional contraction of the CFL generates a force that retracts the hindlimb while maintaining the semi-erect limb posture.

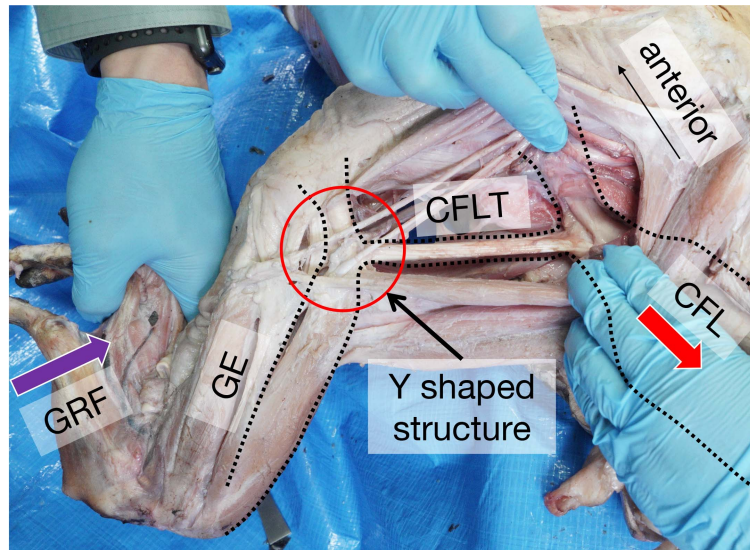


FIGURE 2.2: The Y-shaped junction of the hindlimb where the CFLT connects to the GE tendon. The purple and red arrows indicate the GRF and the traction force of the CFL, respectively.

We only focus on the passive function of the GE in this study and regard the GE remaining at a constant length. Then, it can be hypothesized that:

1. The crocodilian hindlimb musculoskeletal system has a passive interlocking mechanism activated by the CFL contraction and the interaction with the ground.
2. The minimum configuration of this passive interlocking mechanism includes the CFL, the passive GE, and the CFLT.

## 2.3 Crocodilian hindlimb robot

We developed a robot that mimics the crocodilian hindlimb musculoskeletal system (Fig. 2.3). The robot was designed to replicate the passive interlocking mechanism observed in the hindlimb based on the dissection of the hindlimb musculature of the *Crocodylus porosus*. The robot skeletal elements were fabricated using 3D skeletal data from a CT scan of the dissected specimen, printed using tough resin (RESIONE, M68) by the stereolithography 3D printer, Photon Mono X (ANYCUBIC). The printed elements were assembled based on the observed layout of the sacrum, ilium, femur, tibia, fibula, metatarsus, and phalanges. To simplify the design, we assumed that the limbs move in a parasagittal plane during locomoting with a semi-erect limb posture, despite the complexity of the hip, knee, and ankle



joints with multiple degrees of rotational freedom. Consequently, each joint was designed to have a one-degree-of-freedom rotation about the pitch axis, and potentiometers (ALPS ALPINE, RDC501052A) were embedded in the joints (Fig. 2.3A) to measure joint angles (Fig. 2.1A). We also attached a membrane force sensor (LEANSTAR, MD30-60) ventral to the calcaneum to measure the GRF.

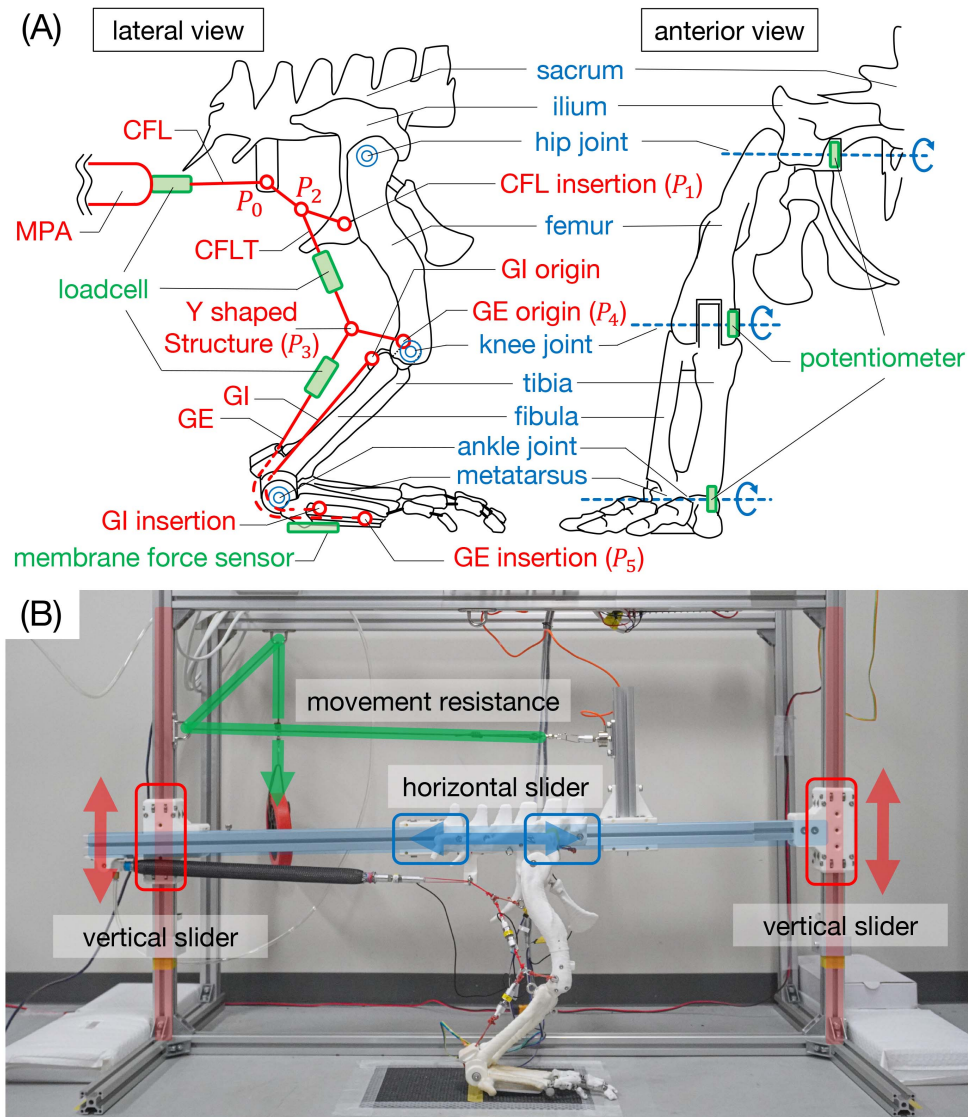


FIGURE 2.3: The crocodilian hindlimb robot. A: Schematic illustration of the crocodilian robot skeletomuscular system and the sensor placement in the lateral and anterior views. B: The vertical and horizontal sliders constrain the motion of the robot. The red and blue arrows indicate the direction of the sliding in the guide mechanism. A ballast connecting to some pulleys provides resistance for forward movement. The green arrow indicates the connection.

The robot replicates the origin and insertion of each muscle and tendon identified from the dissection (Fig. 2.1A) using a high loading capacity (the maximum strength of 54.5 kgf) and bare elastic polyethylene braid (PE line). The tendon strength of birds, which are the closest relative of the crocodilians, typically ranges from 54 to 117 MPa [42]. Since the tendon diameter of the crocodilian CFL inserted onto the fourth trochanter was approximately 6

mm, its maximum tension is expected to range from 150 - 340 kgf. To simulate the tension, bundles of 2 to 4 PE lines are used for the robot, depending on the ease of assembly.

The CFL muscle originates from the posterior edge of the frame and inserts onto the fourth trochanter of the femur. A ring attached to a point  $P_0$  around the third caudal vertebra is used to adjust the direction of the CFL. To simulate the contraction of the CFL, we used a McKibben-type pneumatic actuator (MPA) with a natural length of 205 mm and a contraction capacity of approximately 50 mm under internal pressure of 500 kPa. The GE originates from the lateral femoral epicondyle ( $P_4$ ) and inserts at the ventrodiscal aspect of the metatarsus ( $P_5$ ). The CFLT branches off from CFL at  $P_2$  located posterior to the CFL insertion ( $P_1$ ) and ventrally connects to the Y-shaped junction ( $P_3$ ) located posterior to the origin of the GE ( $P_4$ ). The GE in the robot does not insert onto the calcaneum, unlike that of actual crocodylians, for the sake of simplicity. The CFL, CFLT, and GE tension was measured using load cells (DAYSENSOR, DYM106). To prevent the robot from falling laterally, a guide mechanism (Fig. 2.3B) was used to constrain the robot in the sagittal plane. A ballast weighing 1.2 kg was lifted vertically through pulleys to provide resistance and pull the sacrum posteriorly upon the horizontal movement of the robot. The moving unit of the robot, including the guide mechanism, has a total mass of 4.63 kg.

## 2.4 Results

### 2.4.1 Semi-erect limb posture provided by the passive interlocking mechanism

We conducted experiments with the crocodylian hindlimb robot to evaluate the effectiveness of its interlocking mechanism in achieving a semi-erect limb posture. The initial position of the hindlimb was set up with the hip joint positioned posterior to the ankle joint, as shown in the photo at 5 seconds of Fig. 2.4. We increased the internal pressure of the MPA to 500kPa at a rate of 25 kPa/s and observed how the hindlimb posture changed from its initial position. As depicted in Fig. 4, the robot underwent a series of postural changes from the initial posture to a semi-erect limb posture, until the hindlimb retracted. We divided the experimental results shown in Fig. 5 into four sections for detailed analysis: Phase I (0-4 s), Phase II (4-12 s), Phase III (12-18 s), and Phase IV (18 s onwards).

Phase I: The CFL remained flaccid, and there was no significant change in the posture of each joint.

Phase II: (Tension generation by CFL): The CFL started to put traction force from 4 seconds. The hip joint starts to extend gradually at around 8 seconds. The CFL and CFLT exhibit nearly equal tension during this section. The CFLT, the Y-shaped junction  $P_3$ , and the GE origin  $P_4$  were at nearly the same level, while the tendon from  $P_1$  to  $P_2$  is flaccid. Thus, it is presumed that most of the traction force generated by the CFL acted on  $P_4$  through the CFLT. Due to the flexion of the hip and knee joints in the initial posture, the tendon between  $P_1$  and  $P_2$  is slack, causing the traction force of the CFL to be focused on  $P_4$ .

Phase III (Hip and knee extension): From 12 seconds, the hindlimb maintains a semi-erect limb posture with hip and knee joints extended while being gradually retracted. The CFL and the CFLT tensions reached their peak at the beginning of this phase. Subsequently, the tension in the CFL and CFLT decreased, and the difference between them

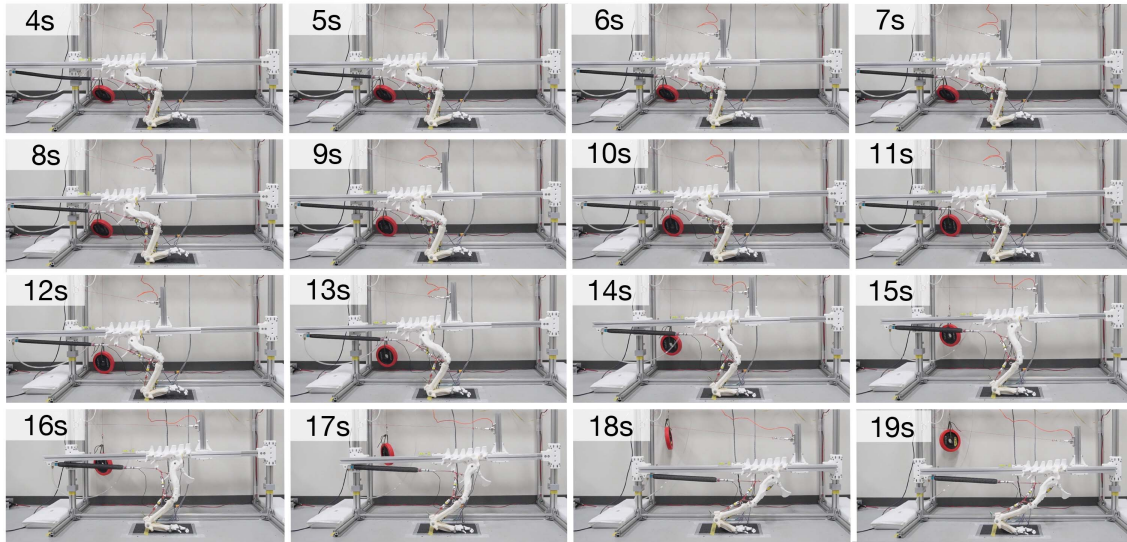


FIGURE 2.4: A sequence of movement of the hindlimb robot in response to changes in the MPA pressure. As the pressure increases, the hip and knee joints gradually extend, causing the hip joint to move forward. A video of this experiment (sv\_1.mp4) is available in Supplemental material.

increased, as shown in Fig. 2.5B. It is therefore considered that the traction force of the CFL primarily acted on the fourth trochanter  $P_2$ , generating propulsive force. The GRF and GE tensions reached their peak soon after, at around 13 seconds, corresponding to the timing when the hip joint was positioned above the ankle joint. The knee was locked or prevented from hyperextension by balancing the flexing torque caused by the GRF and the extending torque caused by the CFL contraction acting through the Y-shaped junction, while the hip joint extended further during propulsion.

Phase IV: The hip and knee joints stopped extending.

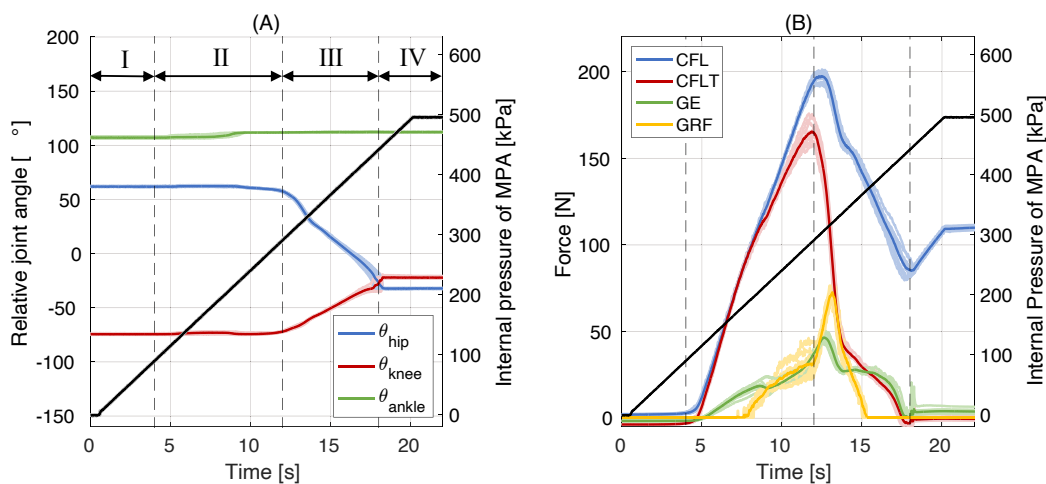


FIGURE 2.5: A: The relative angles of the hip, knee, and ankle joints according to time. B: The tension of the CFL, CFLT, and GE in response to changes in the internal pressure of the MPA. The experiment was conducted 10 times. The darker lines indicate the average of all tests, while lighter lines represent individual test results. The MPA pressure is indicated by the black line.

The results demonstrated that the minimal muscular system comprising CFL, CFLT, and GE passively interlocks through the CFL contraction to achieve coordination of the hip, knee, and ankle joints. This system allows the hindlimb to retract while maintaining a semi-erect limb posture, supporting its own weight, and generating a propulsive movement of the hindlimb. This suggests that this system may play a crucial role in achieving locomotion during the stance phase of the high walk [43], a gait in which crocodylians do not contact their bellies to the ground.

## 2.4.2 Function of coudifemoralis longus muscle tendon and gastrocnemius

To clarify the role of CFLT in connecting the GE and CFL, we performed additional experiments (Figs. 2.6 and 2.7) in which the CFL was contracted with the CFLT disconnected. Under this condition, no tension was generated on the GE because the force generated by the CFL is not conducted through the CFLT. Upon contraction of the MPA, the knee joint rapidly extended from 10.5 s and resulted in hyperextension at 11.2 s. When the CFLT is properly connected, the GE pulls the Y-shaped junction  $P_3$  downwards, creating a force vector  $f_{P_4P_3}$  and a moment arm of  $r_{YJ}$  around the hip joint (Fig. 2.8A). However, when the CFLT is disconnected, the force on the Y-shaped junction is lost; thus, all the traction force of the CFL acts on  $P_1$  ( $f_{P_1P_0}$ ), resulting in a shorter moment arm  $r_{FT}$  around the hip joint compared to  $r_{YJ}$  (Fig. 2.8B).

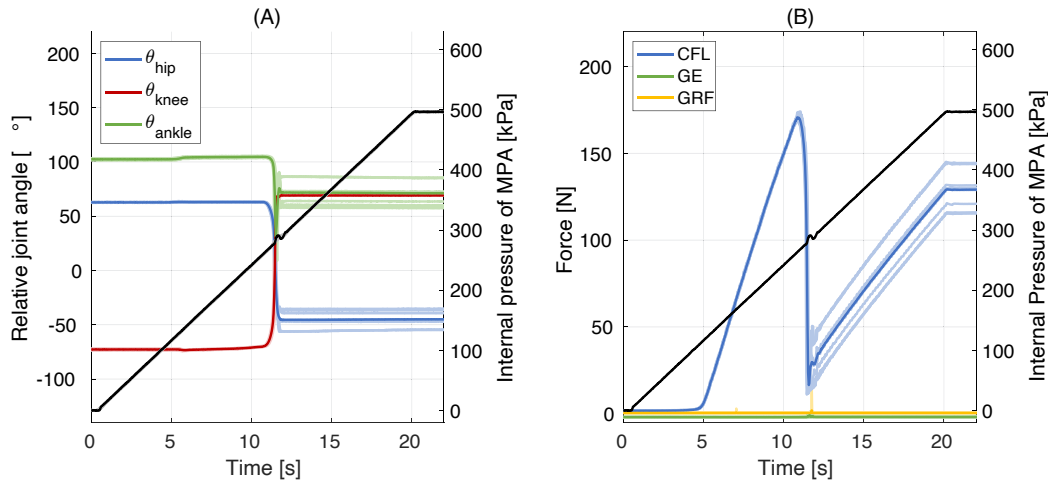


FIGURE 2.6: Movement of each joint in case of CFLT absence. A: Each joint angle. B: Tension acting CFLT and GE, and GRF.

We further conducted a similar experiment with the GE disconnected while the CFLT inserting directly into the lateral femoral epicondyle ( $P_4$ ). At 10.5 seconds, we observed knee joint hyperextension with the traction force of the CFL acting on the distal end of the femur  $P_4$  through the CFLT (Figs. 2.9 and 2.10). In the absence of the GE, the CFLT generates tension  $f_{P_4P_0}$  from  $P_4$  to  $P_0$  (as seen in Fig. 2.8C) due to the nearly aligned position of  $P_0$ ,  $P_1$ ,  $P_2$ , and  $P_4$ . The tension  $f_{P_4P_0}$  is almost parallel to the CFL traction force  $f_{P_1P_0}$  on  $P_1$  (as in the previous test), and the moment arm  $r_{LE}$  is almost equal to  $r_{FT}$ . The additional experiments lead to the conclusion that the Y-shaped junction ( $P_3$ ) formed by CFLT-GE coupling changes the direction of CFLT tension and extends the moment arm  $r_{YJ}$ , facilitating hip extension. Moreover, the Y-shaped junction also prevents hyperextension of the knee joint through the GE passively generating tension opposing the GRF that flexes the knee joint. The inhibitory



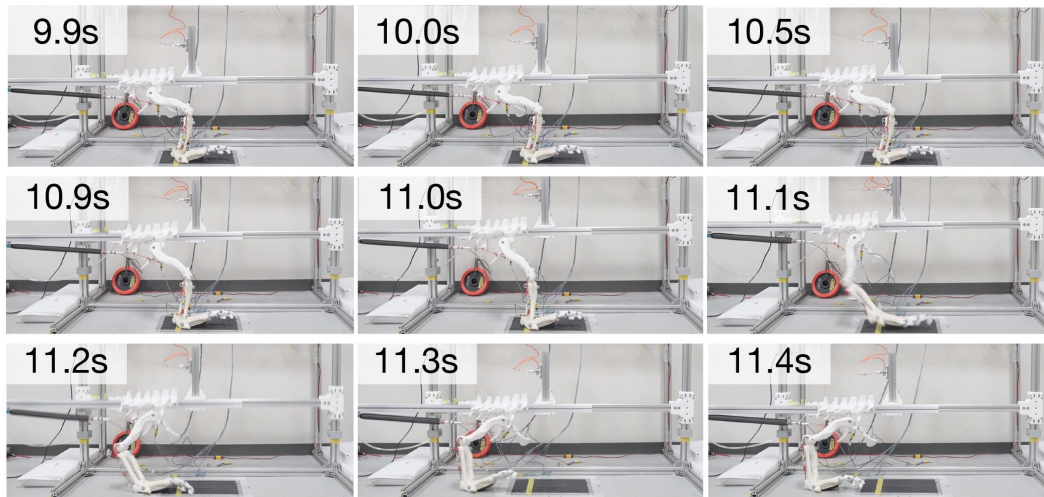


FIGURE 2.7: A sequence of hindlimb motion during the continuous increase of pressure of MPA without CFLT. A video of this experiment (sv\_2.mp4) is available in Supplemental material.

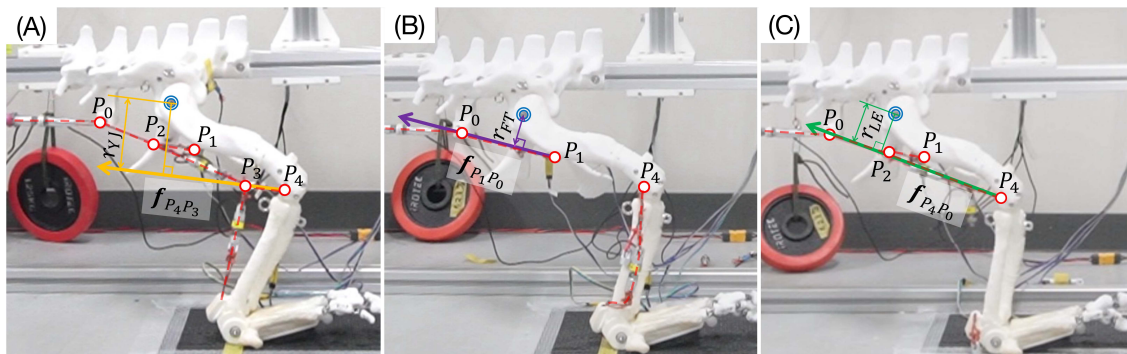


FIGURE 2.8: Moment arms of the hip joint for three cases,  $r_{YJ}$  (yellow),  $r_{LE}$  (purple), and  $r_{FT}$  (green); and the direction of CFL traction force (arrows). A: The CFLT and GE are properly connected. B: The CFLT is disconnected. C: The GE is disconnected.

effect against hyperextension was lost when the GE was disconnected. Consequently, our findings indicate the Y-shaped junction prevents excessive knee extension and lengthens the moment arm for femoral retraction.

### 2.4.3 An additional passive element

The robot constructed above successfully supports the weight with the interlocking mechanism of CFL, CFLT, and GE. Contrarily, the interlocking mechanism insufficiently maintained the natural ankle posture during the experiment; the ankle joint dorsiflexed maximally and the anterior edges of the tibial distal end and the metatarsal proximal end contacted (after 9 s in Fig. 2.11A, where the blue line reached the plateau). Before the experiment, we expected that GE functioned to avoid bone-to-bone contact by generating a torque that plantarflexes the ankle joint, but the experiment indicates that the tension generated by the passive GE is insufficient to maintain the ankle posture against the dorsiflexion torque caused by the GRF. The occurrence of the unnatural ankle joint suggests that the robot requires either active contraction of the GE or additional plantarflexor muscles for the robot

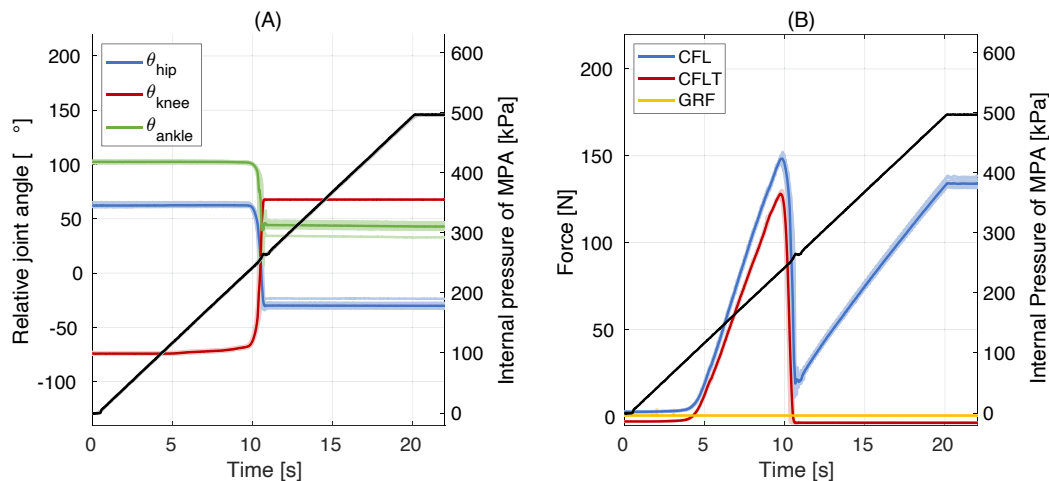


FIGURE 2.9: Movement of each joint when GE disconnected. A: Each joint angle. B: Tension acting CFL and CFLT, and GRF.

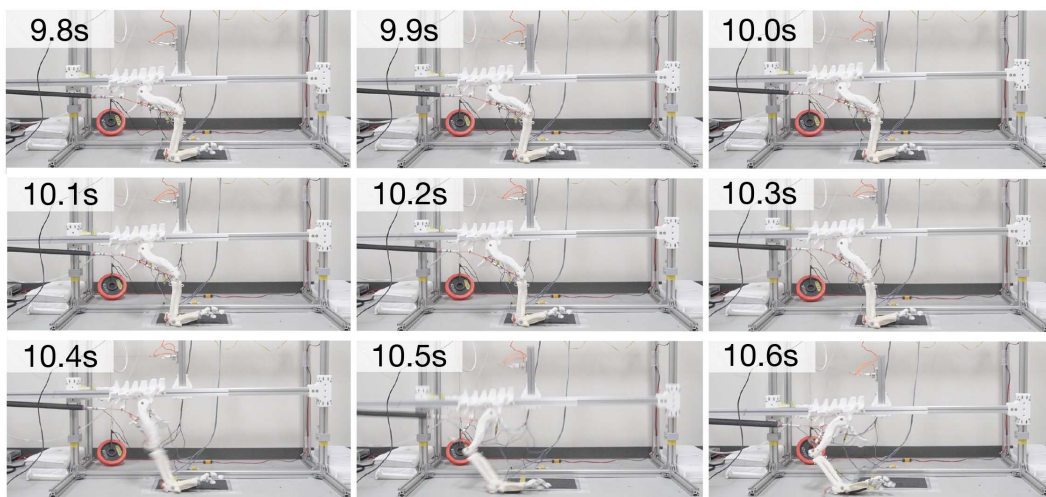


FIGURE 2.10: A sequence of hindlimb motion during the continuous increase of pressure of MPA without GE. A video of this experiment (sv\_3.mp4) is available in Supplemental material.

to achieve the natural ankle posture. To prevent the unnatural ankle posture, we introduce the gastrocnemius internus (GI) muscle, another ankle plantarflexor [29], [38], as a passive element. In crocodylians, the GI is a monoarticular muscle that originates from the posterior surface of the tibial head, joins the GE, and inserts onto the ventrodistal aspect of the metatarsus [38], [39]. With the GI, the ankle joint can attain a more erect posture without bone-to-bone contact at ankle=112°, resulting in propulsive motion (Figs. 2.11 and 2.12). The tension of each muscle, particularly the GE, suggests that a higher traction force is necessary to maintain the ankle posture when the GI is used, as shown in Fig. 2.12.

## 2.5 Discussion and Conclusions

The results of this study indicate that the crocodylian hindlimb has a passive interlocking mechanism for weight bearing and limb propulsion, achieved with a minimal muscular system utilizing only the CFL, CFLT, and GE muscles. The functions of the mechanism are

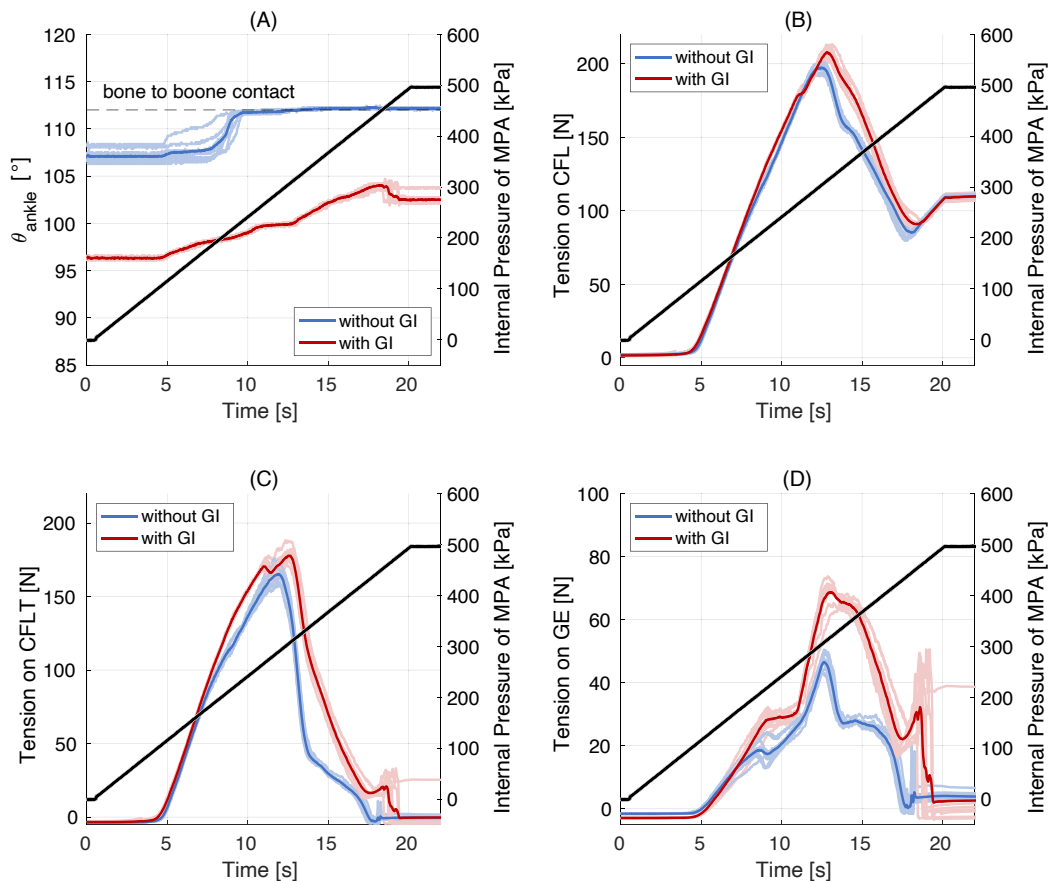


FIGURE 2.11: Comparison of ankle joint angles (A) and tension profiles of CFL (B), CFLT (C), and GE (D) under two conditions: one with the additional passive element GI and one without.

crucial for the semi-erect posture of the crocodilian hindlimb. A previous study by Snyder et al. [36] on lizards reported that the CFL inserts onto the knee capsule and functions to extend the hip, flex the knee, and rotate the femur in coordination with the CFL, thereby extending the moment arm around the hip. Gatesy et al. [37] noted that the traction force of the CFL acts not only on the insertion of the CFL but also on the insertion of the CFLT, providing a larger moment arm and enabling a more efficient stance phase in crocodilians. The studies on both crocodilians and lizards suggest that the moment arm for hip extension may be feasible in the transverse plane, where the femur is needed to abduct. In the sagittal plane, however, CFLT alone is unlikely to increase the moment arm for the hip joint extension since CFL and CFLT are nearly aligned (see Fig. 2.8). Our results thus highlight the importance of the Y-shaped junction connecting the CFLT and the GE in lengthening the moment arm around the hip joint in the sagittal plane through its interaction with the ground. The increased moment arm is likely beneficial for achieving a semi-erect posture, such as in high-walk, in crocodilians.

Our finding suggests that the passive interlocking mechanisms are ubiquitous among terrestrial vertebrates (mammals: [19]–[21], [33]; birds: [22], [24]; crocodilians: this study). The prevailing occurrence of the mechanism further suggests the importance of such a mechanism for accomplishing effective terrestrial locomotion and the presence of similar mechanisms in extinct vertebrates. The presence of interlocking mechanisms in extant archosaurs (birds and crocodilians) strongly suggests that a similar mechanism existed in their



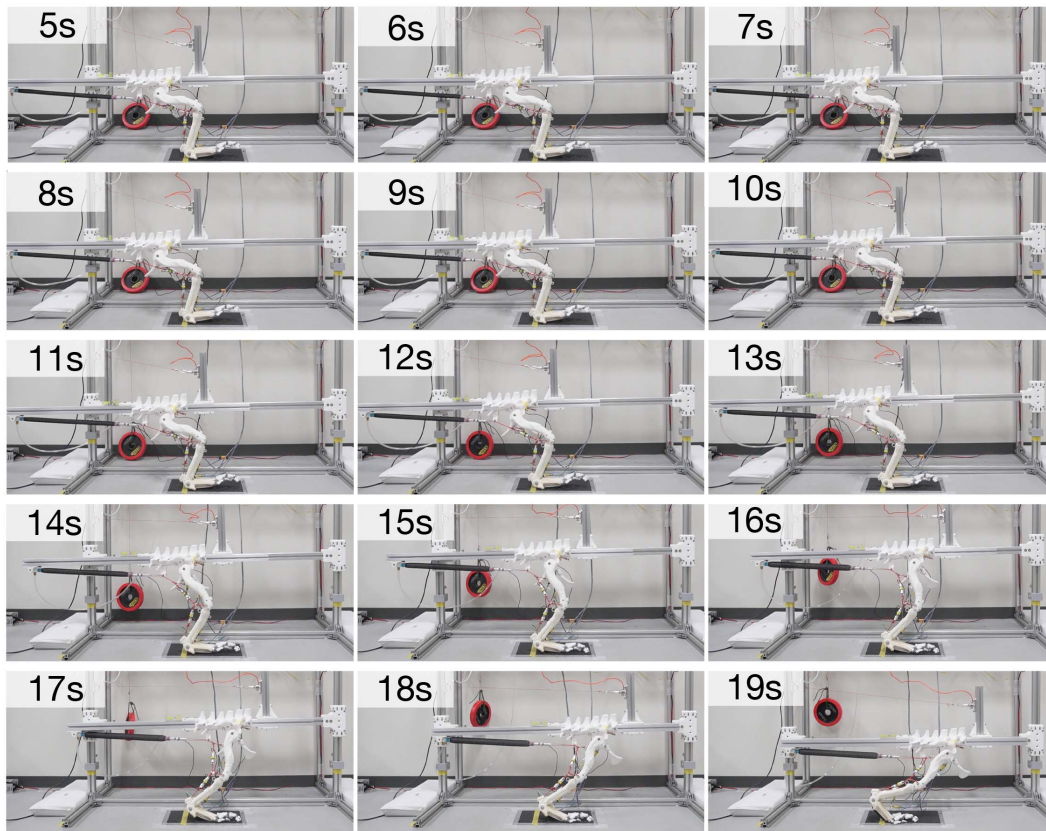


FIGURE 2.12: A sequence of motion using the additional passive element GI to prevent passive plantarflexion of the ankle joint. A video of this experiment (sv\_4.mp4) is available in Supplemental material.

extinct archosaur relatives, non-avian dinosaurs. The CFL is thought to be a large, major propulsive muscle in most of the non-avian dinosaurs as well (e.g., [37], [44], [45]). Although the presence of CFLT cannot be assured due to the lack of osteological correlates, non-avian dinosaurs presumably have the same or alternative anatomical structures to compensate for the function of CFLT in crocodylians to achieve the passive interlocking mechanism. In fact, the mechanism appears to be performed by the different sets of muscles and tendons in birds as their CFL diminished throughout their evolutionary history [37]. The fact that not all muscles and tendons evident from osteological features contribute to the passive mechanism emphasizes the importance of future robotic studies on extant and extinct archosaurs to elucidate the evolution of locomotion in archosaurs.

In future studies, it will be important to compare the joint trajectory of the robot with that of high-walking crocodiles and analyze the force acting on the muscular system, particularly at the Y-shaped junction. Integrating the passive interlocking mechanism in the crocodylian hindlimb into legged robots is expected to reduce the system's degrees of freedom, mechanically and autonomously generate a walking trajectory, and improve energy efficiency during locomotion. Additionally, investigating other passive interlocking mechanism and their linkage with the tail, which is the origin of the CFL and may influence locomotion, is crucial.





## Chapter 3

# Elucidation of the fundamental locomotion mechanism in Crocodylians II

### Note

This chapter is the author's version of the following article:

**Kazuki Ito**, Tetsuya Kinugasa, Sayaka Hida, Koji Yoshida, Ryota Hayashi, Koichi Osuka, "Interlocking mechanism in the hindlimb using a passive musculotendinous structure during the high walk of crocodylians: Validation of the effects of iliotibials as passive element using a robot" , *AROB-ISBC-SWARM 2023*, Beppu, Japan, OS10-7, 2023.

### 3.1 Introduction

Crocodylians are capable of using several gaits in sprawling and semi-erect postures, which is of interest from a bio-mechanical perspective [25], [38], [46]. Many studies have been conducted on the anatomical knowledge of their limbs to elucidate the function of muscles by dissection [29], [38], [47]. The others have used various measurement systems for muscle activity, such as electromyography, motion capture using visible-, infrared-, and/or X- rays, and mathematical models [25], [31], [32], [48]–[52], for revealing the precise active role of each muscle in locomotion.

Some terrestrial vertebrates have joint coordination mechanisms in their limbs using passive interlocking of the muscular system, producing joint trajectories autonomously for locomotion. For instance, horses have a mechanism in which the interaction of some muscles and tendons passively coordinate the lower leg joints only by reciprocating the femur to produce the joint trajectory of gaits (i.e., reciprocal apparatus), and a mechanism that mechanically locks the joints and supports their weight by interacting with the ground reaction force through the passive musculotendinous structure (i.e., stay apparatus) [19], [33]. The passive interlocking of the musculoskeletal system interacting with the environment reduces the redundant degrees of freedom significantly, moderates the computational load for controlling the muscular system and enables the locomotion to adapt to the mechanical characteristics of the body. The normal mode of terrestrial locomotion for crocodylians is the high walk, during which the hindlimbs are more erected and the belly is raised better off the ground than during a sprawl. In some individuals, the crocodile can weigh over

1000 kg [53], and the load on the joints of the limbs during walking is quite significant. The limb joints should be effectively maintained against the weight. Therefore, it is expected that there is a mechanism to maintain the erect-limb posture during high-walking passively by a passive musculotendinous structure, as in the stay apparatus of the horses. However, previous studies on the muscle function in crocodilian locomotion have not focused on joint coordination using the passive interlocking of the musculotendinous system of the limbs, which constrains the range of joint motion, supports the body weight, and produces the joint trajectories for locomotion.

In this study, we focus on joint coordination based on the passive interlocking mechanism interacting with the ground in the crocodilian hindlimb. We have previously identified the musculotendinous structures and their mechanical functions that contribute to locomotion by considering ground reaction forces through the dissection of the hind limbs of *Crocodilus prosus*, and have validated the mechanism by a robot [54]. In this report, we present empirical studies on the mechanical function of the iliotibialis (IT), which is a biarticular muscle coordinating the hip and knee joints, as a passive element in the standing up and propulsive motion during the high walk.

## 3.2 Crocodilian hindlimb robot

In the previous study [54], we developed the crocodilian hindlimb robot that reproduced the skeleton of the hindlimb of crocodilians. The robot was used to test the hypothesis of the mechanism for maintaining the erect-limb posture in the hindlimb during high walking obtained through dissection. Here, we experimentally investigated the mechanical function of the iliotibialis as a passive element using a modified version of the crocodilian hindlimb robot (Fig. 3.1).

The CT-scanned three-dimensional data was used for the robot to synthesize a crocodilian hindlimb. The crocodilian hindlimb can rotate about the roll, yaw, and pitch axes, although the hip, knee, and ankle of the robot are one degree of freedom (DoF) rotational joints around the lateral axis in order to focus on high walking, which is achieved by limb motion in the parasagittal plane. Potentiometers and a pressure sensor enable measuring the angle of each joint and the ground reaction force around the heel. The robot has the caudofemoralis longus (CFL), CFL tendon (CFLT), gastrocnemius externus (GE), gastrocnemius internus (GI), and IT. The McKibben pneumatic actuator (MPA) is used to provide tractive force as the CFL. The non-stretchable wire (polyethylene braid with high load-bearing properties and nylon braid with high abrasion resistance) reproduces the other muscles and tendons as passive elements. The robot is attached to the vertical slide table to constrain the motion in the parasagittal plane. The total weight of the robot except the slide table was 4.78kgf.

## 3.3 Results

### 3.3.1 Functions of the iliotibials as a passive element

The iliotibialis (IT) is a biarticular muscle that originates from the ilium wing and covers the anterolateral portion of the femur, then inserts on the entire surface of the tibia (Fig. 3.2).

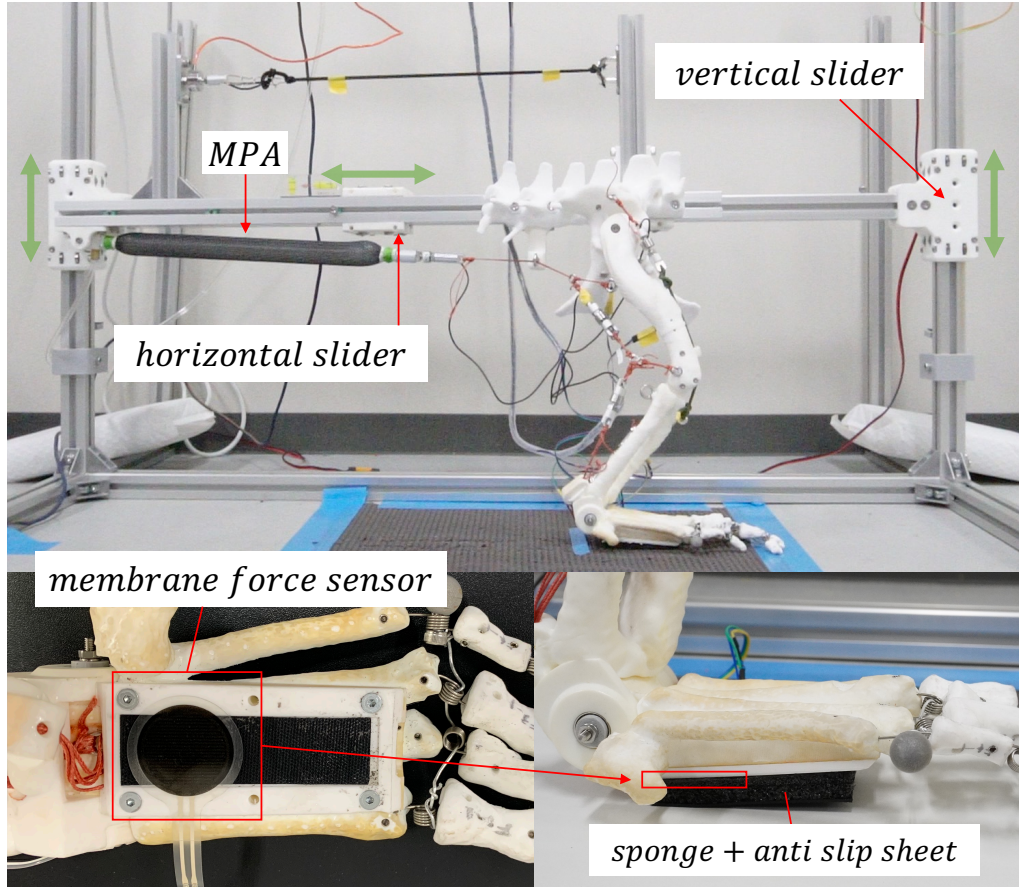


FIGURE 3.1: The hindlimb robot reconstructing the passive musculotendinous system and an MPA as the CFL.

First, we identify the function of the IT as a biarticular muscle for the hip and knee joints. The IT is attached alone to the robot (Fig. 3.3), which is not in contact with the ground. An elastic wire is implemented from the ilium wing to the calcaneum to provide knee flexion tension. We made the hip joint manually extend and flex in the range  $\theta_{hip}$  from  $-70^\circ$  to  $70^\circ$  as demonstrated in Fig. 3.3.

Figure 3.4 represents the knee angle with respect to the hip angle. The relative angle of the hip joint  $\theta_{hip}$  is defined by the angle between the ilium and the femur, and the angle of the knee joint  $\theta_{knee}$  is defined by the angle between the femur and the tibia, where the clockwise direction is positive. The positive direction of the hip and knee joints corresponds to hip extension and knee flexion. Figures 3.3 and 3.4 show that the knee joint angle decreased when the hip is extended from an almost horizontal position (approximately  $-70^\circ$ ) to a vertical posture (approximately  $0^\circ$ ). The IT length is constant when the hip joint is extended, resulting in knee extension. In addition, when the hip joint angle exceeds  $30^\circ$ , the knee flexion angle increases because the IT path between the origin and the insertion begins to decrease.

### 3.3.2 Effect of the iliotibialis on erect-limb posture

Next, the effects of IT on the erect-limb posture during the high walk were investigated. Figure 3.5 shows the minimum musculotendinous structure necessary for maintaining the



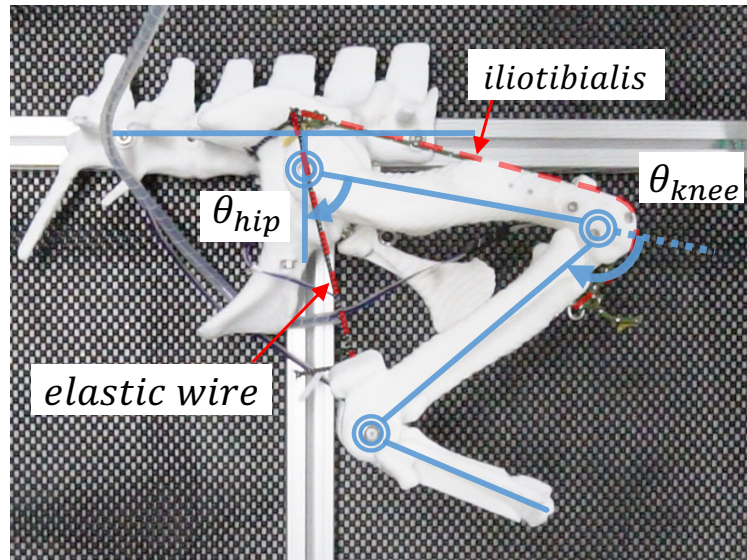


FIGURE 3.2: The effect of IT as the biarticular muscle for the hip and knee joints.

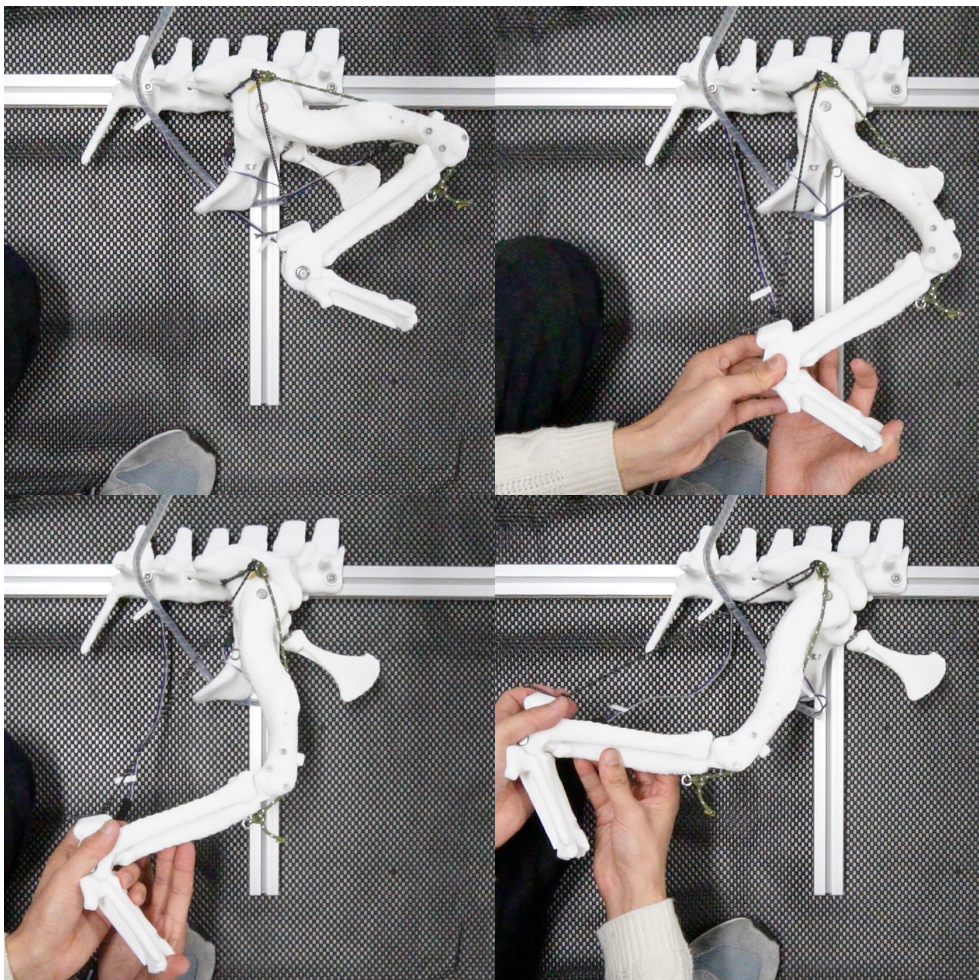


FIGURE 3.3: The effect of IT as the biarticular muscle for the hip and knee joints. The path of IT extends according to the hip extension, and the knee joint extends if the IT length keeps constant.

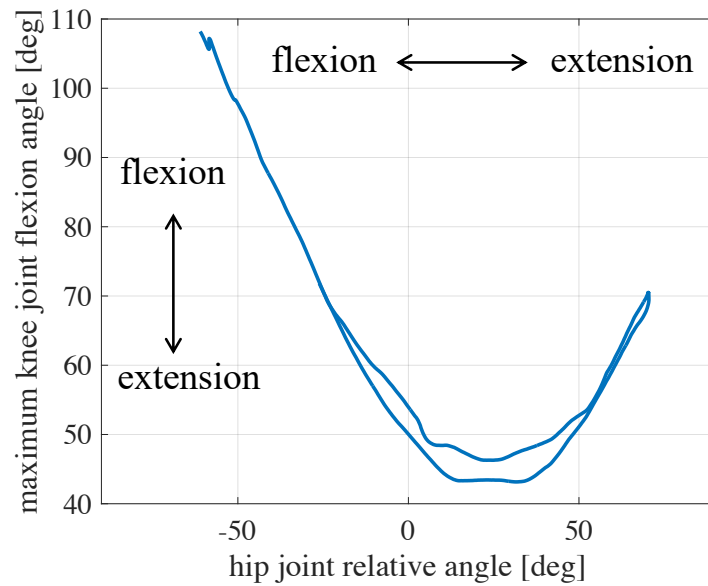


FIGURE 3.4: Hip joint angle and maximum knee joint flexion angle.

erect-limb posture of the hindlimb, as identified in a previous study [54]. This structure enables the erect-limb posture only by active contraction of the caudofemoralis (CFL). Finally, we conducted some experimental tests to verify the IT effect.

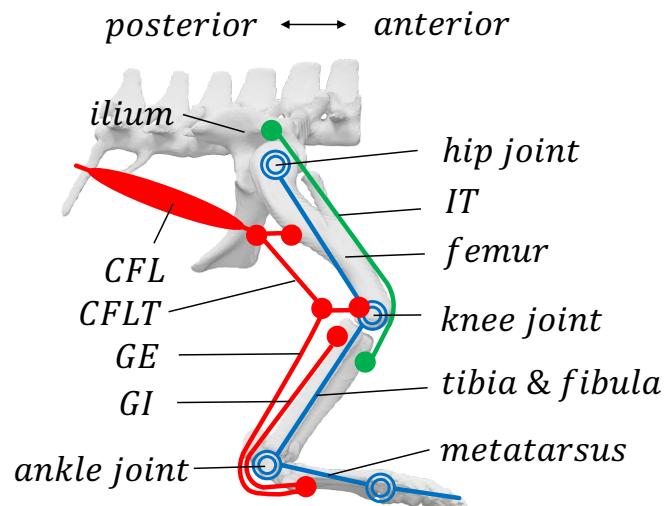


FIGURE 3.5: The minimum musculotendinous structure (red lines) of the hindlimb robot for maintaining the erect-limb posture.

The representative sequence of the limb posture when the MPA as the CFL was contracted gradually, as shown in Fig. 3.6. The hindlimb robot successfully produced the erect-limb posture.

After 6 s, the knee joint of the robot using the IT (above figure) is more extended than that of the robot not having the IT (below). The calcaneus is lifted from the ground after 6 s in the above figure, whereas the robot using the IT keeps the calcaneus on the ground,



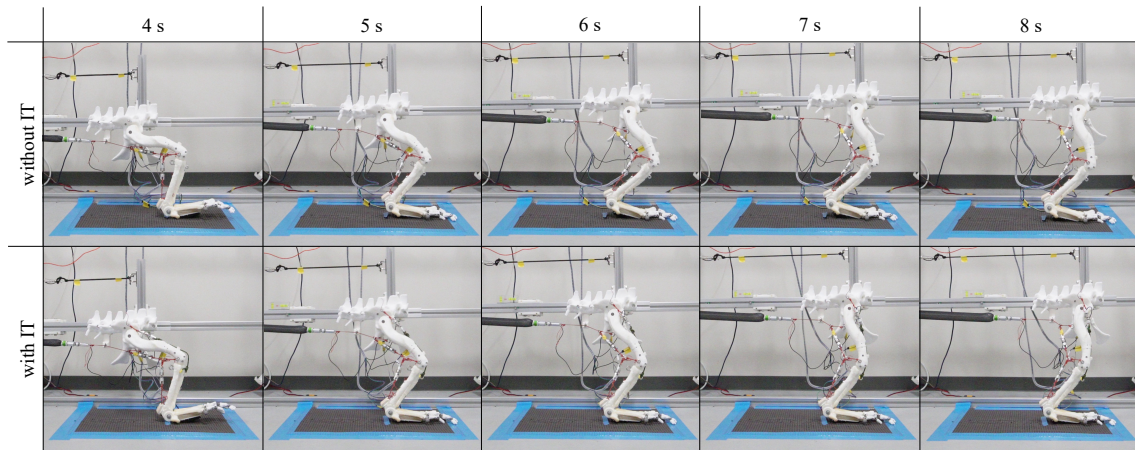


FIGURE 3.6: Representative sequence of standing up and propulsive motion. The above row indicates the motion in the absence of the IT. Below is the case using IT.

swinging the hindlimb backward (i.e., providing propulsive force). The knee is forced to extend by the IT when the CFL extends the hip joint, resulting in a weight shift toward the calcaneus.

Figure 3.7 indicates the ground reaction force (GRF) measured by a pressure sensor attached to the sole around the calcaneus. The GRF around the calcaneus rapidly decreased around 5 s when the robot used the IT. Contrarily, although the GRF reduced by almost half around 7 s, the robot kept it on the calcaneus, swinging the hindlimb backward.

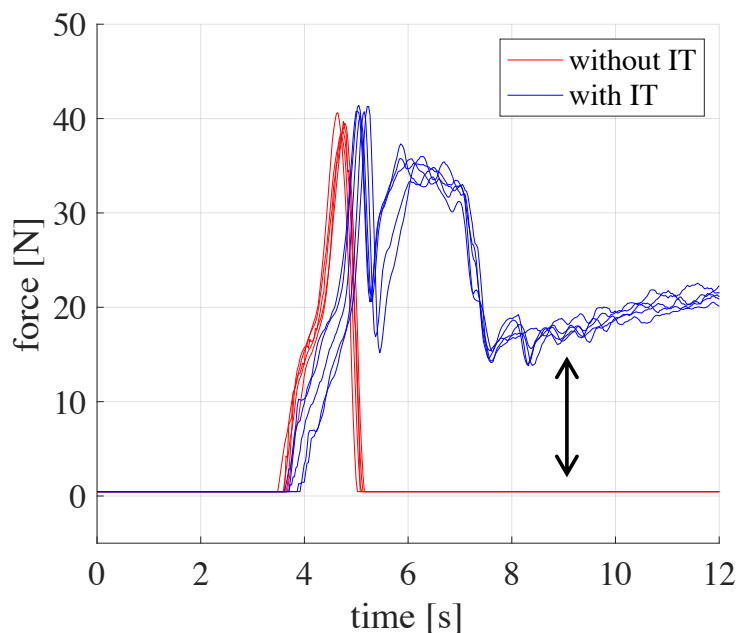


FIGURE 3.7: Ground reaction force around the calcaneus.

Therefore, the important role of the IT as a passive element in the erect-limb posture is an improvement of the knee extension for the active hip extension by the CFL, providing more frictional force around the calcaneus.

## 3.4 Conclusions

In this report, we empirically investigated the passive role of iliotibialis in an erect-limb posture of the crocodilian hindlimb robot. As a passive element, the IT provided joint coordination of the hip and the knee in the erect-limb posture, resulting in more knee extension and more frictional force around the calcaneus.

Future work in this study will aim to understand the active and passive roles of other muscles and tendons in the hindlimbs of crocodilians and the mechanism of periodic movements of the high walk, including the swing phase realized by the integration of these functions.





## Chapter 4

# Elucidation of the fundamental locomotion mechanism in avians

### Note

This chapter is the author's version of the following article:

Kazuki Ito, Sayaka Hida, Tetsuya Kinugasa, Kentaro Chiba, Yu Okuda, Miwa Ichikawa, Tsukasa Okoshi, Ryuji Takasaki, Ryota Hayashi, Koji Yoshida, and Koichi Osuka, “Cam-like mechanism in the intertarsal joints of ratites and its design framework “, *Journal of Robotics and Mechatronics*, 11/28/2023 Accepted.

### 4.1 Introduction

People often mistakenly believe that the knees of birds flex in the direction opposite that of humans. This misconception arises because it is difficult to visually observe the bird's thighs, as they are hidden in feathers (Fig. 4.1A). The joint of birds mistaken for the knee is called the intertarsal joint, which connects the tibiotarsus and tarsometatarsus (Fig. 4.1B). Because the bird intertarsal joint is homologous to the human ankle joint, the tarsometatarsus moves forward (anteriorly) in flexion, unlike the human knee joint, in which the tibia and fibula move posteriorly during flexion. Although the human knee joint and bird intertarsal joint are not homologous, they rotate about the medial-lateral axis and support the weight of the whole body during the stance phase of walking and running [24], [46].

Regarding the intertarsal joint of birds, a functional anatomical study revealed that large ratites, such as ostriches and emus, exhibit an engage – disengage mechanism (EDM) of this joint [24]. EDM is a passive mechanism in which the joint converges to two locally stable equilibrium points, that is, the maximally extended and flexed states, from the locally unstable equilibrium points at which the intertarsal joint is partially flexed. This mechanism is achieved only by passive elements, which consist of articular surfaces between the distal end of the tibiotarsus and the proximal end of the tarsometatarsus and ligaments and muscles with minimal contraction capability. EDM was earlier described as “Schnappbewegung” (snapping motion) [55], [56] and can also be observed in the elbow joints of various mammals [57]–[62]. The passive property of the EDM is thought to play a crucial role in bird walking.

In the human knee joint, which functions similarly to the bird's intertarsal joint, the lower limb swings forward in a relaxed state, with the knee slightly flexed during the first half of the swing phase of walking. That is, the link lower than the knee swings later than

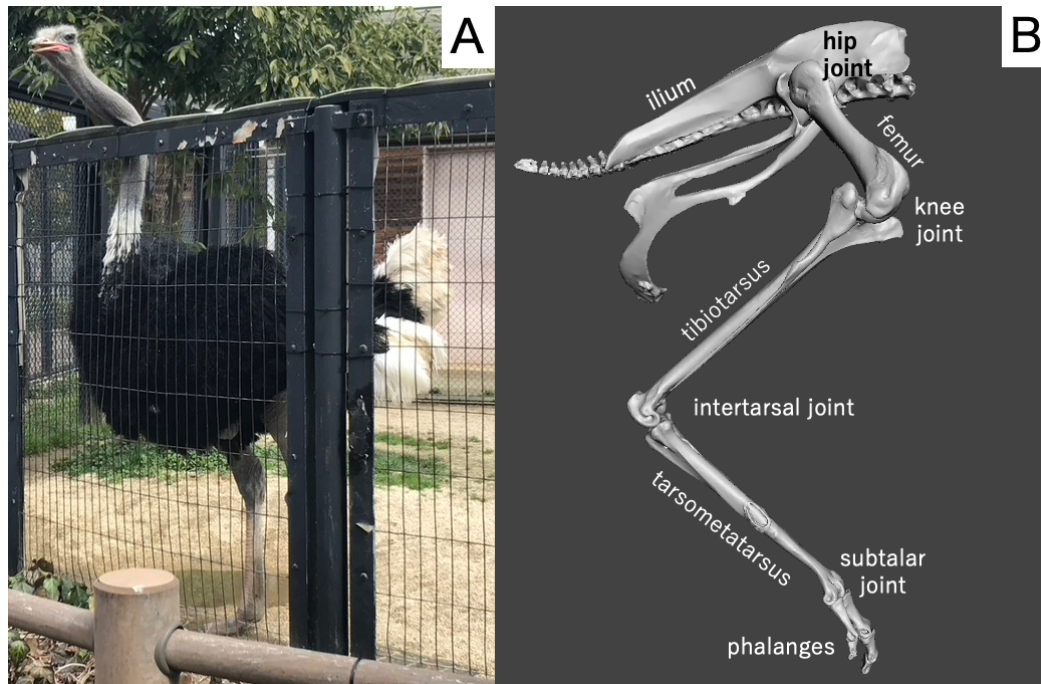


FIGURE 4.1: Ostrich (*Struthio camelus*) at Fukuyama City Zoo (A) and right posterior postcranial skeleton in lateral view (B).

the femur, which enables the leg to swing without having the toes touch the ground, thus preventing stumbling. After the toes are swung through, the forward-swinging femur is decelerated to extend the knee, and the foot sole lands after the leg is extended straight. This passive knee motion is a well-known phenomenon in robotics, and it is called passive dynamic walking [63]. However, the bird's intertarsal joint flexes in the reverse direction of the human knee joint, and the free oscillation of the leg under the influence of gravity does not induce flexion or extension, which may lead one to believe that the toes stumble against the ground. Therefore, birds must actively flex their intertarsal joints during the swinging phase. The intertarsal joint begins to flex in the first half of the swing phase to lift the foot off the ground and move toward a maximally flexed posture, which is a stable equilibrium point. In the latter half of the swing phase, the intertarsal joint is extended, and the foot is carried to the ground in the maximally extended posture; this is maintained in the stance phase to support the bird's weight. The extended posture of the intertarsal joint in the stance phase is the other stable equilibrium point engaged in the EDM. As in previously recognized passive mechanisms in bird [22], [24], [34], crocodilian [64], and horse limbs [33], [62], the stability of the EDM during the stance phase is potentially reinforced by the interaction between muscles, tendons, and the ground reaction force. Thus, the EDM may provide the key to understanding how birds deliberately flex and extend their intertarsal joints. The previous study investigated the role of the medial and lateral condyles at the distal end of the tibiotalarsus that causes the deformation of muscles and ligaments in the EDM [24]. However, because the elastic deformation or tension of the muscles and ligaments involved were not measured, the details of how the passive elements around the joint generate tension to achieve EDM remain unclear. If the EDM can be replicated using a physical model, it should be possible to measure the displacement of the muscles and ligaments of the joint, which may lead to the elucidation of the detailed principles of EDM and its design method.

In this study, to examine the EDM observed in the intertarsal joint of ratites, we dissected an emu to confirm the arrangement and functions of the passive elements around the joint and established a physical model using a replica of an ostrich hindlimb skeleton to reveal the principles of the EDM. Specifically, we measured the passive torque of the constructed intertarsal joint and the displacements of the springs, simulating the ligaments, for various postures to show that the articular surface performs a cam-like function. Furthermore, we demonstrated that the tibiotarsal distal articular surface can be replicated by employing a specific ligament arrangement and displacements.

## 4.2 Materials and methods

To fabricate a physical model, we first dissected an emu, *Dromaius novaehollandiae*, to confirm the EDM and arrangement of the ligaments and muscles of the intertarsal joint. The specimen used for dissection was a young adult (approximately 30 kg) of unknown age and sex, which was frozen immediately after natural death. The emu was provided by Japan Eco System Co., Ltd.

The physical model was 3D printed using a 3D printer, ANYCUBIC Photon Mono X-6K, with the RESIONE M58 resin. The 3D data for printing was provided free of charge on Sketchfab by the Idaho Virtualization Laboratory under the license CC BY-NC-ND 4.0 Deed [65] (Fig. 4.2). The physical model was printed in a half-scale. The model consists of the right tibiotarsus, tarsometatarsus, and proximal-most phalanx of the medial digit. The muscle and ligaments on the medial and lateral sides of the intertarsal joint were arranged according to Schaller et al. [24] and the observations of the emu's anatomy from the dissection, which are described in the following section. The muscle and ligaments were replicated using extension springs HP040-015-0.5 (0.922 N/mm, Showa Spring Co., Ltd.) for ligamentum collaterale mediale longum (LCML) and m. fibularis brevis (MFB) and HP040-019-0.5 (0.583 N/mm, Showa Spring Co., Ltd.) for ligamentum collaterale mediale (LCM) and ligamentum collaterale laterale (LCL), which are connected with nylon cords (0.570 mm in diameter, 20 kgf, Varivas Co., Ltd.) to M2 screws affixed at the origins and insertions of the ligaments (Figs. 4.2 and 4.3). The springs were slightly pre-tensioned to maintain the joint articulation and constrain the natural range of motion.

With this physical model, the elastic forces generated by the passive elements on the intertarsal joint were measured using a spring scale (ST-01 100g/ 1g, Sanko Seikohjyo Co., Ltd.). The spring scale was attached to an M3 screw affixed to the point on the tarsometatarsus located 125 mm from the origin of the LCML (Fig. 4.3A). The generated force was measured in intervals of 10° within the joint range of motion (Fig. 4.3B).

## 4.3 Result

### 4.3.1 EDM and muscle and ligaments arrangement of the emu hindlimb

First, we confirmed the existence of the EDM and the associated muscle and ligaments in the intertarsal joints through the dissection of the emu specimen. Our observations confirm that the emu has the relatively long LCML and the short LCM parallelly arranged on the medial side (Fig. 4.4A – D), and the MFB, a short muscle with limited contractile action, and the short LCL arranged to cross each other on the laterals side of the intertarsal joint (Fig. 4.4E

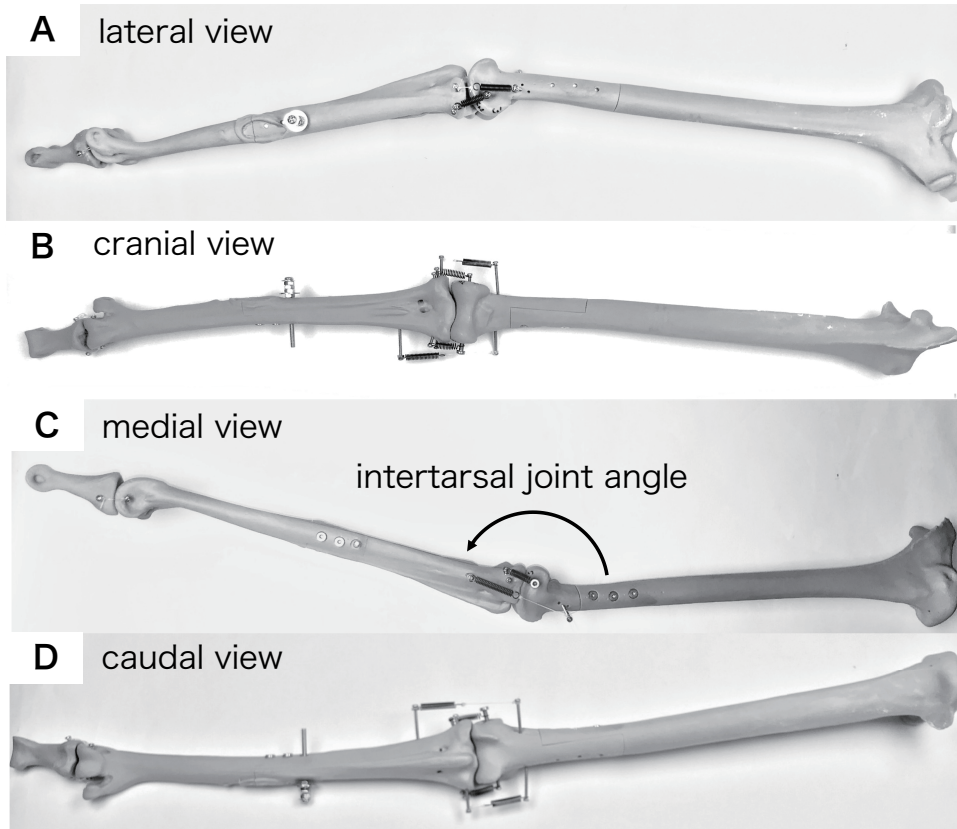


FIGURE 4.2: Physical model using 3D-printed right hindlimb of ostrich [65].

– H) as in ostriches [24]. We further confirmed the virtually identical EDM in the emu as in ostriches [24]; the joint snaps back to the extended posture when released from a slightly flexed posture (at approximately  $120^\circ$  according to Schaller et al. [24]) from the maximally extended state, and snaps towards the flexing direction ( $< 115^\circ$  according to Schaller et al. [1]) when further flexed.

#### 4.3.2 EDM in the intertarsal joint of the physical model

Next, we describe the forces acting on the intertarsal joint, displacements of the muscle system, and the EDM of the physical model. Table 4.1 lists the lengths  $l_{LCML}(\theta)$  and  $l_{LCM}(\theta)$  of the two medial ligaments, and Table 4.2 lists the displacements of the lateral muscle and ligament. The angle  $\theta$  of the intertarsal joint is defined as the relative angle between the tibiotarsus and tarsometatarsus (Fig. 4.2C). The displacements of the medial ligaments are expressed by  $d_{LCML}(\theta) = l_{LCML}(\theta) - l_{LCML}(44^\circ)$  and  $d_{LCM}(\theta) = l_{LCM}(\theta) - l_{LCM}(165^\circ)$ .  $l_{LCML}(44^\circ)$  and  $l_{LCM}(165^\circ)$  are the minimum values (52.4 and 22.8 mm) of the respective ligaments.

The tibiotarsus of the physical model was kept immobile, and the tarsometatarsus was flexed by applying an external force from the maximally extended posture of  $165^\circ$ . If the tarsometatarsus is released when the angle is over  $110^\circ$ , the joint snaps back to and becomes stabilized at the maximally extended posture owing to the positive force acting on the joint by the elastic force of the spring (Fig. 4.5A). Contrarily, if the joint is flexed beyond the point that the angle becomes lower than  $110^\circ$ , the joint snaps to and becomes stabilized at

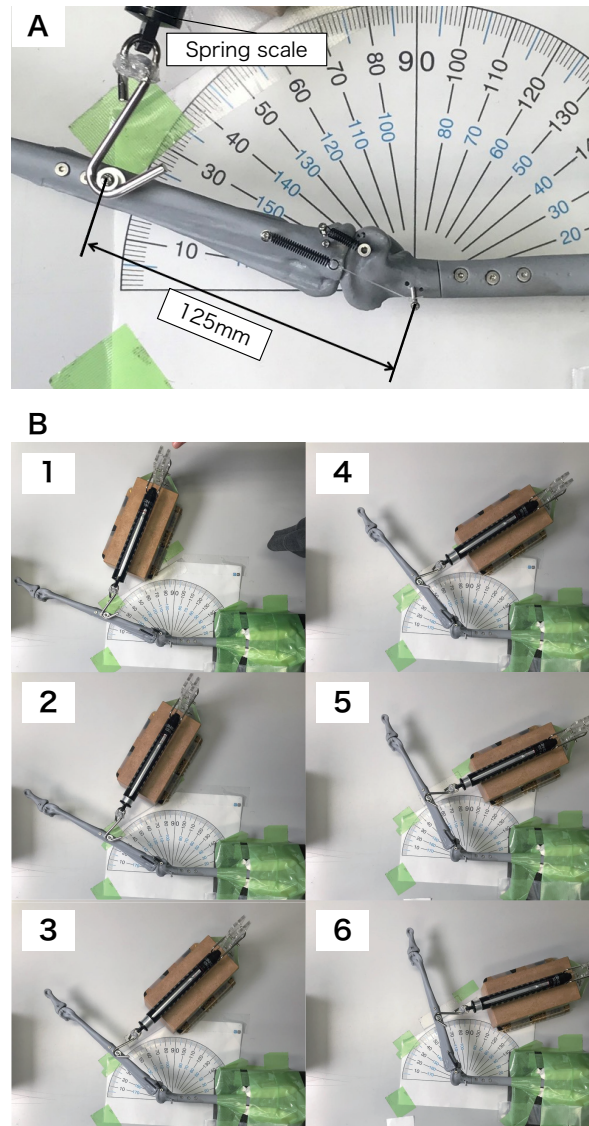


FIGURE 4.3: Experimental setup (A) and sequential photographs of experiment for flexion (B)

the maximally flexed posture ( $40^\circ$ ), at which the end of each bone segment contacts, due to the negative elastic force on the joint. The observations indicate that the intertarsal joint has an unstable equilibrium point within the range of  $100^\circ$  to  $110^\circ$ , around which a vector field is formed by the forces acting in the flexing and extending directions. Conversely,  $165^\circ$  and  $40^\circ$  can be regarded as stable equilibrium points in the extended (Fig. 4.6B) and flexed postures. However, the spring tension within the vicinity of the stable equilibrium point in the flexed posture is weak; therefore, the joint angle can vary around  $70^\circ$  owing to the effects of friction and gravity.

#### 4.3.3 Design of articular surface, critical for achieving the EDM

The direction of the elastic force on the intertarsal joint alternates between  $100^\circ$  and  $110^\circ$  of the joint angle (Fig. 4.5A). In Fig. 4.5B, the trend of the LCML displacement has an upward



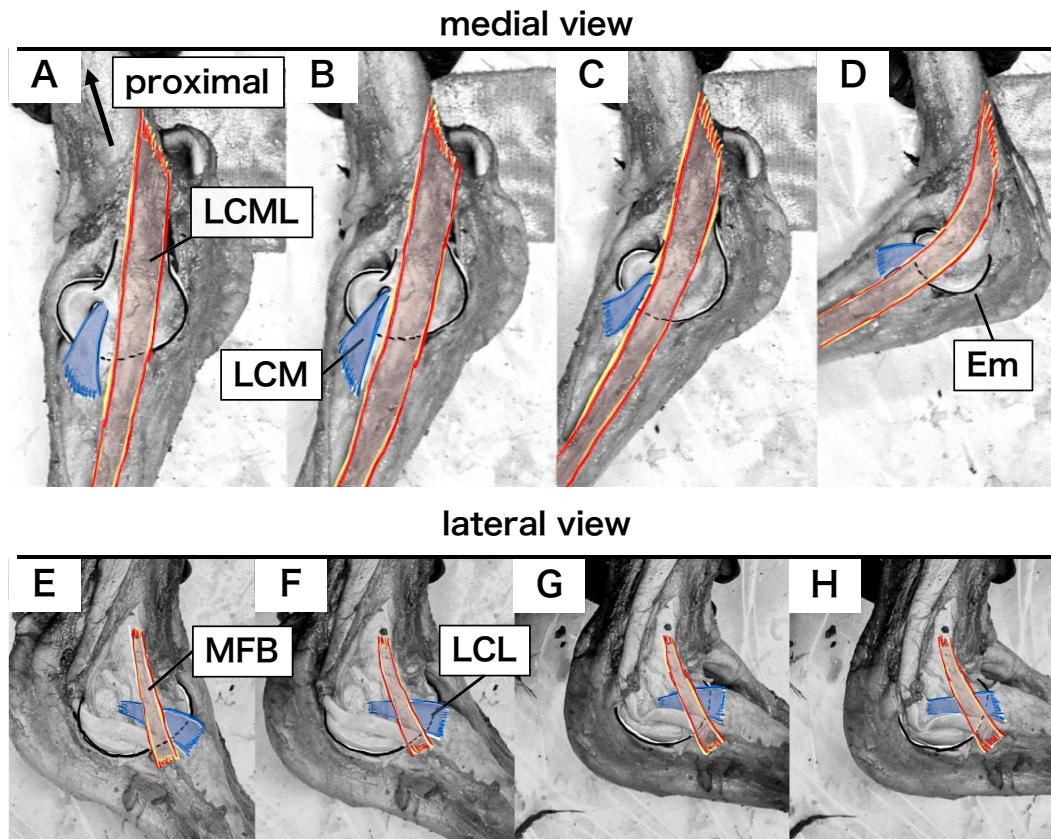


FIGURE 4.4: Dissected intertarsal joint of emu. In the medial view (A-D), the orange and blue lines represent the LCML and LCM, respectively. In the lateral view (E-H), the orange and blue lines represent the MFB and LCL, respectively. The black line indicates the outline of the distal end of the tibiotarsus.

convex shape peaking at  $120^\circ$  on the medial side of the joint, generating an elastic force towards the extended posture, which appears to be responsible for the EDM to snap back the joint. The trend of the LCM displacement has an upward convex shape peaking at 3 mm and  $90^\circ$ , and it becomes almost constant around 0.4 mm (displacement: 0 mm) over  $140^\circ$  and gradually decreases to 1.5 mm towards the maximally flexed posture ( $44^\circ$ ). Thus, the EDM for the flexing direction is achieved by the additional tension of the LCM at angles smaller than  $140^\circ$ . On the lateral side, the trend of the LCL displacement is similar to but smaller than that of the LCM. Thus, it appears to have a slight effect on the EDM (see further discussion in Section 4.4). The displacement of the MFB sharply increases as the joint approaches the maximally extended posture. The displacements of the LCML and the LCM result from the morphology of the distal and cranial rims of the condylus medialis of the distal tibiotarsus (DrM and CrM, respectively) (Table 4.1 and Fig. 4.6); the articular surface in lateral view is not circular with a single center but more similar to oval with two ellipse center. The elliptical outline of the condyles stretches the LCML and the LCM when the joint angle is over or less than  $100^\circ$ - $110^\circ$ , respectively, causing the tarsometatarsus rotation with alternating the rotational centers between origins of the LCML and the LCM on the tibiotarsus. This indicates that the intertarsal joint has a special two-axis cam-like structure. Based on this observation, we can design the articular surface to achieve the EDM using the displacements of the two medial ligaments. Furthermore, because the line connecting the

TABLE 4.1: Lengths of ligaments LCML and LCM

$\theta$	$l_{LCML}$	$l_{LCM}$	$\theta$	$l_{LCML}$	$l_{LCM}$
[°]	[mm]	[mm]			
100	66.4	25.3	100	66.4	25.3
44	52.4	24.3	110	67.9	24.7
50	53.7	24.8	120	68.1	24.3
60	56.1	25.2	130	67.7	23.7
70	58.9	25.2	140	66.9	23.2
80	61.6	25.7	150	65.5	22.9
90	64.2	25.8	165	63.8	22.8

TABLE 4.2: Displacements of ligaments MFB and LCL

$\theta$	MFB	LCL	$\theta$	MFB	LCL
[°]	[mm]	[mm]			
100	0.2	1.6	100	0.2	1.6
35	0	0.8	110	0.5	1.5
40	0	0.9	120	0.6	1.3
50	0	1.6	130	0.8	1.2
60	0	2.1	140	1.1	1.1
70	0	2.3	150	1.8	1.3
80	0	2.1	160	2.9	1.4
90	0	2.0	165	3.6	2.1

origins of the LCM and LCML corresponds to the intertarsal joint angle  $\theta$  of approximately  $130^\circ$  (Fig. 4.6D), the dominant ligament in the EDM is assumed to switch from the LCML to the LCM at this angle. Based on this assumption, we can design the cam in the intertarsal joint by applying the following procedure.

First, the radius  $r_{DrM}$  of the cam base circle is set at the distance between the origin of the LCML and DrM (34.3 mm, as determined via measurements, Fig. 4.6B) at the maximally extended posture ( $\theta = 165^\circ$ ). The center of the base circle  $C_{DrM}$  is the origin of the LCML and is set as the coordinate origin. The cam surface of the distal articular surface (i.e., DrM) can be expressed as follows using the displacement of the LCML.

$$R_{LCML}(\theta) = l_{LCML}(\theta) - (l_{LCML}(165^\circ) - r_{LCML}) \quad (4.1)$$

$$x_{LCML}(\theta) = R_{LCML}(\theta) \cos \theta + x_{C_{LCML}} \quad (4.2)$$

$$y_{LCML}(\theta) = R_{LCML}(\theta) \sin \theta + y_{C_{LCML}} \quad (4.3)$$

Next, we determined the length of the LCM so that the cranial articular surface (i.e., CrM) forms a continuous outline to the DrM at  $\theta = 130^\circ$ ; the radius of the base circle of the CrM is determined as  $r_{CrM} = l_{LCML}(130^\circ) - d_{C_{CrM}}$ , where the center of the base circle  $C_{CrM}$  is set at the origin of the LCM ( $C_{CrM} = (x_{C_{CrM}}, y_{C_{CrM}}) = (-19.6, 22)$ ), and the distance between the two centers is  $d_{C_{CrM}} = 29.8$  mm. Subsequently, the cam surface of the CrM is expressed as follows.

$$R_{LCM}(\theta) = R_{LCML}(130^\circ) - d_{C_{LCM}} \quad (4.4)$$

$$x_{LCM}(\theta) = R_{LCM}(\theta) \cos \theta + x_{C_{LCM}} \quad (4.5)$$

$$y_{LCM}(\theta) = R_{LCM}(\theta) \sin \theta + y_{C_{LCM}} \quad (4.6)$$



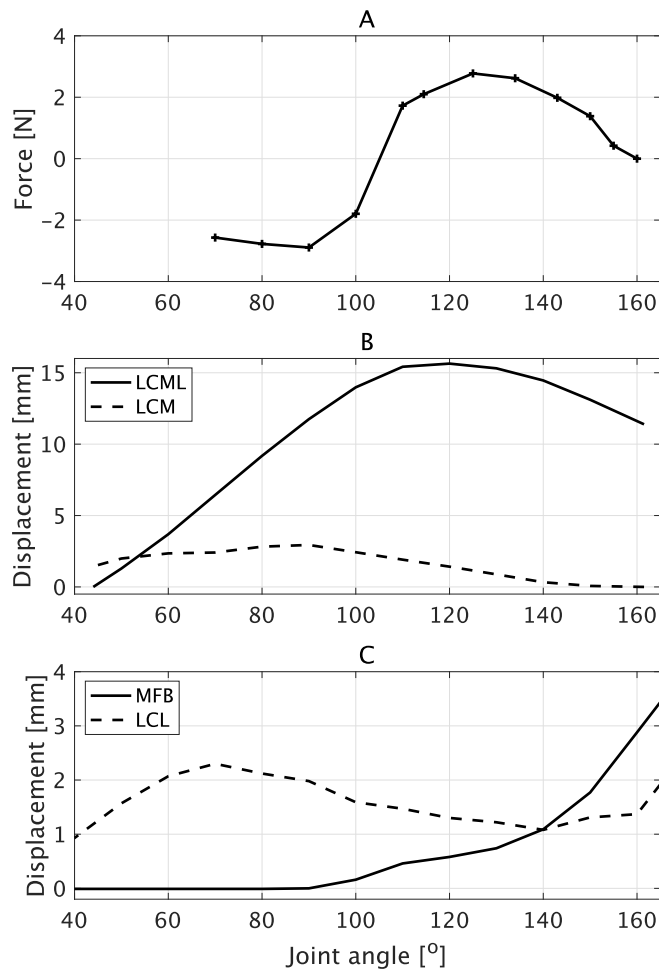


FIGURE 4.5: Joint elastic force (A), displacements of LCML and LCM (B), and displacements of the MFB and LCL (C).

The designed cam surface shows that the DrM and the CrM are divided at the angle of  $130^\circ$ , and the shift of the dominant ligament occurs at the same angle (Fig. 4.7). The replicated articular surface accurately represents the range of the CrM between the joint angle of  $44^\circ$  and  $130^\circ$  and the DrM between  $130^\circ$  and  $165^\circ$  (Fig. 4.8).

## 4.4 Discussion

We first discuss whether the arrangement of the ligaments and muscles necessary for achieving the EDM was appropriately replicated in the physical model in comparison with the dissection results. Although the dissection was conducted using an emu and the physical model was produced based on the digital data of an ostrich, the aforementioned results in Section 4.3.1 clearly indicate that the anatomical features around the intertarsal joints are consistent between the two species, making the comparison meaningful.

The arrangement of the ligaments in the physical model does not fully replicate that in the dissected specimen, but the differences do not appear to influence the performance of the EDM significantly. We arranged the LCML and LCM in parallel along the long axis of the tarsometatarsal on the medial side of the intertarsal joint at the maximally extended posture

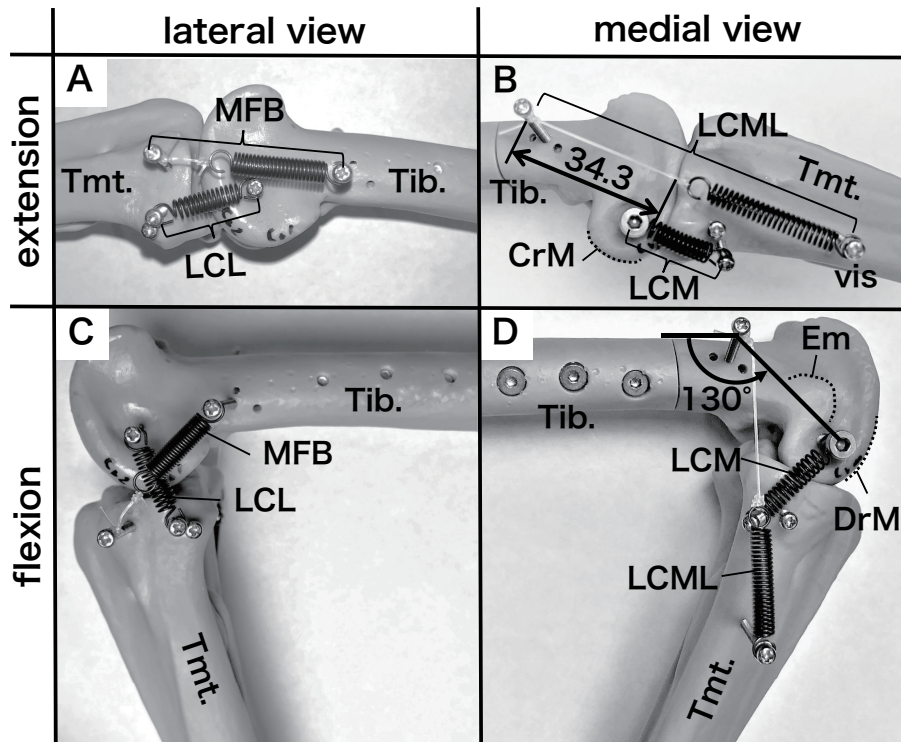


FIGURE 4.6: Extended (A and B) and flexed (C and D) postures of replicated intertarsal joint.

in the physical model (Fig. 4.6B), as in the dissected emu specimen (Fig. 4.4A). However, the LCML in the physical model slides over the epicondylus medialis (Em) cranially, which is located on the medial surface of the tibiotarsal distal end, at the flexed posture whereas the ligament does not in the dissected specimen (Figs. 4.4D and 4.6D). This discrepancy occurs because we could not physically replicate the membranous ligament, originating at the condylar rim, connecting to and preventing the over-slide of the LCML. This suggests that the elastic force of the LCML did not act as much in the flexed posture in the physical model as it did in vivo. Therefore, the passive action of the EDM in the flexed posture observed in the dissected specimen was not fully replicated. On the lateral side, the LCL and the MFB were arranged to intersect each other, forming the 'X' configuration of those ligaments (Fig. 4.6C), as in the dissected specimen (Fig. 4.4H). The configuration of the ligaments, however, was not fully replicated in the extended posture; the LCL and MFB were arranged at an oblique angle with respect to each other without intersecting (Fig. 4.6A) but completely intersected in the dissected specimen (Fig. 4.4E). Regardless of the discrepancy, the physical model successfully replicated the EDM using the cam surface of the joint as well as the muscle and the ligaments. Ultimately, the disparity between the physical model and the dissected specimen does not dispute the validity of our findings.

Next, we discuss the roles of the ligaments and the muscle, which are critical for achieving the EDM of the intertarsal joint, based on their displacement pattern (Fig. 4.5B and C). The LCML displacement pattern suggests that it generates an elastic force towards the extended posture, responsible for the EDM to snap back the joint. The similar displacement pattern of the LCM and the LCL suggests that the elastic forces of both structures conjunctively produce the force to flex the joint. However, the maximum displacement of the LCM

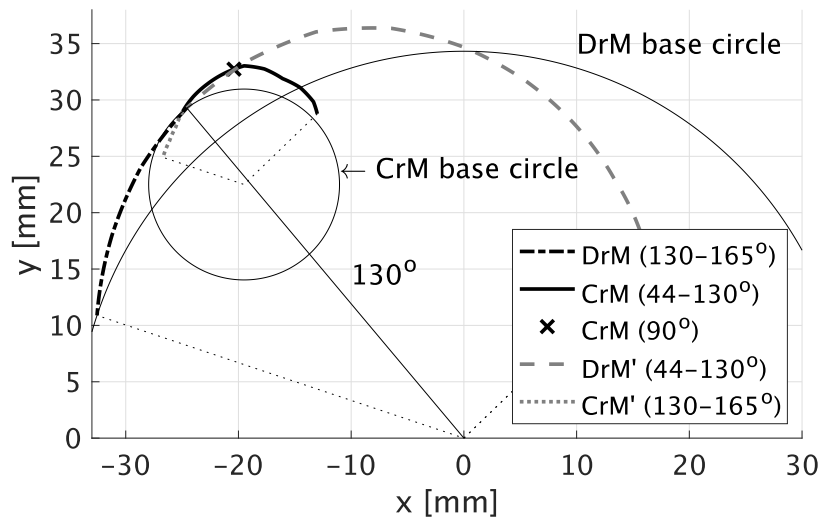


FIGURE 4.7: Designed Cam surface. The cam surface is represented by the dash-dot line (DrM) and the solid line (CrM). DrM' and CrM' represent the virtual extensions of the DrM and CrM.

(3 mm) and the LCL displacement (1.2 mm) infers the different roles of the elements; the LCM plays the dominant role in achieving the EDM, whereas the basic role of the LCL is the maintenance of the joint coherence (Note that both elements employed with the same type of spring, and therefore the displacement reflects the magnitude of the force acting on each element). The MFB begins to extend at the joint angle of  $90^\circ$  and is rapidly displaced with an increasing joint angle, suggesting that its role is to maintain joint coherence in the extended posture and prevent hyperextension.

Finally, we discuss the suggestions for the more appropriate cam surface design to replicate the structure seen in ratites. The designed articular surface does not connect smoothly at the position ( $\theta = 130^\circ$ ), where the dominant role for the EDM alternates between the LCML and the LCM (DrM and CrM in Fig. 4.7). The designed surfaces of the DrM and the CrM are roughly identical between the joint angles of  $90^\circ$  and  $130^\circ$ , although that of the CrM is slightly bulged outward (Fig. 4.7). Therefore, the  $130^\circ$  line in Fig. 4.7, which connects the origins of the LCML and the LCL, is not necessarily the switching point; instead, the centers of the cam base circles can gradually shift in this range ( $90^\circ < \theta < 130^\circ$ ) as in the dissected specimen. In future studies, it will be ideal to form a smooth surface via spline interpolation or other approaches to design an actual robotic intertarsal joint to replicate the gradual transition of the rotational centers of the base circles.

## 4.5 Conclusions

This study successfully designed and established a physical model of an ostrich intertarsal joint that can achieve EDM. Using the physical model, we measured the displacements of the muscle and the ligaments around the joint, demonstrating that the EDM was achieved owing to the interaction of the muscle, the ligaments, and the cam-shaped distal end of the

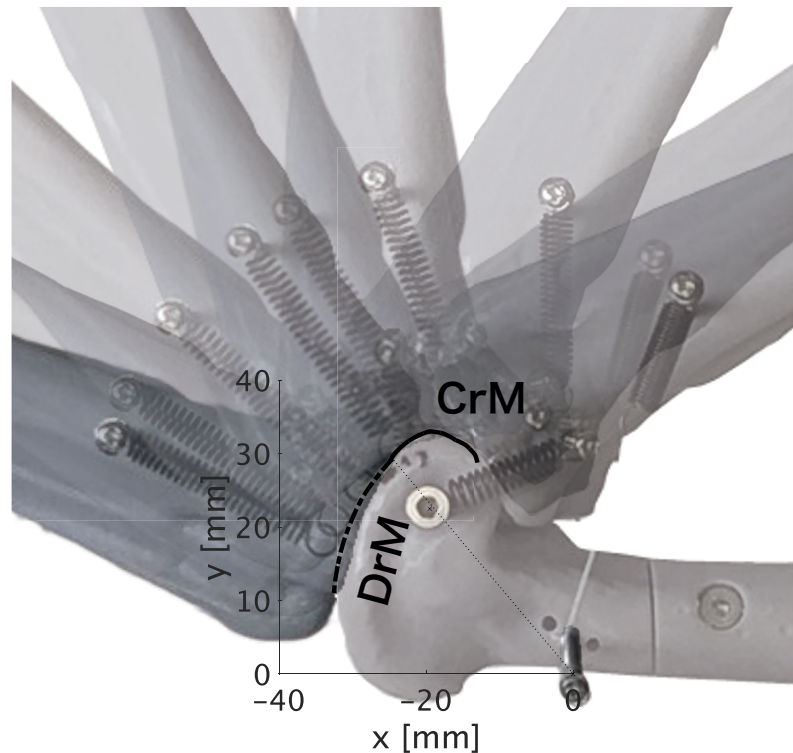


FIGURE 4.8: Cam surface and intertarsal joint motion. The cam surface is represented by the dash-dot line (DrM) and the solid line (CrM). The transparent images of the medial side of the tibiotarsal distal end are superimposed as the origin of the LCML matches the center of the base circle of the DrM, showing the distal end functions as a cam, and the tarsometatarsus functions as the follower.

tibiotarsus. Because it is difficult to measure the extensions or elastic forces of the muscle and the ligaments through dissection or *in vivo*, the approach of this study is significant to elucidate the biomechanical aspect of the EDM in the intertarsal joint. Conversely, this study further demonstrates we can design a cam surface by adjusting the arrangement and displacement of certain ligaments (the LCML and the LCM).

The previous study addressed the EDM in the ostrich intertarsal joints and suggested that the protrusions on the medial (Em) and lateral sides of the distal tibiotarsi play a crucial role in achieving the EDM. However, the function of the EDM resembles that of a cam, as revealed in this study, and we argue that it is more rational to regard the articular surface morphology of the tibiotarsal distal end rather than the protrusions as a fundamental structure to achieve the EDM.

Although nearly all conventional robots employ pivotal rotating joints, elucidating the effects of structures that have local equilibrium points, such as those used in this study, may provide hints for achieving more natural postures and locomotion of robots. For example, the passive function of maintaining joint extension is effective in the stance phase, whereas the function alternating flexion and extension of certain joints across an unstable equilibrium point may provide design guidelines for synergetic contraction of multiple muscles or reciprocal control to trigger flexion and extension during the swing phase. As a follow-up, we plan to investigate whether natural and efficient locomotion in living animals can be

achieved by introducing joints with nonlinear properties, such as EDM, to robots. In addition, because the EDM achieved in this study was based on static experiments, it is necessary to clarify the function of the EDM in dynamic locomotion.

## Chapter 5

# Construction of locomotion mechanisms in dinosaurs

### Note

This chapter is the author's version of the following article:

Kazuki Ito, Tetsuya Kinugasa, Tsukasa Okoshi, Kentaro Chiba, Ryuji Takasaki, Damdinsuren Idersaikhan, Ryota Hayashi, Koji Yoshida, and Koichi Osuka, "Can Dinosaurs' Hindlimb Maintain their Stance Posture Using the Passive Interlocking Mechanism Confirmed in Crocodylian Hindlimb?", *AROB-ISBC-SWARM 2024*, OS15-5, Beppu, Japan, 2024.

### 5.1 Introduction

Animals possess a musculoskeletal tendinous system that comprises multiple joints and redundant muscle configurations, resulting in a highly complex multi-degree-of-freedom system. Revealing the essential mechanisms required for animal locomotion proved to be challenging but attracted much scientific attention not only in biology but also in robotics. Merely elucidating how individual muscles generate force might not inherently lead to a comprehensive understanding of overall locomotion. Functional anatomical studies demonstrate that passive interlocking mechanisms achieved by the coordination of multiple muscles, tendons, and bones are vital to producing remarkably smooth limb movements with minimal activation of muscles in horses [19], birds [24], [26], and crocodiles [25], [64]. Reproducing such passive mechanisms by synthesizing robots has been shown to emerge the natural motion of animals in studies [22], [33], [34], [64], [66], [67]. These studies underscore the significance of comprehending the intricately connected muscle systems and replicating them through physical models to reveal the underlying mechanisms of animal locomotion.

The approach to understanding locomotion through robotic replications is not exclusive to extant species; it can be extended to those that are extinct. The locomotion and musculoskeletal system supporting it were lost through fossilization, and therefore, validating their efficacy through the replication of physical models is highly informative to locomotive strategies of extinct animals. Previous studies have employed computer simulations to analyze the locomotion of extinct species e.g., [16], [18]. However, mathematical models inherently lose information during the modeling process, and there might be numerous aspects that can only be understood through the replication of physical models.



FIGURE 5.1: A reconstructed skeleton of *Protoceratops andrewsi* (cast) at the Museum of Dinosaur Research, Okayama University of Science.

This study, therefore, aims to elucidate and reconstruct the musculoskeletal tendinous systems present in extinct species by establishing a physical model based on actual fossil specimens. This report presents a physical model based on a remarkably well-preserved fossil specimen of a non-avian dinosaur, *Protoceratops andrewsi* (Fig. 5.1). We emulate the passive interlocking mechanism supported by certain muscles and tendons observed in the hindlimbs of crocodiles, extant relatives of non-avian dinosaurs. Using the physical model with the emulated passive systems, we demonstrate the ability to stand upright and maintain a stance posture in *Protoceratops* through robotic experiments.

## 5.2 Material and Method

To reconstruct a physical model of a dinosaur, we used a cast of *Protoceratops andrewsi* skeleton with the musculotendinous system for maintaining a stance posture implemented based on the passive interlocking mechanism of the crocodylian hindlimb [64].

### 5.2.1 Skeletal model of *Protoceratops andrewsi*

A cast of the nearly complete *Protoceratops andrewsi* skeleton was utilized for this study. This species is a small-bodied quadruped herbivorous ceratopsian dinosaur and is represented by numerous well-preserved skeletons from the Upper Cretaceous Djadokhta Formation in the Gobi Desert, Mongolia [68]. It was collected at Tugrikin Shireh on August 28, 1993, during the Hayashibara Museum of Natural Sciences and the Mongolian Paleontological Center Joint Expedition [69]. The specimen preserves a nearly complete skeleton, lacking only the rostral region of the skull and the tip of the tail. It measures approximately 1.7 meters in length and is estimated to weigh around 106-179 kilograms based on the estimation formula by Campione and Evans [70]. The specimen is minimally deformed by taphonomic processes. The skeleton is now housed in the Institute of Paleontology of the Mongolian Academy of Sciences in Ulaanbaatar, Mongolia, and the specimen number is MPC-D 100/531. The skeletal cast was reconstructed in a standing posture at the former

Hayashibara Museum of Natural Sciences in Okayama, Japan (Fig. 5.1) [71], and later transferred to the Museum of Dinosaur Research, Okayama University of Science. The reconstructed standing posture, including each joint angle, is congruent with that of the independent study of *Protoceratops* locomotion [72]. Three-dimensional digital models of the pelvic girdle and each hindlimb element were created based on the isolated casts of the bones using photogrammetry [73] and X-ray computed tomography (CT) scanning. The photogrammetric models were created using Metashape Standard version 1.7.3 (Agisoft, Russia). The casts were CT scanned using Latheta LCT-200 (Hitachi Aloca Medical, Japan). The obtained CT images were rendered using VGSTUDIO MAX 3.4 (Volume Graphics, Germany) and segmented using 3DSlicer version 5.3 [74].

### 5.2.2 Stance mechanism based on the passive interlocking of the musculotendinous system in crocodylian hindlimb

We implemented the musculotendinous system onto the skeletal model of *Protoceratops* based on the passive interlocking mechanism of the crocodylian hindlimb, maintaining a stance posture. The mechanism achieves a stance posture using the caudofemoralis longus (CFL), the branched tendon of the CFL (CFLT), and the gastrocnemius externus (GE) in crocodylians (Fig. 5.2A [64]). The CFL, the largest muscle around the hindlimbs, originates from the third to fifteenth caudal vertebrae and inserts into the fourth trochanter on the posterior side of the femur. A thick tendon (CFLT) branches slightly distal to the CFL insertion, connecting to the GE, and forms a Y-shaped junction (Fig. 5.2B). The GE originates from the lateral femoral epicondyle, descends alongside the tibia, and inserts into the flexor digitorum longus around the metatarsi, which inserts into the ventrodorsal aspect of the phalanges [38].

This musculotendinous arrangement is based on our previous anatomical studies of *Crocodylus porosus* [64] and other previous studies of multiple crocodylian species [29], [38]. The mechanism of crocodylian hindlimbs to support weight and maintain a stance posture is performed through the traction generated by the active contraction of the CFL and the ground reaction forces (GRF). The active contraction of the CFL  $F_{CFL}$  results in traction of the femur, causing extension of the hip joint, and simultaneously generates the tension of the CFLT  $T_{CFL}$  posterodorsally (Fig. 5.2B). If the hindfoot makes contact with the ground when the CFL is activated, the GRF affects the ankle joint's dorsiflexion, resulting in tension  $T_{GRF}$  that pulls the Y-shaped junction posterovernally along the GE. The active contraction of the CFL  $F_{CFL}$  results in traction of the femur, causing extension of the hip joint, and simultaneously generates the tension of the CFLT  $T_{CFL}$  posterodorsally (Fig. 5.2B). At this moment, considering the combined forces acting on the Y-shaped junction formed by the CFLT and GE -  $T_{CFL}$  and  $T_{GRF}$  - the resultant force  $F_{CFL+GRF}$  pulls the Y-shaped junction posteriorly.  $F_{CFL+GRF}$  acts as a force that pulls the lateral femoral epicondyle, which is the origin of the GE, posteriorly through the Y-shaped junction, leading to the extension of the knee joint if the foot does not slip. Essentially, upon hindfoot contact with the ground, the stance posture in the hindlimb can be accomplished and maintained solely through the traction exerted by the CFL and the passive joint coordination in crocodylians. This interlocking mechanism within the crocodylian hindlimb musculotendinous system for maintaining a stance posture was verified through robotic experiments in our previous study [64].



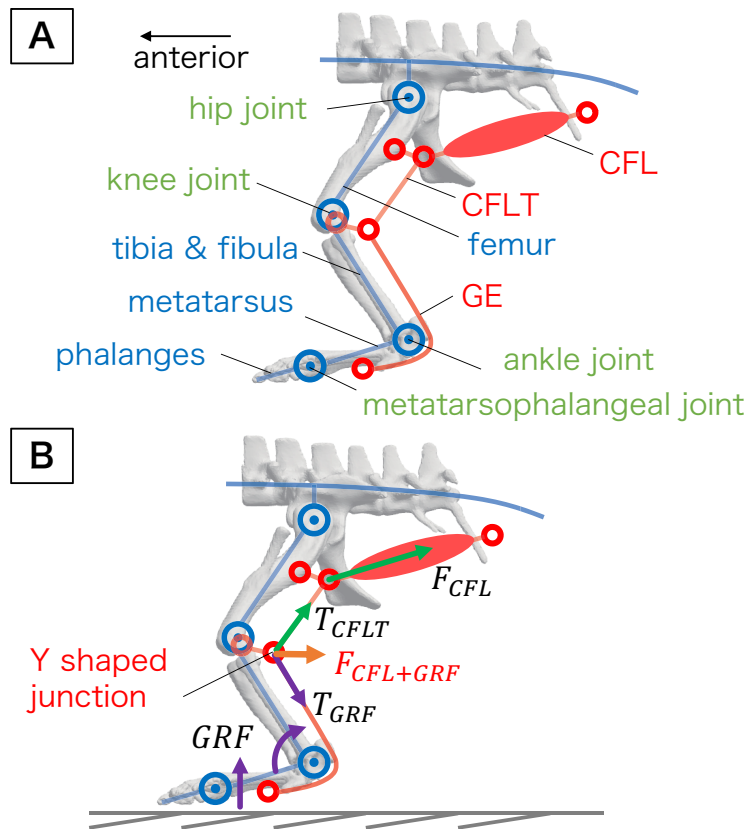


FIGURE 5.2: A. The schematic diagram of the stance posture maintenance mechanism in crocodilian hindlimbs. B. summarized representations of generated forces.

## 5.3 Result

### 5.3.1 Reconstruction of the *Protoceratops* hindlimb musculoskeletal tendinous system

We implemented the musculotendinous system to the *Protoceratops* hindlimb based on that of crocodilians, primarily focusing on the passive interlocking mechanism (Fig. 5.3). To reconstruct soft tissue structures of extinct animals that are rarely fossilized, paleontologists have utilized inferences from extant relatives (e.g., [8]). The origin and insertion points of the CFL, CFLT, and GE are regarded as consistent among archosaurs, including extant crocodilians, extinct non-avian dinosaurs, and extant birds [12], [13], [15], [16], [22], [27], [28], [36], [37], [75]–[85]. Therefore, these muscles can be implemented in the *Protoceratops* model with high certainty. Additionally, we introduced the gastrocnemius internus (GI) and the iliotibialis (IT) muscles, which are also consistent among archosaurs, as passively functioning elements (e.g., [14], [16]). The GI originates from the medial surface of the proximal end of the tibia and inserts onto the plantar surface of the metatarsals in crocodilians [29], [38]. In our previous research [64], introducing the GI into the crocodilian hindlimb musculoskeletal model limits excessive dorsiflexion of the ankle joint, avoiding collision between the tibia and metatarsi. Furthermore, we assumed that the addition of the GI to the *Protoceratops* skeleton is essential to maintain the digitigrade posture observed in non-avian

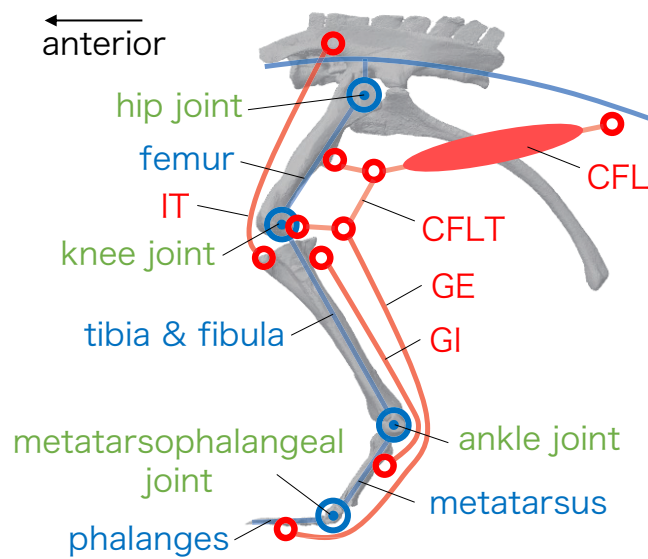


FIGURE 5.3: Reconstructed musculoskeletal tendinous system to achieve a stance posture in *Protoceratops*.

dinosaurs by passively restricting the range of dorsiflexion in the ankle joint. Such passive support of the ankle joint by elastic stretch of the muscles was also predicted to have been present in dinosaurs by Bishop et al. [16] and Sellers et al. [18]. The IT in crocodilians originates from the dorsal border of the iliac blade and inserts into the cnemial crest of the tibia [29], [38]. Our previous study [67] revealed that introducing the IT into the crocodilian hindlimb musculoskeletal model results in passive extension of the knee joint, coordinating with the extension of the hip joint. The inclusion of IT is assumed to be critical to maintaining a more upright stance for dinosaurs compared to crocodilians.

### 5.3.2 Design of the *Protoceratops* hindlimb robot

We designed the *Protoceratops* hindlimb robot (Fig. 45.4), combining the pelvic and hindlimb elements with the hip joint, knee joint, ankle joint, and metatarsophalangeal joint (only the second digit) as single-axis rotational joints (Fig. 5.4B). These joints were equipped with potentiometers to measure the relative angles (Fig. 5.4A). We fixated the constructed pelvic and hindlimb elements onto the aluminum frames that imitating dorsal and caudal vertebral column. Additionally, a single-axis rotational joint was positioned at the equivalent point of the shoulder joints and connected to imitated forelimbs (Fig. 5.4C). The imitated forelimbs are equipped with casters to slide on the ground, enabling movement in the horizontal plane. To prevent lift force due to their lighter weight compared to the hindlimbs, we attached 5 kg weights to the forelimbs. We then implemented the artificial musculotendinous system (Fig. 5.3). The CFL was implemented using two McKibben-type pneumatic actuators (MPAs) arranged in parallel. Other passive muscles and tendons were reconstructed using Kevlar lines. The natural lengths of the GI, GE, and IT elements were configured to be adjustable. The dimensions of the robot are approximately 1.6 m in length, 0.7 m in height, and 0.6 m in width, weighing around 16 kg.

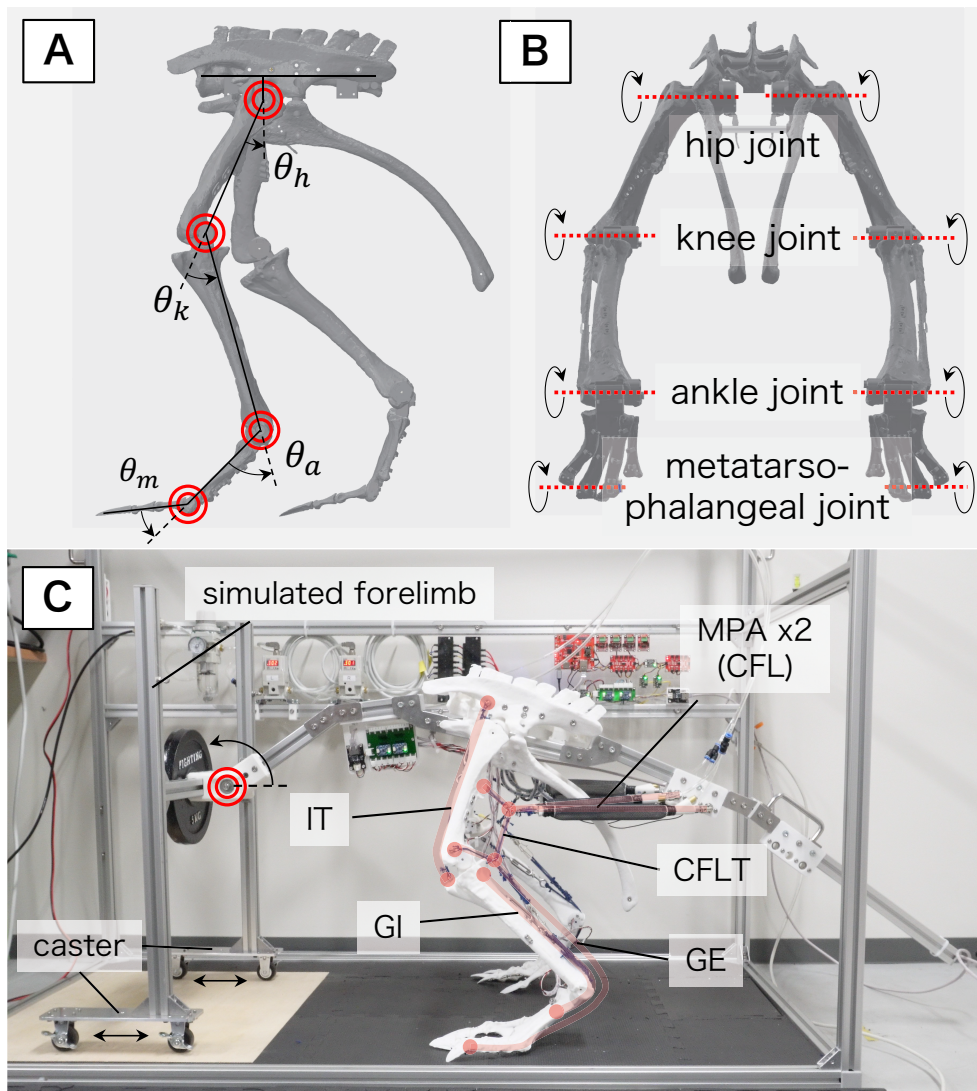


FIGURE 5.4: A. Left lateral view of *Protoceratops* hindlimb region showing the positions of joint axes. B. Anterior view of the hindlimb region. C. Experimental system using the physical model of the *Protoceratops* hindlimb.

### 5.3.3 Experiment of upright standing and maintaining the posture

The experiments verified that the *Protoceratops* hindlimb robot successfully performs standing upright motion and maintains the stance posture (Fig. 5.5). The experiments started from an initial posture resembling a crouched posture with flexed knee and hip joints. The pressure within the MPAs, representing the CFL, was increased at a constant rate from the atmospheric pressure, causing gradual contraction. Around the relative pressure of 200 kPa, the hip and knee joints began extending. At approximately 300 kPa, the posture resembles the stance posture of the reconstructed skeleton, illustrated in Fig. 5.1. We replicated the experiment ten times and recorded the relative angles of the joints in each hindfoot according to the MPA pressure (Fig. 5.6). The results showed that the robot successfully stood upright and maintained the stance almost identically regardless of uncertainties (e.g., differences in initial condition) in all tests.

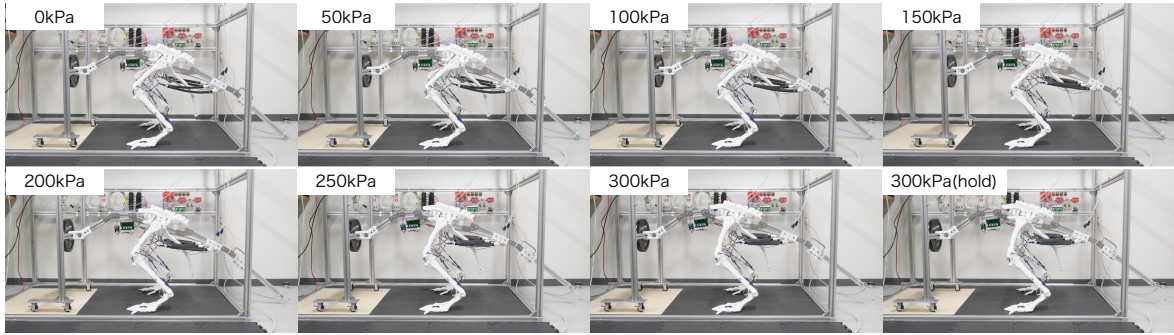


FIGURE 5.5: A sequence of movement of *Protoceratops* hindlimb robot in response to the change of the MPA pressure.

## 5.4 Conclusions

This report demonstrates that the implementation of the passive interlocking mechanism, seen in crocodylian hindlimbs, enables *Protoceratops andrewsi* to achieve a stance posture solely by the activation of the CFL with the coordination of the passive musculotendinous structures and GRF. The importance of such passive mechanisms in the study of dinosaur locomotion has been raised but not investigated (e.g., [16], [18]). The robotic approaches of this study, in contrast, directly contributed to understanding passive mechanisms in dinosaur locomotion. The measurement of the forces acting upon each muscle and tendon element, as well as ground reaction forces, will facilitate a more thorough investigation into the mechanics behind how dinosaur musculoskeletal systems achieve the stance posture relevant to their locomotion.

Now, we have the *Protoceratops* robot that is capable of standing upright, and the apparatus serves as an effective platform to investigate other musculoskeletal systems to achieve different aspects of locomotion (e.g., walking) in *Protoceratops*. This study highlights that constructing physical models based on original fossil specimens is a highly effective scheme to emulate the locomotion and the underlying musculoskeletal tendinous systems in various extinct species beyond non-avian dinosaurs.

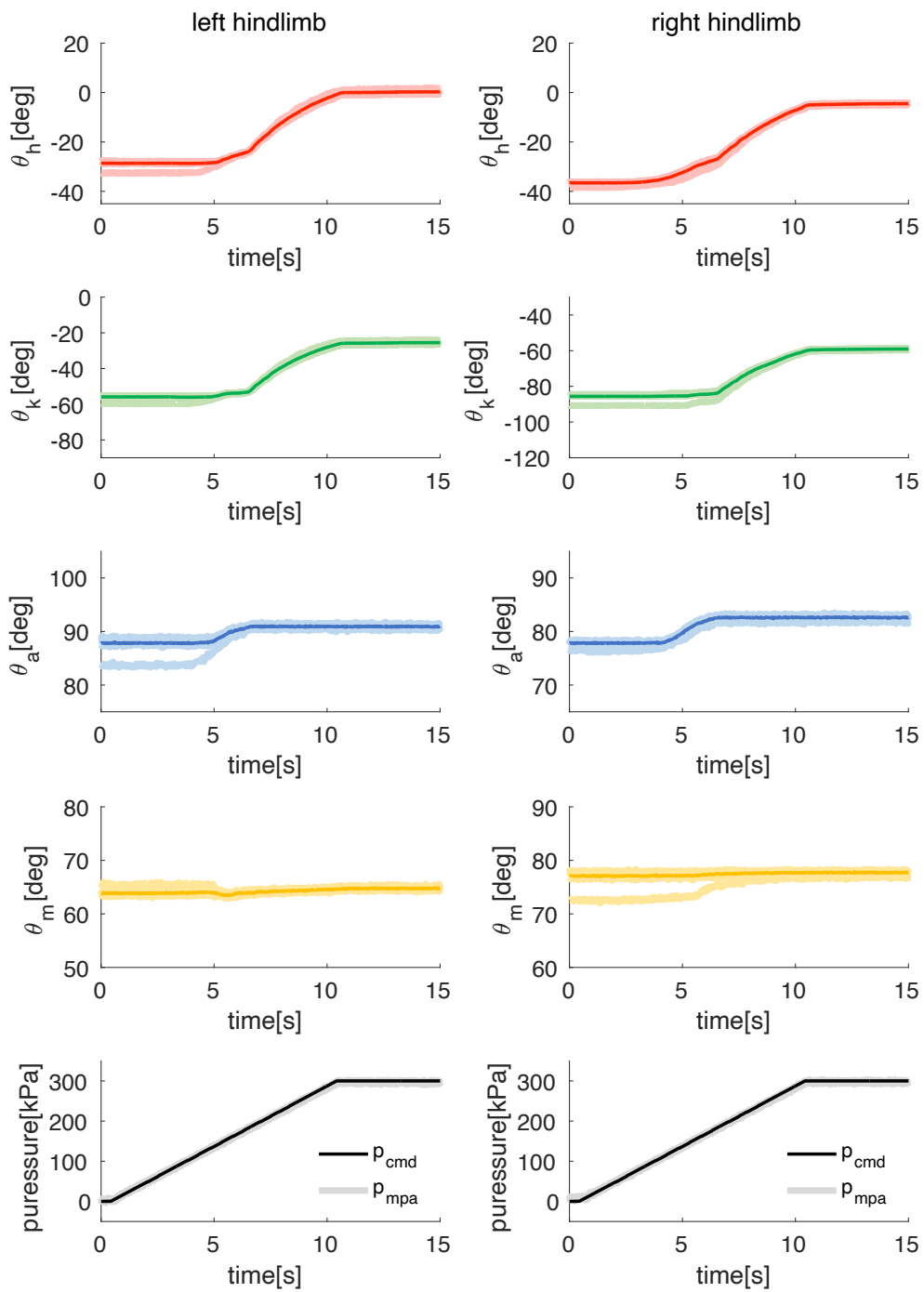


FIGURE 5.6: The relative angle of each joint according to the MPA pressure. The lighter solid lines represent the variations in the relative angles over ten trials, while the darker solid line represents their averages.

## Chapter 6

# General discussion

### 6.1 Evaluation of the efficacy of the proposed approach

In order to reveal the locomotion mechanism of dinosaurs in which the active function and passive function of the musculoskeletal system are harmonized, we first followed STEP1 of the proposed approach. We revealed the stance mechanism, which is the basis of locomotion, based on the mechanical functional morphology of the crocodylian musculoskeletal system, as shown in Chapters 2 and 3. Then, in Chapter 5, we succeeded in realizing the stance posture of the dinosaur hindlimb by applying the mechanical functional morphology that realizes the stance posture of the crocodylian hindlimb to the dinosaur skeleton. The approach of constructing the muscular system of the dinosaur hindlimb is based on the mechanical functional morphology of the crocodylian hindlimb, which is different from the approach of reconstructing the dinosaur muscular system based on the extant phylogenetic bracket that has been used so far. Then, are there differences between our muscular system and the dinosaur muscular system reconstructed based on the EPB? In this study, we confirmed how the muscles CFL, CFLT, GE, GM, and IT that make up the dinosaur muscle system were inferred in previous studies [12], [15], [16], [78], [79].

The EPB assesses the presence of specific soft tissues by evaluating them through Levels of Inference, which indicate three levels of confidence based on the evidence of correlation within the encompassing taxa that serve as a reference. Firstly, when both extant species bracketing an extinct organism share a specific soft tissue and its associated osteological features, it constitutes the highest level of inference (Level 1). This suggests a very high probability that the extinct organism also possessed that soft tissue. Secondly, when only one of the extant species has the specific soft tissue, it is considered an intermediate level of inference (Level 2). In this case, since the soft tissue is not universal in both extant species, it becomes uncertain whether the extinct species had that feature. Lastly, when neither of the extant species possesses the specific soft tissue, it is classified as the lowest level of inference (Level 3). Here, the inference is highly speculative, and any hypothesis about the presence of that soft tissue in the extinct species is based on very weak evidence. Additionally, in the EPB, when inferring soft tissues without osteological evidence, such as attachment marks on bones, three corresponding levels (Level 1', 2', 3') are defined.

First, for CFL, GE, GI, IT, the highest level of inference (Level 1 or 1') has been predicted for their presence in the hindlimb musculoskeletal system of dinosaurs, as shown by Carrano et al. [15], Schachner et al. [78], Piechowski et al. [12], Bishop et al. [16], and Smith et al. [79]. This suggests a very high probability of their existence in this context. On the other hand, the inference for the tendon CFLT, which diverges from the CFL, has been estimated



only by Carrano et al., and it is at an inference Level 2 [24]. In the case of CFLT, a difference arises between the proposed approach and the EPB methodology.

The most crucial difference is that the EPB approach [12], [16], [78], [79] does not recognize CFLT as a component of the muscular system. Since the musculoskeletal system is composed of dozens of muscles, it may not be considered that tendons that do not have active functions exist, as it would require a huge amount of effort to infer all of their existence. In addition, since CFLT exists only in crocodylians and its function has not been shown to be necessary so far, it may not have been considered in the EPB. Furthermore, there is also a difference in the possibility of the existence of CFLT. Carrano et al. inferred the CFLT at Level 2, suggesting that the CFLT in the musculoskeletal system of *Tyrannosaurus Rex* is reduced or absent. On the other hand, in the muscular system that realizes the stance of crocodylians and dinosaurs revealed in this study, CFLT was an essential element that realizes the passive interlocking of joints. Based on this result, the CFLT existed with a very high probability.

However, even if the proposed approach can be used to propose a locomotion mechanism for dinosaurs, it is difficult to guarantee its rationality. In order to understand a more rational mechanism, it is essential to construct a mechanism in a broader framework, such as all reptiles or all terrestrial vertebrates, rather than just the closest species of dinosaurs. For example, since CFLT has been confirmed to exist in lizards [36], [86], it is also essential to understand the locomotion mechanism based on the mechanical functional morphology of the lizard hindlimb.

## 6.2 Summary of this dissertation

Dinosaurs were one of the most successful species of terrestrial vertebrates that ever existed on Earth, and they succeeded in long-term prosperity and unparalleled diversification of their bodies. Their forms ranged from bipedal and quadrupedal to small and large, with some exceeding 20 m in length. The locomotion mechanism that supported their diverse bodies and prosperity was very versatile in relation to their body size and was well adapted to the terrestrial environment of the Earth. If such an excellent locomotion design principle is revealed, we might enrich engineering knowledge, such as the development of walking robots.

In order to reveal the design principle of locomotion of dinosaurs, it is necessary to clarify the locomotion mechanism based on the mechanical function realized by the morphology of the limb's musculoskeletal system, which is the source of locomotion. Such locomotion of terrestrial vertebrates is realized not only by the active action of muscles but also by the passive behavior of the skeleton, muscles, tendons, and the interaction with the environment. Against this background, this study aims to clarify the locomotion mechanism of dinosaurs in which the active function and the passive function of the musculoskeletal system, which is the source of locomotion, are well combined.

However, the only remaining element that makes up the musculoskeletal system of dinosaurs is the skeleton. Therefore, the morphology and function of soft tissues such as muscles and tendons need to be restored based on the musculoskeletal system of dinosaurs' relatives, crocodiles, and avians. For this purpose, this study first clarifies the fundamental locomotion mechanism of crocodiles and avians, which are closely related species. Then, the fundamental mechanism of locomotion of closely related species is applied to the skeleton of dinosaurs to construct the musculoskeletal system, and it is verified whether the same



movement as that of closely related species can be realized. Finally, the fundamental mechanisms based on crocodiles and avians are integrated to construct the locomotion mechanism of dinosaurs.

In this doctoral dissertation, as part of the proposed approach, we first attempted to elucidate the fundamental locomotion mechanisms of crocodylians and avians by using dissection and physical modeling. Next, we constructed a musculoskeletal system of dinosaurs based on the mechanisms obtained from extant sisters and verified whether it is possible to realize locomotion similar to extant sisters.

Chapter 2, we attempted to elucidate the mechanism by which crocodylians achieve a standing posture during the stance phase of locomotion (high walk) without touching their bellies to the ground and by keeping their limbs upright, as dinosaurs do, by using dissection and physical modeling. In the dissection, we hypothesized that the standing posture of the hindlimb is achieved by the passive coordination of the main joints of the hindlimb by the traction force of the caudifemoralis longus muscle, which originates from the tail and stops at the femur, and the ground reaction force obtained by the interaction with the environment. To verify this hypothesis, we created a physical model of the skeleton by CT scanning the hindlimb bones and reconstructing them with joints. Then, we constructed a robotic model of the musculoskeletal system by placing caudifemoralis longus, gastrocnemius externus, and a tendon connecting the two muscles. When traction force was applied to this model, it was able to achieve a standing posture, and further increasing the traction force generated a movement similar to the stance phase of a high walk. Furthermore, when the gastrocnemius muscle internus was added to this musculoskeletal system as a passive muscle, it prevented the collision between the tibia and the metatarsal bone caused by excessive dorsiflexion of the ankle joint. This result revealed that gastrocnemius internus passively restricts the range of motion of the ankle joint in the dorsiflexion direction by elongating at its natural length.

Chapter 3, we experimentally investigated the mechanical function of the iliotibialis muscle, a two-joint muscle that spans the hip and knee joints, using the physical model of the crocodylian hindlimb bones created in Chapter 2. As a result, it was revealed that the iliopsoas restrict the range of motion of hip extension and knee flexion by elongating at its natural length, thereby coordinating the movements of both joints. Furthermore, adding the iliotibialis muscle to the stance mechanism of the crocodylian hindlimb revealed that it assists in knee extension and increases the frictional force around the calcaneus throughout the stance phase.

Chapter 4, we investigated in detail the mechanism by which the engage-disengage mechanism (EDM), known to extend or flex the joint passively, is realized in the intertarsal joint of running birds using dissection and physical modeling. First, we investigated the muscles and ligaments that contribute to the action of the EDM by dissection and then constructed a physical model to reproduce the function of the EDM using a three-dimensional model of the ostrich skeleton. As a result, it was shown that the articular surface of the distal end of the metatarsal bone has a cam-like function by measuring the passive rotational torque of the intertarsal joint and the displacement of the spring that mimics the ligament. Furthermore, it was revealed that the articular surface shape that realizes the EDM can be determined mainly by the arrangement and displacement of the two medial ligaments, LCML and LCM. The mechanism of passively generating joint movement by the cam-like shape of the distal end of the bone and the constraint of the ligament may exist in

joints other than the intertarsal joint, providing a new perspective on joint control. In addition, by introducing such a joint into the design of a walking machine, it is possible to realize the passive interlocking of joint movement and simplify the control of the swing phase of locomotion.

Chapter 5, we attempted to verify the possibility of realizing a standing posture by introducing the standing mechanism of the crocodilian hindlimb into the skeleton of dinosaurs homologously. First, we constructed a hindlimb skeletal model of dinosaurs using the skeleton of *Protoceratops andrewsi*, and then constructed a physical model of the hindlimb musculoskeletal system by constructing a muscle system that passively interlocks to achieve a standing posture as observed in the crocodilian hindlimb. Using this model, we achieved a standing posture as in crocodilians by actively contracting the caudifemoralis longus muscle. Furthermore, it was confirmed that even if the initial posture was different, it converged to a specific stance posture, indicating the possibility of controlling the trajectory by passively restricting the joint's range of motion by the muscle's passive behavior.

The locomotion mechanism of dinosaurs that could be revealed in this doctoral dissertation was limited to the mechanism that realizes the standing posture of the hindlimb. However, we were able to show a locomotion mechanism in which the active function and the passive function of the musculoskeletal system are well combined, which could not be revealed by the reconstruction of the morphology of the muscle system by extant phylogenetic bracketing as in previous studies [16], [17]. In previous studies on locomotion based on the musculoskeletal dynamics model of dinosaurs, the primary approach was to construct locomotion by adjusting the timing of activation of many muscles by trajectory tracking or optimization methods. However, as shown in this study, the musculoskeletal system of dinosaurs autonomously controls part of the locomotion by the coordination of multi-joint caused by the insert at multiple points of muscles and tendons and the connection with other muscle systems and the restriction of the range of motion of the joint caused by the elastic tension due to the elongation at the natural length of the muscles and tendons. These functions are the essence of the morphology of the musculoskeletal system, and unraveling the mechanical intention of the morphology will lead to a better understanding of the mechanism of natural locomotion.

### 6.3 Future work

The locomotion mechanism of dinosaurs that could be revealed in this dissertation was limited to the fundamental mechanism of achieving a stance posture of the hindlimb. This result is only a tiny part of the locomotion mechanism of dinosaurs. In order to understand the overall locomotion mechanism of dinosaurs, it is necessary to clarify the mechanisms of the stance phase, the swing phase, the coordination of the left and right limbs, and the movement of the forelimbs. To this end, it is necessary to fully elucidate the basic locomotion mechanisms of crocodilians and avians, which are the basis for constructing dinosaur locomotion.

In addition, if we can reveal the locomotion mechanism based on the morphology and function of the musculoskeletal system of crocodilians and avians according to the approach of this study and reproduce it by a physical model, it is necessary to evaluate whether it is plausible. This evaluation can be performed by comparing the observed data of actual animal locomotion, such as the range of motion of the joints [25], [31], [46], [50], [52], ground

reaction force [31], walking patterns of each limb [43], and muscle activation patterns [31], [32], [50]. However, for the locomotion of dinosaurs constructed based on the locomotion mechanism of closely related species, it is impossible to evaluate it based on the observed data of actual locomotion because they are extinct. In this regard, the range of motion of the joints estimated from the skeleton [16], [44], [87] and the footprints that preserve the behavior of dinosaur locomotion [88] will be clues for the evaluation.

Finally, the ultimate goal of this study was to construct a general locomotion design principle that can be applied to various forms based on the locomotion mechanism of dinosaurs. In order to achieve this goal, it is necessary to apply the locomotion mechanism of dinosaurs revealed in this study to skeletons of dinosaurs with various sizes and gaits and verify whether locomotion can be realized. In this case, it is important to know what elements can be parameters when applying them to the skeleton of dinosaurs. For example, in this study, when the stance mechanism of the crocodylian hindlimb was applied to the skeleton of dinosaurs, the stance posture was realized only by the active traction of the caudifemoralis longus muscle by adjusting the length of each muscle and tendon as parameters. These parameters will be revealed by applying them to skeletons of dinosaurs with various forms. The other parameters are expected to include the presence or absence of active action of each muscle, viscoelasticity of the muscle system, and the timing of contraction of each muscle when there are multiple active muscles.

Furthermore, once the elements of the parameters are known, the next task is to determine the values of the parameters. In this study, when the stance mechanism of the crocodylian hindlimb was applied to the dinosaurs' skeleton, the muscle system's length that realizes the standing posture was searched for by trial and error. However, suppose a musculoskeletal dynamics model is constructed, and the condition of each muscle length or tension that maintains the standing posture by the balance of muscle tension is obtained. In that case, it can be used as indices. However, when determining the parameter value based on the mechanical analysis, it is expected that the problem of which solution to choose will arise when multiple solutions exist. In order to solve this problem, it is necessary to clarify the indicators derived from the locomotion of crocodylians and avians, which are the basis of the dinosaur's mechanism.

Through the above process, if the locomotion mechanism based on the morphology and mechanical function of the musculoskeletal system of dinosaurs and the parameters applied to various forms are revealed, the framework for realizing universal terrestrial locomotion might be constructed (Fig. 6.1).

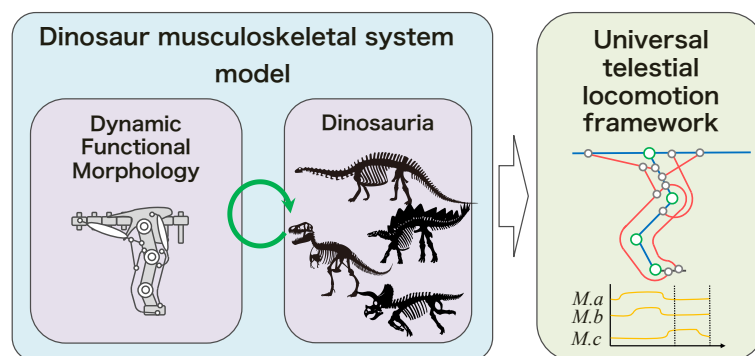


FIGURE 6.1: The process of constructing the universal terrestrial locomotion framework.



## *Acknowledgements*

I am deeply indebted to Prof. Koichi Osuka of Osaka University for his unwavering support as the primary supervisor of this doctoral dissertation. Since my admission to the doctoral program at Osaka University, Prof. Osuka has been instrumental in guiding my research journey, offering invaluable advice on research policies and generous financial support. I extend my heartfelt gratitude to Prof. Tetsuya Kinugasa of Okayama University of Science, who inspired me to pursue a career in robotics research. His constant support throughout my academic journey, from my senior undergraduate year to my postdoctoral program, has been invaluable. My sincere thanks go to Prof. Sinobu Isigaki, Dr. Kentaro Chiba, and Dr. Yu Okuda, all from the Okayama University of Science, for their guidance in the study of dinosaurs and the comparative anatomy of vertebrates. Their provision of opportunities for me to conduct dissections on various animals, including crocodiles and birds, has significantly enriched my research. I am grateful to Prof. Masato Ishikawa and Prof. Mitsuru Higashimori, both from Osaka University, for accepting sub-supervisors' roles and providing numerous valuable suggestions for this doctoral dissertation. There are many others who have contributed to my study, too numerous to list, to whom I owe deep gratitude for their assistance.

Additionally, my gratitude extends to Dr. Ryuji Takasaki of the University of Toronto, Mr. Tsukasa Okoshi, and Ms. Miwa Ichikawa, both from Okayama University, for their pivotal roles in creating 3D data of animal skeletons and assisting in animal dissections. I am also deeply thankful to all the students and staff in the Osuka-Sugimoto laboratory at Osaka University and everyone in the Kinugasa-Yoshida, Hayashi, and Kondo laboratories for their guidance, discussions, and collaboration throughout my student life.

Lastly, I wish to express my profound gratitude to my family—my father, Mikio; my mother, Yuri; my sister, Kanako; and all of my family. They have been my pillars of strength and support; their unwavering faith and love have guided me throughout this life. I am eternally grateful for their support. Thank you.



# Bibliography

- [1] D. Naish, *Dinosaurs : how they lived and evolved*, eng. London, England : Natural History Museum, 2016.
- [2] S. C. Wang and P. Dodson, "Estimating the diversity of dinosaurs," *Proceedings of the National Academy of Sciences*, vol. 103, no. 37, pp. 13 601–13 605, 2006.
- [3] E. J. O Gorman and D. W. E. Hone, "Body Size Distribution of the Dinosaurs," *PLoS ONE*, vol. 7, no. 12, P. Dodson, Ed., e51925, 2012.
- [4] F. Seebacher, "A new method to calculate allometric length-mass relationships of dinosaurs," *Journal of Vertebrate Paleontology*, vol. 21, pp. 51–60, 2001.
- [5] A. Larramendi, "Shoulder Height, Body Mass and Shape of Proboscideans," *Acta Palaeontologica Polonica*, vol. 61, no. 3, pp. 537–574, 2016.
- [6] R. M. Alexander, *Dynamics of Dinosaurs & Other Extinct Giants*. New York: Columbia University Press, 1989.
- [7] H. Bryant and A. Russell, "The occurrence of clavicles within Dinosauria: Implications for the homology of the avian furcula and the utility of negative evidence," *Journal of Vertebrate Paleontology - J VERTEBRATE PALEONTOL*, vol. 13, pp. 171–184, 1993.
- [8] L. Witmer, "The Extant Phylogenetic Bracket and the importance of reconstructing soft tissues in fossils," in *Thomason JJ, editor. Functional morphology in vertebrate paleontology*, Cambridge, UK: Cambridge University Press, 1995, pp. 19–33.
- [9] S. H. Burch, "Complete forelimb myology of the basal theropod dinosaur Tawa hallae based on a novel robust muscle reconstruction method," *Journal of Anatomy*, vol. 225, no. 3, pp. 271–297, 2014.
- [10] A. Otero, "Forelimb musculature and osteological correlates in Sauropodomorpha (Dinosauria, Saurischia)," *PLOS ONE*, vol. 13, no. 7, e0198988, 2018.
- [11] K. K. Voegelé, P. V. Ullmann, M. C. Lamanna, and K. J. Lacovara, "Appendicular myological reconstruction of the forelimb of the giant titanosaurian sauropod dinosaur *Dreadnoughtus schrani*," *Journal of Anatomy*, vol. 237, no. 1, pp. 133–154, 2020.
- [12] R. Piechowski and M. Tałanda, "The locomotor musculature and posture of the early dinosauriform *Silesaurus opolensis* provides a new look into the evolution of Dinosauromorpha," *Journal of Anatomy*, vol. 236, no. 6, pp. 1044–1100, 2020.
- [13] J. R. HUTCHINSON, "The evolution of femoral osteology and soft tissues on the line to extant birds (Neornithes)," *Zoological Journal of the Linnean Society*, vol. 131, no. 2, pp. 169–197, 2001.
- [14] J. R. HUTCHINSON, "The evolution of pelvic osteology and soft tissues on the line to extant birds (Neornithes)," *Zoological Journal of the Linnean Society*, vol. 131, no. 2, pp. 123–168, 2001.



- [15] M. T. Carrano and J. R. Hutchinson, "Pelvic and hindlimb musculature of *Tyrannosaurus rex* (Dinosauria: Theropoda)," *Journal of Morphology*, vol. 253, no. 3, pp. 207–228, 2002.
- [16] P. J. Bishop, A. R. Cuff, and J. R. Hutchinson, "How to build a dinosaur: Musculoskeletal modeling and simulation of locomotor biomechanics in extinct animals," *Paleobiology*, vol. 47, no. 1, pp. 1–38, 2021.
- [17] J. R. Hutchinson, F. C. Anderson, S. S. Blemker, and S. L. Delp, "Analysis of Hindlimb Muscle Moment Arms in *Tyrannosaurus rex* Using a Three-Dimensional Musculoskeletal Computer Model: Implications for Stance, Gait, and Speed," *Paleobiology*, vol. 31, no. 4, pp. 676–701, 2005, Publisher: Paleontological Society.
- [18] W. I. Sellers, L. Margetts, R. A. Coria, and P. L. Manning, "March of the Titans: The Locomotor Capabilities of Sauropod Dinosaurs," *PLOS ONE*, vol. 8, no. 10, e78733, 2013.
- [19] M. Hildebrand, "The Mechanics of Horse Legs," *American Scientist*, vol. 75, no. 6, pp. 594–601, 1987.
- [20] P. R. van Weeren, M. O. Jansen, A. J. van den Bogert, and A. Barneveld, "A kinematic and strain gauge study of the reciprocal apparatus in the equine hind limb," *Journal of Biomechanics*, vol. 25, no. 11, pp. 1291–1301, 1992.
- [21] Keith M. Dyce, Wolfgang O. Sack, and Cornelis Johannes Gerardus Wensing, *Dyce, Sack, and Wensing's Textbook of Veterinary Anatomy*, 3rd ed. Philadelphia; London: Saunders, 2002.
- [22] Noble S. Proctor, *Manual of ornithology : avian structure & function*. New Haven : Yale University Press, 1998.
- [23] P. M. Galton and J. D. Shepherd, "Experimental Analysis of Perching in the European Starling (*Sturnus vulgaris*: Passeriformes; Passeres), and the Automatic Perching Mechanism of Birds," *Journal of Experimental Zoology Part A: Ecological Genetics and Physiology*, vol. 317, no. 4, pp. 205–215, 2012.
- [24] N. U. Schaller, B. Herkner, R. Villa, and P. Aerts, "The intertarsal joint of the ostrich (*Struthio camelus*): Anatomical examination and function of passive structures in locomotion," *Journal of Anatomy*, vol. 214, no. 6, pp. 830–847, 2009.
- [25] A. L. A. Wiseman, P. J. Bishop, O. E. Demuth, A. R. Cuff, K. B. Michel, and J. R. Hutchinson, "Musculoskeletal modelling of the Nile crocodile (*Crocodylus niloticus*) hindlimb: Effects of limb posture on leverage during terrestrial locomotion," *Journal of Anatomy*, vol. 239, no. 2, pp. 424–444, 2021.
- [26] J. W. Rankin, J. Rubenson, and J. R. Hutchinson, "Inferring muscle functional roles of the ostrich pelvic limb during walking and running using computer optimization," *Journal of The Royal Society Interface*, vol. 13, no. 118, p. 20160035, May 2016.
- [27] S. Haughton, "Notes on Animal Mechanics: No. 6. On the Muscular Anatomy of the Crocodile," *Proceedings of the Royal Irish Academy (1836-1869)*, vol. 9, pp. 268–277, 1864, Publisher: Royal Irish Academy.
- [28] J. Sutton, "The Nature of Ligaments: Part IV," *Journal of anatomy and physiology*, vol. 20, no. Pt 1, 1885.

- [29] V. Allen, J. Molnar, W. Parker, A. Pollard, G. Nolan, and J. R. Hutchinson, "Comparative architectural properties of limb muscles in Crocodylidae and Alligatoridae and their relevance to divergent use of asymmetrical gaits in extant Crocodylia," *Journal of Anatomy*, vol. 225, no. 6, pp. 569–582, 2014.
- [30] D. Suzuki and S. Hayashi, "Myology of crocodiles II : Pectoral girdle and forelimb," vol. 89, 2010, pp. 83–102.
- [31] S. M. Reilly, J. S. Willey, A. R. Biknevičius, and R. W. Blob, "Hindlimb function in the alligator: Integrating movements, motor patterns, ground reaction forces and bone strain of terrestrial locomotion," *Journal of Experimental Biology*, vol. 208, no. 6, pp. 993–1009, 2005.
- [32] A. R. Cuff, M. A. Daley, K. B. Michel, *et al.*, "Relating neuromuscular control to functional anatomy of limb muscles in extant archosaurs," *Journal of Morphology*, vol. 280, no. 5, pp. 666–680, 2019.
- [33] K. Miyashita, Y. Masuda, M. Gunji, A. Fukuhara, K. Tadakuma, and M. Ishikawa, "Emergence of Swing-to-Stance Transition from Interlocking Mechanism in Horse Hindlimb," in *2020 IEEE/RSJ International Conference on Intelligent Robots and Systems (IROS)*, 2020, pp. 7860–7865.
- [34] A. Badri-Spröwitz, A. Aghamaleki Sarvestani, M. Sitti, and M. A. Daley, "BirdBot achieves energy-efficient gait with minimal control using avian-inspired leg clutching," *Science Robotics*, vol. 7, no. 64, eabg4055, 2022.
- [35] C. E. Doyle, J. J. Bird, T. A. Isom, *et al.*, "An Avian-Inspired Passive Mechanism for Quadrotor Perching," *IEEE/ASME Transactions on Mechatronics*, vol. 18, no. 2, pp. 506–517, 2013.
- [36] R. C. Snyder, "Adaptations for bipedal locomotion of lizards," *American Zoologist*, vol. 2, no. 2, pp. 191–203, 1962.
- [37] S. M. Gatesy, "Caudofemoral musculature and the evolution of theropod locomotion," *en, Paleobiology*, vol. 16, no. 2, pp. 170–186, 1990.
- [38] D. Suzuki, K. Chiba, Y. Tanaka, and S. Hayashi, "Myology of crocodiles III : Pelvic girdle and hindlimb," *Fossils*, vol. 90, pp. 37–60, 2011.
- [39] A. Otero, P. Gallina, and Y. Herrera, "Pelvic musculature and function of Caiman latirostris," *The Herpetological Journal*, vol. 20, pp. 173–184, Jul. 2010.
- [40] P. O. Fuller, T. E. Higham, and A. J. Clark, "Posture, speed, and habitat structure: Three-dimensional hindlimb kinematics of two species of padless geckos," *Zoology*, vol. 114, no. 2, pp. 104–112, Apr. 2011.
- [41] D. K. Riskin, C. J. Kendall, and J. W. Hermanson, "The crouching of the shrew: Mechanical consequences of limb posture in small mammals," *en, PeerJ*, vol. 4, e2131, Jun. 2016.
- [42] A. P. Summers and K. T. J., "The evolution of tendon — morphology and material properties," *Comparative Biochemistry and Physiology Part A: Molecular and Integrative Physiology*, vol. 133, pp. 1159–1170, 2002.
- [43] S. M. Reilly and J. A. Elias, "Locomotion in Alligator mississippiensis: Kinematic effects of speed and posture and their relevance to the sprawling-to-erect paradigm," *Journal of Experimental Biology*, vol. 201, no. 18, pp. 2559–2574, 1998.

- [44] J. R. Hutchinson, "The evolution of locomotion in archosaurs," *Comptes Rendus Palevol*, Cent ans après Marey : Aspects de la morphologie fonctionnelle aujourd'hui, vol. 5, no. 3, pp. 519–530, 2006.
- [45] W. S. Persons IV and P. J. Currie, "The Tail of Tyrannosaurus: Reassessing the Size and Locomotive Importance of the *M. caudofemoralis* in Non-Avian Theropods," *The Anatomical Record*, vol. 294, no. 1, pp. 119–131, 2011.
- [46] S. M. Gatesy, "Hind limb movements of the american alligator (*alligator mississippiensis*) and postural grades," *Journal of Zoology*, vol. 224, no. 4, pp. 577–588, 1991.
- [47] A. Otero, P. Gallina, and Y. Herrera, "Pelvic musculature and function of *Caiman latirostris*," *The Herpetological Journal*, vol. 20, pp. 173–184, 2010.
- [48] R. W. Blob and A. A. Biewener, "In vivo locomotor strain in the hindlimb bones of *Alligator mississippiensis* and *Iguana iguana*: Implications for the evolution of limb bone safety factor and non-sprawling limb posture," *Journal of Experimental Biology*, vol. 202, no. 9, pp. 1023–1046, 1999.
- [49] J. S. Willey, A. R. Biknevicius, S. M. Reilly, and K. D. Earls, "The tale of the tail: Limb function and locomotor mechanics in *Alligator mississippiensis*," *Journal of Experimental Biology*, vol. 207, no. 3, pp. 553–563, 2004.
- [50] S. M. Reilly and R. W. Blob, "Motor control of locomotor hindlimb posture in the American alligator (*Alligator mississippiensis*)," *Journal of Experimental Biology*, vol. 206, no. 23, pp. 4327–4340, 2003.
- [51] J. R. Hutchinson, D. Felkner, K. Houston, *et al.*, "Divergent evolution of terrestrial locomotor abilities in extant Crocodylia," *Scientific Reports*, vol. 9, no. 1, p. 19302, 2019.
- [52] M. Iijima, V. D. Munteanu, R. M. Elsey, and R. W. Blob, "Ontogenetic changes in limb posture, kinematics, forces and joint moments in American alligators (*Alligator mississippiensis*)," *Journal of Experimental Biology*, vol. 224, no. 23, jeb242990, 2021.
- [53] A. Britton, R. Whitaker, and N. Whitaker, "Here be a dragon: Exceptional size in a saltwater crocodile (*Crocodylus porosus*) from the Philippines," *Herpetological review*, vol. 43, no. 4, pp. 541–546, 2012.
- [54] I. Kazuki, H. Sayaka, K. Tetsuya, *et al.*, "Crocodylian knee locking mechanism and intralimb coordination of a hindlimb in the stance phase during high walking," in *Proceedings of the 2022 JSME Conference on Robotics and Mechatronics*, Sapporo, Japan, 2022, 2A1–S06.
- [55] C. Bell, *Die Hand und ihre Eigenschaften*. Translated from the English by F Kottenkamp, original: *The hand, its mechanism and vital endowment as evincing design*. Stuttgart : Paul Reff, 1847.
- [56] K Langer, "Ueber die Fu\ss gelenke der V\{a}gel.," *Denkschr Kaiser-Akad Wissenschaften Wien*, vol. 16, pp. 93–130, 1859.
- [57] H. JW, "Das ellenbogengelenk und seine mechanik," *Jena: Verlag Gustav Fischer*, 1897.
- [58] R. H, "Die bedeutung der federnden gelenke oder schnappgelenke.," *Schweiz Arch Tierheilkd*, vol. 64, pp. 76–87, 1922.
- [59] A. O, "Über die wirkung der ligamenta collateralia nebst bemerkungen über die sogenannten schnappgelenke.," *Z Anat Entwicklungsgesch*, vol. 76, pp. 1–15, 1925.

- [60] P. A., "Zur kenntnis der sogenannten schnappgelenke. i. die ursache des federungsphänomens nebst einigen bemerkungen über die fossae nudatae des ellenbogengelenkes beim pferde.," *Anat Embryol*, vol. 89, pp. 710–745, 1929.
- [61] S. E. F. J. W. K.-H. W. K. Nickel R Schummer A, "Lehrbuch der anatomie der haustiere. 6th edn, vol. 1," 1992.
- [62] M. Hildebrand, *Analysis of Vertebrate Structure*. Wiley, 1995.
- [63] T. McGeer, "Passive dynamic walking," *CSS-IS TR*, vol. 88, no. 2, 1988.
- [64] K. Ito, T. Kinugasa, K. Chiba, *et al.*, "The robotic approach to the passive interlocking mechanism in the hindlimb musculoskeletal system of *Crocodylus porosus*," *Advanced Robotics*, vol. 37, no. 18, pp. 1187–1197, 2023.
- [65] I. V. Laboratory, *Ostrich*.
- [66] A. Abourachid, C. Chevallereau, I. Pelletan, and P. Wenger, "An upright life, the postural stability of birds: A tensegrity system," *Journal of The Royal Society Interface*, vol. 20, no. 208, p. 20230433, 2023.
- [67] K. Ito, T. Kinugasa, S. Hida, K. Yoshida, R. Hayashi, and K. Osuka, "Interlocking mechanism in the hindlimb using a passive musculotendinous structure during the high walk of crocodylians: Validation of the effects of iliotibials as passive element using a robot," vol. Proceedings of the Joint Symposium of AROB-ISBC-SWARM 2023, Beppu, Japan, Jan. 2023, pp. 1205–1208.
- [68] B. Brown and E. M. Schlaikjer, "The structure and relationships of *Protoceratops*," *Annals of the New York Academy of Sciences*, vol. 40, no. 3, pp. 133–266, 1940.
- [69] K.-i. Ishii, M. Watanabe, S. Suzuki, S. ishigaki, R. Barsbold, and K. Tsogtbaatar, *Hayashibara Museum of Natural Sciences Research Bulletin Vol. 1*. Okayama, Japan: Hayashibara Museum of Natural Sciences, Jul. 2000.
- [70] N. E. Campione and D. C. Evans, "A universal scaling relationship between body mass and proximal limb bone dimensions in quadrupedal terrestrial tetrapods," *BMC Biology*, vol. 10, no. 1, p. 60, 2012.
- [71] Y. Matsumoto, "Amounting method using a mock-up system and templates," *Fossils*, vol. 91, pp. 31–38, 2012.
- [72] V. S. Tereshchenko, "A reconstruction of the locomotion of *Protoceratops*," *Paleontologiceskij Zurnal*, pp. 107–121, 1996.
- [73] J. Idei, S. Hida, K. Ito, T. Kinugasa, R. Hayashi, and K. Yoshida, "Dynamical Model and Numerical Simulation for Animal Locomotion Based on its Skeleton.," in *52th Student Council Meeting for Graduation Research in Chugoku and Shikoku Branches of The Japan Society of Mechanical Engineers*, Kochi, Japan, 2020, 11a2.
- [74] A. Fedorov, R. Beichel, J. Kalpathy-Cramer, *et al.*, "3d Slicer as an image computing platform for the Quantitative Imaging Network," *Magnetic Resonance Imaging*, vol. 30, no. 9, pp. 1323–1341, 2012.
- [75] R. Fechner, "Morphofunctional evolution of the pelvic girdle and hindlimb of dinosauromorpha on the lineage to sauropoda," 2009.

- [76] A. Gunther and R. Owen, "Xix. Contribution to the anatomy of Hatteria (Rhynchocephalus, Owen)," *Philosophical Transactions of the Royal Society of London*, vol. 157, no. 0, pp. 595–629, 1997.
- [77] M. Langer, "The pelvic and hind limb anatomy of the stem-sauropodomorph *Saturnalia tupiniquim* ( Late Triassic , Brazil )," 2003.
- [78] E. R. Schachner, P. L. Manning, and P. Dodson, "Pelvic and hindlimb myology of the basal archosaur *Poposaurus gracilis* (archosauria: Poposauroidea)," *Journal of Morphology*, vol. 272, no. 12, pp. 1464–1491, 2011.
- [79] D. K. Smith, "Hind limb muscle reconstruction in the incipiently opisthopubic large therizinosaur *Nothronychus* (Theropoda; Maniraptora)," *Journal of Anatomy*, vol. 238, no. 6, pp. 1404–1424, 2021.
- [80] V. H. Gadow, "Beiträge zur Myologie der hinteren Extremität der Reptilien," in *Morphologisches Jahrbuch*, vol. 7, Leipzig: Wilhelm Engelmann, 1882, pp. 329–465.
- [81] L. Dollo, "Sur la signification du "trochanter pendant" des dinosauriens," vol. 19, 1888, pp. 215–224.
- [82] S. G. J. Mivart, "Notes on the myology of *Iguana tuberculata*," *Proceedings of the Zoological Society of London*, vol. 1867, pp. 766–797, 1867.
- [83] A. S. Romer, "The Pelvic Musculature of Ornithischian Dinosaurs," *Acta Zoologica*, vol. 8, no. 2-3, pp. 225–275, 1927.
- [84] P. Galton, "The pelvic musculature of the dinosaur *Hypsilophodon* (Reptilia: Ornithischia)," *Postilla*, no. 131, 1969.
- [85] J. R. Hutchinson, "The evolution of hindlimb tendons and muscles on the line to crown-group birds," *Comparative Biochemistry and Physiology Part A: Molecular & Integrative Physiology*, vol. 133, no. 4, pp. 1051–1086, 2002.
- [86] F. E. Nelson and B. C. Jayne, "The effects of speed on the in vivo activity and length of a limb muscle during the locomotion of the iguanian lizard *Dipsosaurus dorsalis*," *Journal of Experimental Biology*, vol. 204, no. 20, pp. 3507–3522, 2001.
- [87] J. D. Hutson and K. N. Hutson, "A test of the validity of range of motion studies of fossil archosaur elbow mobility using repeated-measures analysis and the extant phylogenetic bracket," *Journal of Experimental Biology*, vol. 215, no. 12, pp. 2030–2038, 2012.
- [88] Peter L. Falkingham, Daniel Marty, and Annette Richter, *Dinosaur Tracks*. Indiana, United States: Indiana University Press, 2016.

# List of research achievements

## Journal

1. **Kazuki Ito**, Tetsuya Kinugasa, Kentaro Chiba, Yu Okuda, Ryuji Takasaki, Sayaka Hida, Tsukasa Okoshi, Ryota Hayashi, Koji Yoshida, and Koichi Osuka, “The robotic approach to the passive interlocking mechanism in the hindlimb musculoskeletal system of *Crocodylus porosus*” , *Advanced Robotics*, Vol. 37, No. 18, pp. 1187-1197, DOI: 10.1080/01691864.2023.2256375, 2023.
2. **Kazuki Ito**, Sayaka Hida, Tetsuya Kinugasa, Kentaro Chiba, Yu Okuda, Miwa Ichikawa, Tsukasa Okoshi, Ryuji Takasaki, Ryota Hayashi, Koji Yoshida, and Koichi Osuka, “Cam-like mechanism in the intertarsal joints of ratites and its design framework “ , *Journal of Robotics and Mechatronics*, in submission.

## International Conference, Symposium

1. **Kazuki Ito**, Tetsuya Kinugasa, Tsukasa Okoshi, Kentaro Chiba, Ryuji Takasaki, Damdinsuren Idersaikhan, Ryota Hayashi, Koji Yoshida, and Koichi Osuka, ” Can Dinosaurs’ Hindlimb Maintain their Stance Posture Using the Passive Interlocking Mechanism Confirmed in Crocodylian Hindlimb?” , *AROB-ISBC-SWARM 2024*, Beppu, Japan, 2024.
2. **Kazuki Ito**, Tetsuya Kinugasa, Sayaka Hida, Koji Yoshida, Ryota Hayashi, Koichi Osuka, ” Interlocking mechanism in the hindlimb using a passive musculotendinous structure during the high walk of crocodylians: Validation of the effects of iliotibials as passive element using a robot” , *AROB-ISBC-SWARM 2023*, Beppu, Japan, OS10-7, 2023.
3. **Kazuki Ito**, Tetsuya Kinugasa, Kentaro Chiba , Yu Okuda , Ryuji, Takasaki , Sayaka Hida , Koji Yoshida , Ryota Hayashi , Koichi Osuka: “INTERLOCKING MECHANISMS OF CROCODYLIAN HINDLIMB JOINTS USING A PASSIVE MUSCULOTENDINOUS STRUCTURE DURING THE HIGH WALK” , *Society of Vertebrate Paleontology 82nd Annual Meeting*, Toronto, Canada, 2022.
4. **Kazuki Ito**, Tetsuya Kinugasa, Shinobu Ishigaki, Daiki Fujimoto , Ryota Hayashi , Koji Yoshida, “ANALYSIS OF “OFF-TRACKING” IN THE TURNING QUADRUPED TRACKWAY” , *Society of Vertebrate Paleontology 79th Annual Meeting 2019*, Brisbane, Australia, 2019.

## Domestic Conference, Symposium

1. **Kazuki Ito**, Keisuke Naniwa, Yushuke Tsunoda, Tetsuya Kinugasa, Koichi Osuka, “Development of control system for the ”d-FlexCraw” : High maintainability and scalability controller design with ROS2” , JSME Conference on Robotics and Mechatronics (ROBOMECH 2023), Nagoya, A2-H24, 2023.
2. **Kazuki Ito**, Tetsuya Kinugasa, Yu Okuda, Kentaro Chiba, Sayaka Hida, Ryuji Takasaki, Ryota Hayashi, Koji Yoshida, Koichi Osuka, “Stay Apparatus in Crocodilian Hindlimb Based on the “Y” Shaped Muscular System and Robotic Implementation.” , 28th Robotics symposia, pp. 71 – 74, 2023.
3. **Kazuki Ito**, Tetsuya Kingasa, Sayaka Hida, Koji Yoshida, Ryota Hayashi, Koichi Osuka, “Erect-limb posture using passive interlocking inherent in musculoskeletal system by crocodilian hindlimb robot.” , The 35th SICE Symposium on Distributed Autonomous Systems, Osaka, 2B1-1, 2023.
4. **Kazuki Ito**, Ssayaka Hida, Tetsuya Kinugasa, Yu Okuda, Kentaro Chiba, Ryuji Takasaki, Koichi Osuka, “Crocodilian knee locking mechanism and intralimb coordination of a hindlimb in the stance phase during high walking: Investigation based on the dissection of *Crocodylus prosus* and a physical model” , JSME Conference on Robotics and Mechatronics (ROBOMECH 2022), Sapporo, 2A1-S06, 2020.
5. **伊東 和輝**, 衣笠 哲也, 藤本 大樹, 石垣 忍, 林 良太, 吉田 浩治, "大型四足歩行生物の旋回運動に関する力学的考察", 日本古生物学会 2021 年年会, P14, 2021.
6. **Kazuki Ito**, Tetsuya Kinugasa, Daiki Fujimoto, Shinobu Ishigaki, Ryota Hayashi, Koji Yoshida, ” Mechanics for Turning of Quadrupedal Walking: Synthetic Approach on Turning of Sauropod “ , 24th Robotics symposia, Unatsuki, 5A4, 2019.

## Others

### International Conference, Symposium

1. Tetsuya Kinugasa, **Kazuki Ito**, Naoki Miyamoto<sup>3</sup>, Takahiro Nose, Seiji Yuasa, Ryota Hayashi, Koji Yoshida, “Autonomous Panel Fixing for Free-Access Floors” , 2022 SICE Annual Conference (SICE), Kumamoto, Japan, ThA02.4, Japan.
2. Tetsuya Kinugasa, **Kazuki Ito**, Shinobu Ishigaki, Daiki Fujimoto, Ryota Hayashi, and Koji Yoshida : “Mechanics of “Off-tracking” in the Turning Sauropod Trackway and Numerical Simulation using Dynamic Model” , The 4th International Symposium on ASIAN DINOSAURS in Mongolia, Ulaanbaatar, Mongolia, 2019.

### Domestic Conference, Symposium

1. 木村 魁斗, **伊東 和輝**, 衣笠 哲, 市川 美和, 大越 司, 千葉 謙太郎, 奥田 ゆう, 杉本 靖博, 浪花 啓右, 中西 大輔, 大須賀 公一, “ワニ類後肢における股関節の内外転自由度を考慮した立位姿勢維持メカニズムの検証” , 第 24 回計測自動制御学会システムインテグレーション部門講演会, 新潟, 1G2-07, 2023.



2. 片山 貴仁, 角田 祐輔, 浪花 啓右, **伊東 和輝**, 大須賀 公一, “履帯型掘削ロボット“Antler”の開発”, 第 24 回計測自動制御学会システムインテグレーション部門講演会, 新潟, 1D1-03, 2023.
3. 建部 俊介, 近藤 翔太, **伊東 和輝**, 浪花 啓右, 角田 祐輔, 衣笠 哲也, 大須賀 公一, “双胴柔軟クローラ型ロボット“d-FlexCraw”の三次元姿勢取得と可視化”, 第 24 回計測自動制御学会システムインテグレーション部門講演会, 新潟, 1D1-04, 2023.
4. 山本 誠也, **伊東 和輝**, 角田 祐輔, 浪花 啓右, 大須賀 公一, “水を喰らって自己の構造体にする対河道閉塞用水排除ロボット“i-CentiPot-Aqua”の提案”, 第 24 回計測自動制御学会システムインテグレーション部門講演会, 新潟, 1D1-05, 2023.
5. 浪花 啓右, **伊東 和輝**, 杉本 靖博, 角田 祐輔, 大須賀 公一, “徹底的に立ち往生しないことを目指した移動機構”, 第 24 回計測自動制御学会システムインテグレーション部門講演会, 新潟, 1D1-06, 2023.
6. 浪花 啓右, **伊東 和輝**, 角田 祐輔, 大須賀 公一, “徹底的に立ち往生しないことを目指した超多球面脚モジュールロボット:K3(KyuKyaKu)”, 第 67 回 システム制御情報学会 研究発表講演会, 京都, OS03 344-3, 2023.
7. 山本 誠也, **伊東 和輝**, 角田 祐輔, 浪花 啓右, 大須賀 公一”, “開いた設計に基づく柔軟多脚ロボットの開発—異なる脚形状における移動性能の評価”, 第 67 回 システム制御情報学会 研究発表講演会, 京都, OS03 344-4, 2023.
8. Runze Xiao, **Kazuki Ito**, Takahiro Goto, Yusuke Tsunoda, Keisuke Naniwa, Koichi Osuka, ” The Development of a Multi-Jointed Mobile Robot with a Torso Featuring Flexible and Rigid Switchability for Navigation in Unknown 3D Environments”, 第 67 回 システム制御情報学会 研究発表講演会, 京都, OS03 344-5.
9. 浪花啓右, **伊東和輝**, 佐藤悠弥, 角田祐輔, 衣笠哲也, 谷口寿俊, 三谷泰浩, 大須賀公一,” 双胴柔軟クローラ型ロボット“d-FlexCraw”の不整地走行実験検証”, JSME Conference on Robotics and Mechatronics (ROBOMECH 2023), Nagoya, 1P1-I07, 2023.
10. 阪本徹太, 末岡裕一郎, **伊東和輝**, 杉本靖博, 大須賀公一, 浅間一, 永谷圭司”, 群ロボットシステムの異常対応に向けた自律分散的救助アーキテクチャの提案と実装”, JSME Conference on Robotics and Mechatronics (ROBOMECH 2023), Nagoya, 1A2-G03, 2023.
11. 檜田 沙耶香, **伊東 和輝**, 衣笠 哲也, 吉田 浩治, 林 良太:「走鳥類の足根間関節に見られるカム様メカニズムとその設計法の検討」, 第 35 回自律分散システム・シンポジウム, 大阪, 2B1-2, 2023.
12. 山本 誠也, **伊東 和輝**, 角田 祐輔, 浪花 啓右, 大須賀 公一, ” 水陸両用柔軟多脚ロボット“i-CentiPot-Amphibian Jr.”の開発”, 第 35 回自律分散システム・シンポジウム, 大阪, 2C1-4, 2023.
13. 浪花 啓右, **伊東 和輝**, 角田 祐輔, 大須賀 公一, “超多球面脚モジュールロボット: K3(KyuKyaKu)”, 第 23 回計測自動制御学会 システムインテグレーション部門講演会, 千葉, 3P2-G09, 2022.
14. 阪本徹太, 末岡裕一郎, **伊東 和輝**, 大須賀公一, “頑健な群ロボットシステムに向けたスタック協調回避行動の設計”, 第 23 回計測自動制御学会 システムインテグレーション部門講演会, 千葉, GS03-06, 2022.

15. 能瀬 貴大, 伊東 和輝, 宮本 直輝, 杉本 泰基, 衣笠 哲也, 湯浅 誠二, 吉田 浩治, 林 良太, ” フリーアクセスフロア施工のためのパネル固定部材取付ロボット”, 日本機械学会 中国四国支部 第 60 期総会・講演会, 高知, 09b1, 2022.
16. Junya Idei, Sayaka Hida, K. Ito, Tetsuya Kinugasa, Ryota Hayashi, and Koji Yoshida, “Dynamical Model and Numerical Simulation for Animal Locomotion Based on its Skeleton.”, 52th Student Council Meeting for Graduation Research in Chugoku and Shikoku Branches of The Japan Society of Mechanical Engineers, Kochi, 11a2, 2021.
17. 衣笠哲也, 石垣忍, 伊東 和輝, 藤本 大樹, 林 良太, 吉田 浩治, ” 旋回する四足歩行動物の行跡に見る軌道差と動力学モデル解析, 日本古生物学会 168 回例会, 神奈川, A12m, 2019.

## Patent

1. 特開 2022-119283, 衣笠 哲也, 伊東 和輝, 宮本 直輝, 能瀬 貴大, 土谷 嘉紀, 湯浅 誠二, ”無人作業車”, 2022.

## Awards

1. 日本機械学会 ロボティクス・メカトロニクス部門 ベストデモンストレーション表彰, 6/29/2023.
2. 第 28 回ロボティクスシンポジウム 学生奨励賞, 3/15/2023.
3. 第 35 回自律分散システム・シンポジウム 萌芽研究部門 優秀研究奨励賞, 1/27/2023.